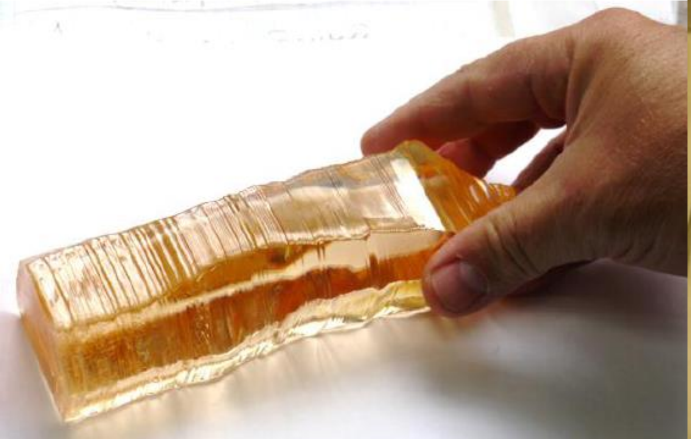

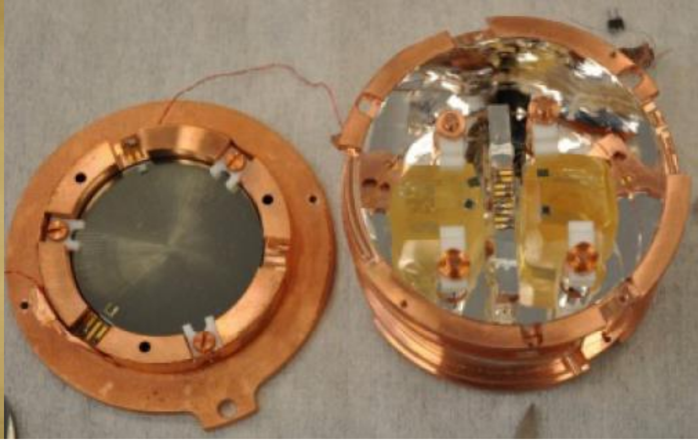

Study of double beta decay using $ZnMoO_4$ cryogenic scintillating bolometers and $^{116}CdWO_4$ crystal scintillators

Dmitry CHERNYAK

chernyak@kinr.kiev.ua http://lpd.kinr.kiev.ua

Institute for Nuclear Research NASU, Kyiv, Ukraine



Mozumi seminar, Kamioka, Japan, 2 March 2016

Outline

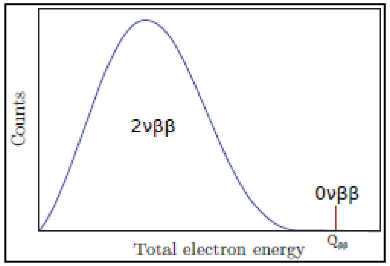

Introduction

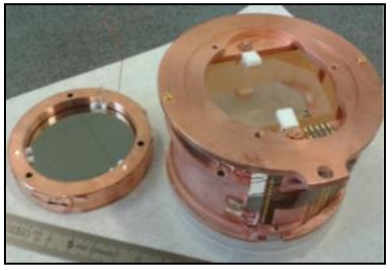

Development of cryogenic low background detectors based on $Zn^{100}MoO_4$ crystal scintillators to search for 0ν2β of ^{100}Mo

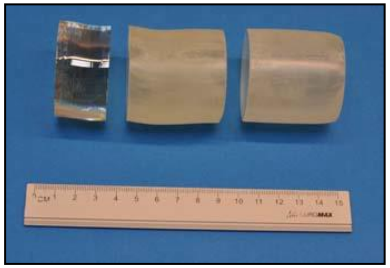

Search for double beta decay of ^{116}Cd with enriched $^{116}CdWO_4$ crystal scintillators

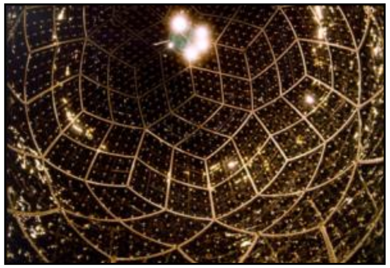

Future plans

2β decay

Double beta decay (2β) is a rare nuclear transition which changes the nuclear charge by two units.

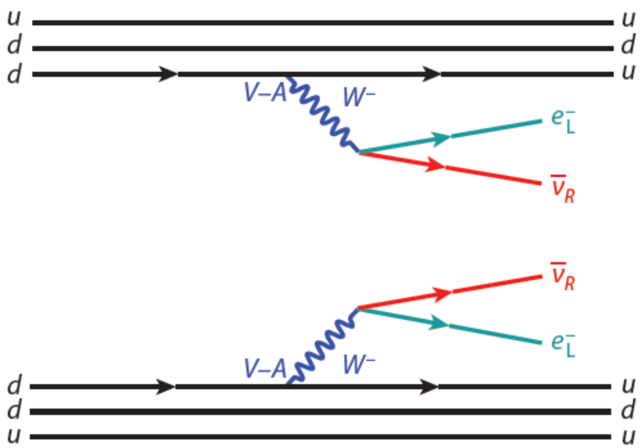

Two-neutrino double beta decay (2ν2β)

2β⁻: $(A, Z) \rightarrow (A, Z+2) + 2e^- + 2\bar{\nu}_e$

Allowed by the Standard Model,

was observed for 11 isotopes:

^{48}Ca, ^{76}Ge, ^{82}Se, ^{96}Zr, ^{100}Mo, ^{116}Cd, ^{128}Te, ^{130}Te, ^{136}Xe, ^{150}Nd, ^{238}U

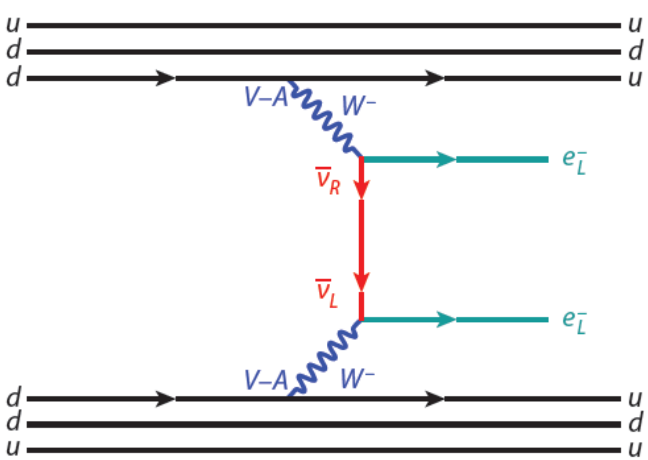

Neutrinoless double beta decay (0ν2β)

2β⁻: $(A, Z) \rightarrow (A, Z+2) + 2e^-$

Process without emission of neutrino or antineutrino

Forbidden by the Standard Model,

is not observed

Neutrino oscillations and 0ν2β decay

$\langle m_\nu \rangle = |\Sigma m_j U_{ej}^2|$ – effective neutrino Majorana mass

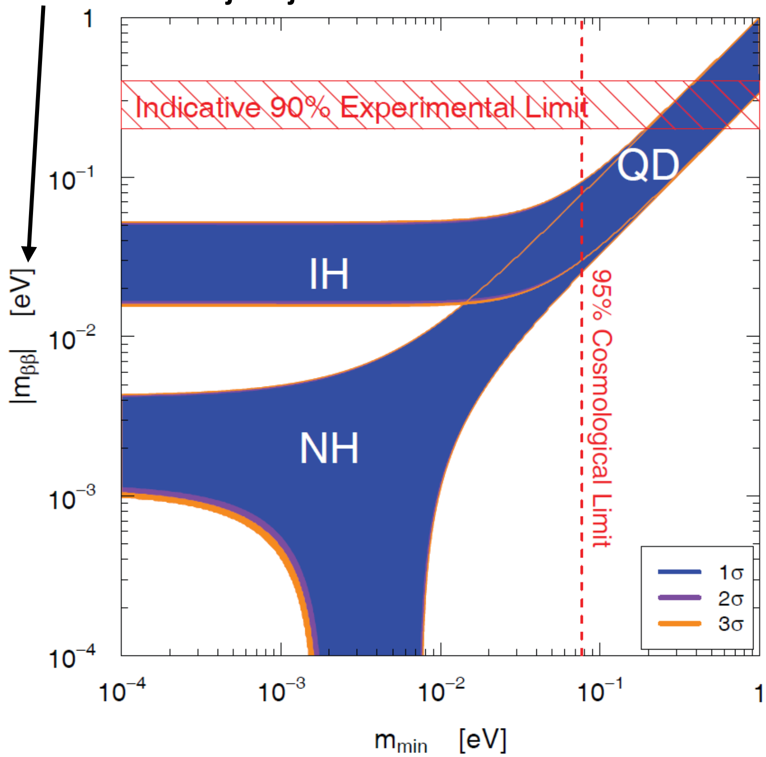

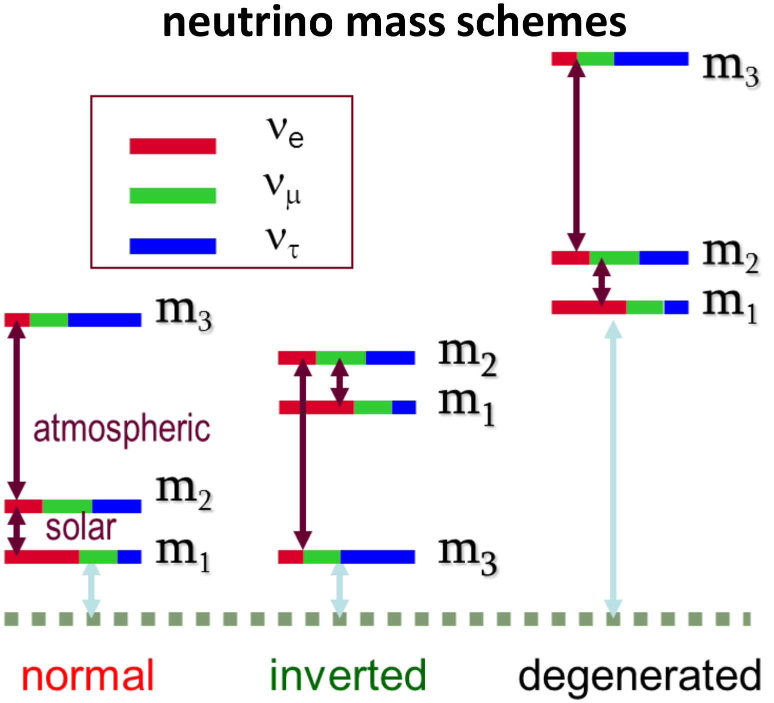

Observation of 0ν2β:

- help to test leptogenesis
- prove the lepton number violation
- establish the Majorana nature of the neutrino
- help to determine neutrino mass hierarchy and estimate the effective Majorana mass of neutrino

Sensitivity of 2β experiments

$$T_{1/2} \propto \varepsilon \cdot \delta \sqrt{\frac{m \cdot t}{R \cdot BG}}$$

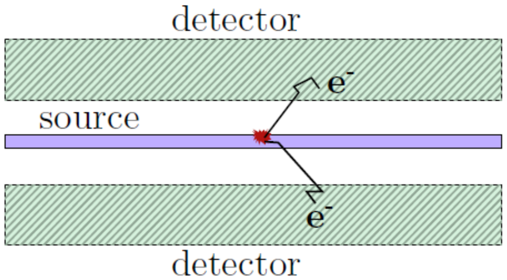

ε – detection efficiency
δ – abundance of candidate nuclei in the detector
m – mass of detector
t – time of measurements
R – energy resolution
BG – background

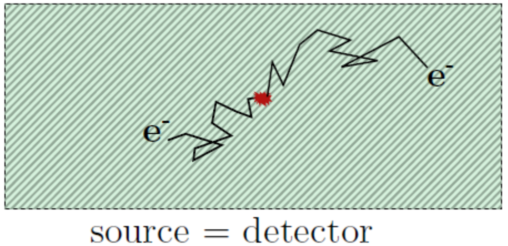

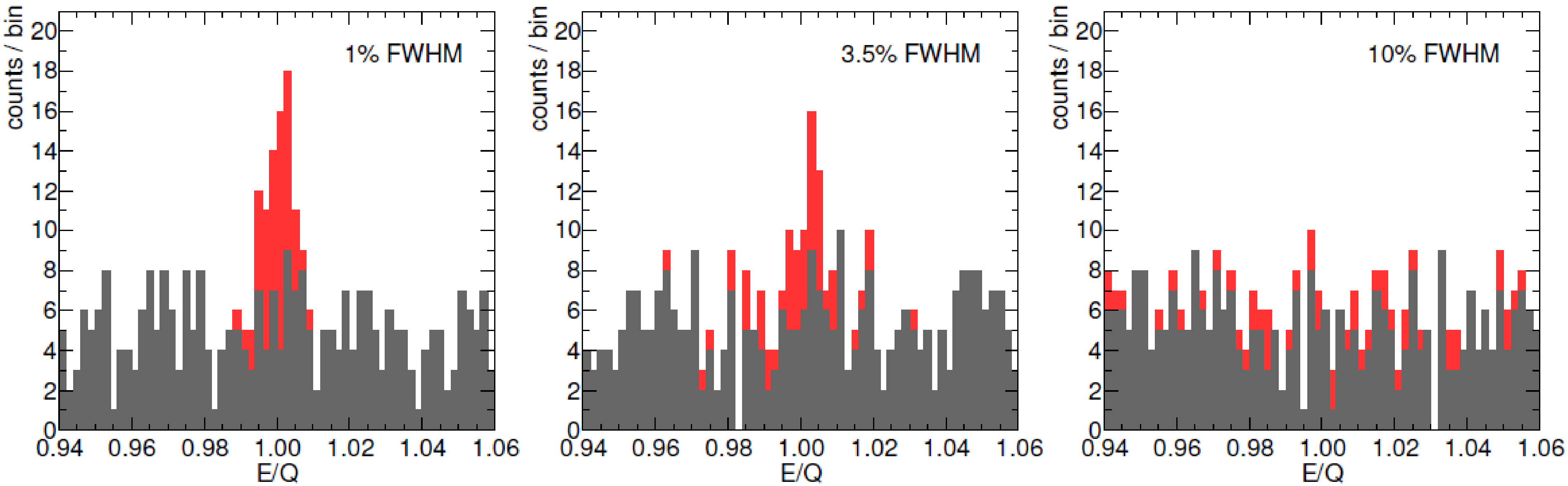

Stefano Dell'Oro et al., Neutrinoless double beta decay: 2015 review, arXiv:1601.07512

Most sensitive 2β decay experiments

Isotope	Experiment	$T_{1/2}^{2\nu}$, years	$T_{1/2}^{0\nu}$, years
^{48}Ca	NEMO-3 ELEGANT VI	$(4.4^{+0.5}_{-0.4}(\text{stat}) \pm 0.4(\text{syst})) \times 10^{19}$	$> 1.3 \times 10^{22}$ $> 5.8 \times 10^{22}$
^{76}Ge	IGEX HM GERDA-I	$(1.45 \pm 0.15) \times 10^{21}$ $(1.74^{+0.18}_{-0.16}) \times 10^{21}$ $(1.84^{+0.14}_{-0.10}) \times 10^{21}$	$\geq 1.57 \times 10^{25}$ $\geq 1.9 \times 10^{25}$ $= (2.23^{+0.44}_{-0.31}) \times 10^{25}$ $> 2.1 \times 10^{25}$
^{82}Se	NEMO-3	$(9.6 \pm 0.1(\text{stat}) \pm 1.0(\text{syst})) \times 10^{19}$	$> 3.6 \times 10^{23}$
^{96}Zr	NEMO-3	$(2.35 \pm 0.14\ (\text{stat}) \pm 0.16\ (\text{syst})) \times 10^{19}$	$> 9.2 \times 10^{21}$
^{100}Mo	NEMO-3	$(7.16 \pm 0.01\ (\text{stat}) \pm 0.54\ (\text{syst})) \times 10^{18}$	$> 1.1 \times 10^{24}$
^{116}Cd	Solotvina NEMO-3	$(2.9^{+0.4}_{-0.3}) \times 10^{19}$ $(2.88 \pm 0.04\ (\text{stat}) \pm 0.16\ (\text{syst})) \times 10^{19}$ [79]	$> 1.7 \times 10^{23}$ $> 1.6 \times 10^{22}$
^{130}Te	NEMO-3 CUORICINO	$(7.0 \pm 0.9\ (\text{stat}) \pm 1.1\ (\text{syst})) \times 10^{20}$	$> 1.0 \times 10^{23}$ $\geq 2.8 \times 10^{24}$
^{136}Xe	EXO-200 KamLAND-Zen	$(2.165 \pm 0.016\ (\text{stat}) \pm 0.059\ (\text{syst})) \times 10^{21}$ $(2.38 \pm 0.02\ (\text{stat}) \pm 0.14\ (\text{syst})) \times 10^{21}$	$> 1.1 \times 10^{25}$ $> 1.9 \times 10^{25}$
^{150}Nd	NEMO-3	$(9.11^{+0.25}_{-0.22}(\text{stat}) \pm 0.63(\text{syst})) \times 10^{18}$	$> 1.8 \times 10^{22}$

Claim for the observation of 0ν2β decay in ^{76}Ge by a part of the Heidelberg-Moscow collaboration **is strongly disfavored** by GERDA result combined with data from HM and IGEX experiments: $T_{1/2}^{0\nu}$ **> 3.0 × 10^{25} (90% C.L.)** [M. Agostini et al., Phys. Rev. Lett. 111 (2013) 122503]

Required sensitivity for the next-generation 2β experiments

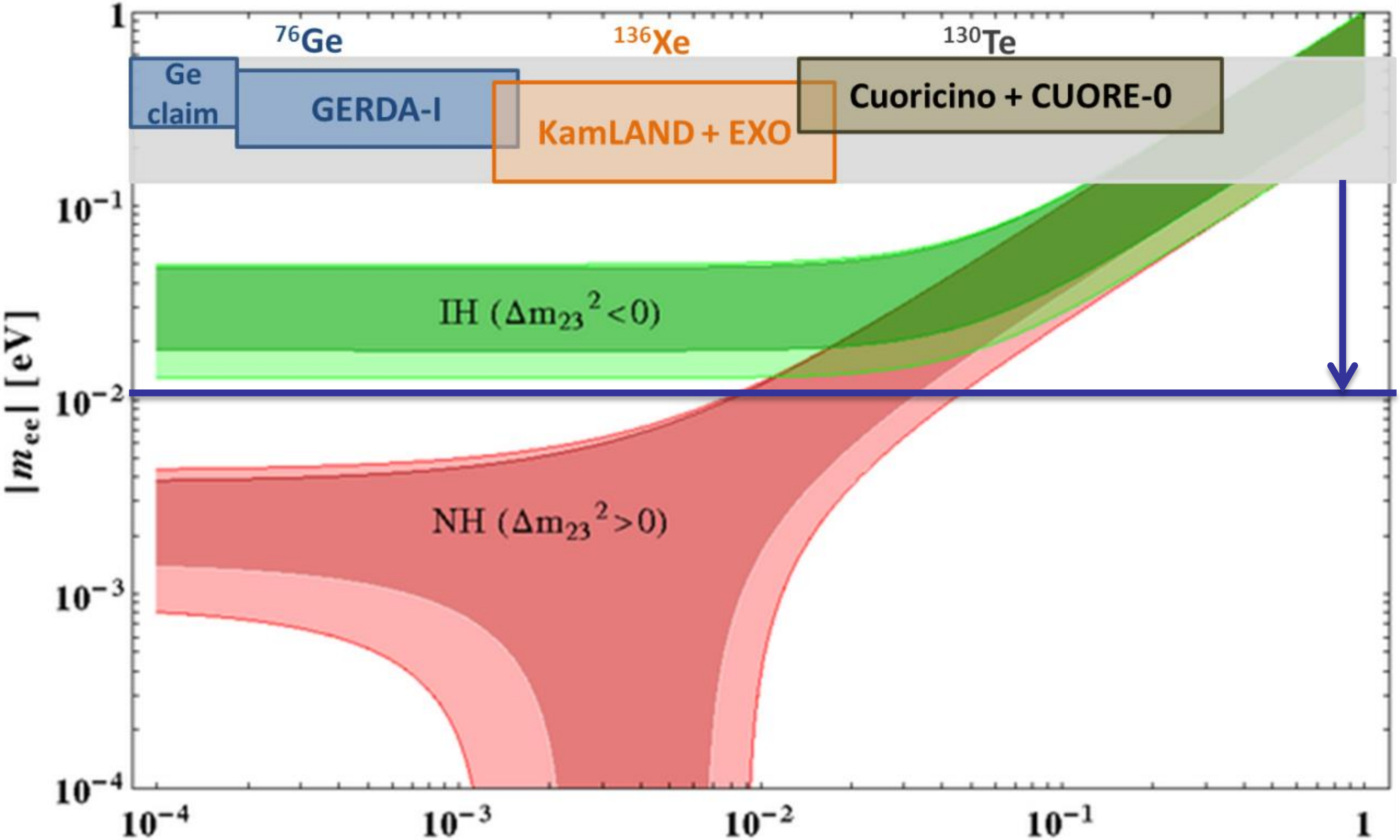

To fully explore the inverted scheme, the sensitivity should be:

$\langle m_\nu \rangle \sim$ **0.01 eV** $\rightarrow$ $T_{1/2} \sim 10^{27} - 10^{28}$ **yr**

Development of cryogenic low background detectors based on $Zn^{100}MoO_4$ crystal scintillators to search for $0\nu2\beta$ of ^{100}Mo

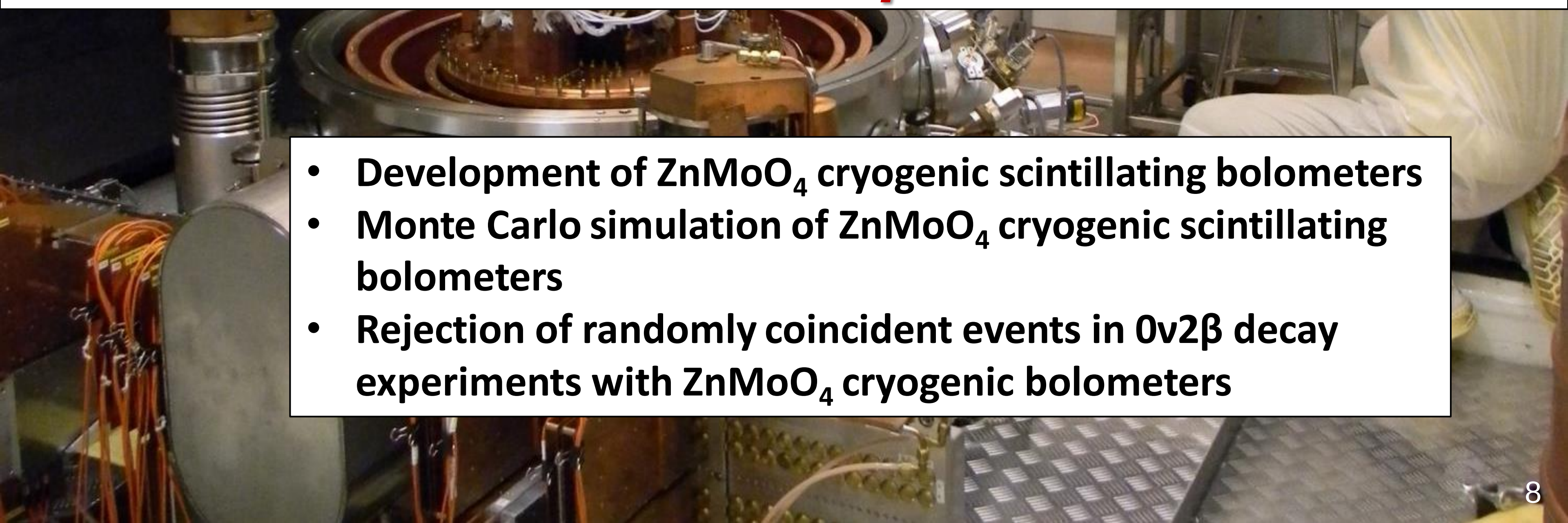

- Development of $ZnMoO_4$ cryogenic scintillating bolometers
- Monte Carlo simulation of $ZnMoO_4$ cryogenic scintillating bolometers
- Rejection of randomly coincident events in $0\nu2\beta$ decay experiments with $ZnMoO_4$ cryogenic bolometers

2β decay of ^{100}Mo

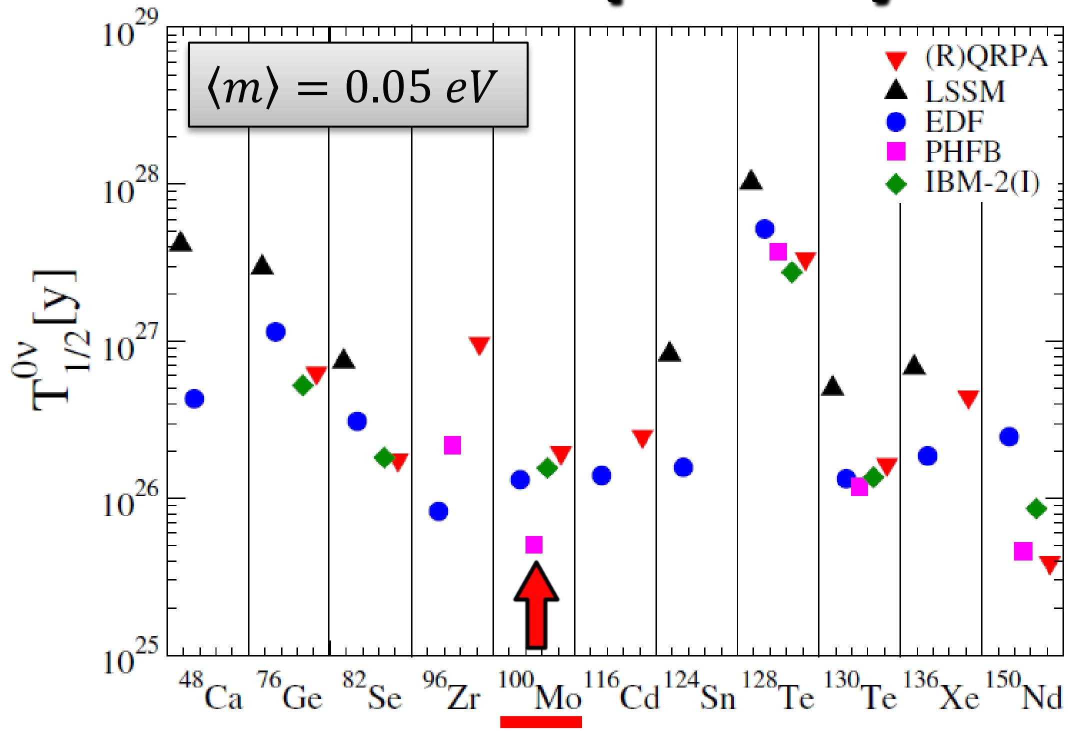

J.D.Vergados, H.Ejiri, F.Simkovic, Rep. Prog. Phys. 75 (2012) 106301

- **Large transition energy : $Q_{2\beta}$ = 3034.4(17) keV**
- **Considerable natural isotopic abundance δ = 9.82% and possibility of enrichment by centrifugation**
- **Favorable theoretical estimations of the decay probability**

Latest results for 2β decay of ^{100}Mo:

$$T^{2\nu}_{1/2}(2\nu2\beta) = (7.16 \pm 0.54)\times10^{18}\ \text{y}\ [1, 2]$$

$$T^{2\nu}_{1/2}(0^{+} \rightarrow 0^{+}_{1}) = (6.9 \pm 0.7)\times10^{20}\ \text{y}\ 90\%\ \text{C.L.}\ [3, 4]$$

$$\mathbf{T^{0\nu}_{1/2} > 1.1\times10^{24}\ y\ 90\%\ C.L.,\ \langle m_\nu \rangle < (0.3\text{–}0.9)\ eV}\ [5]$$

[1] L. Simard (NEMO-3) J Phys. Conf. Proc. 375 (2012) 042011
[2] L Cardani et al., J. Phys. G: Nucl. Part. Phys. 41 (2014) 075204
[3] R.Arnold et al., Nuclear Physics A 925(2014) 25
[4] P. Belli et al., NPA 846 (2010) 143
[5] R. Arnold et al. (NEMO-3) Phys. Rev. D 89 (2014) 111101(R)

Cryogenic bolometers

Bolometers

(CUORE)

Deposited energy is converted into phonons which induce a measurable temperature rise

Scintillating bolometers

(LUMINEU, LUCIFER, AMoRE)

If **bolometer is the scintillator**, a small but significant fraction of the deposited energy is converted into scintillation photons

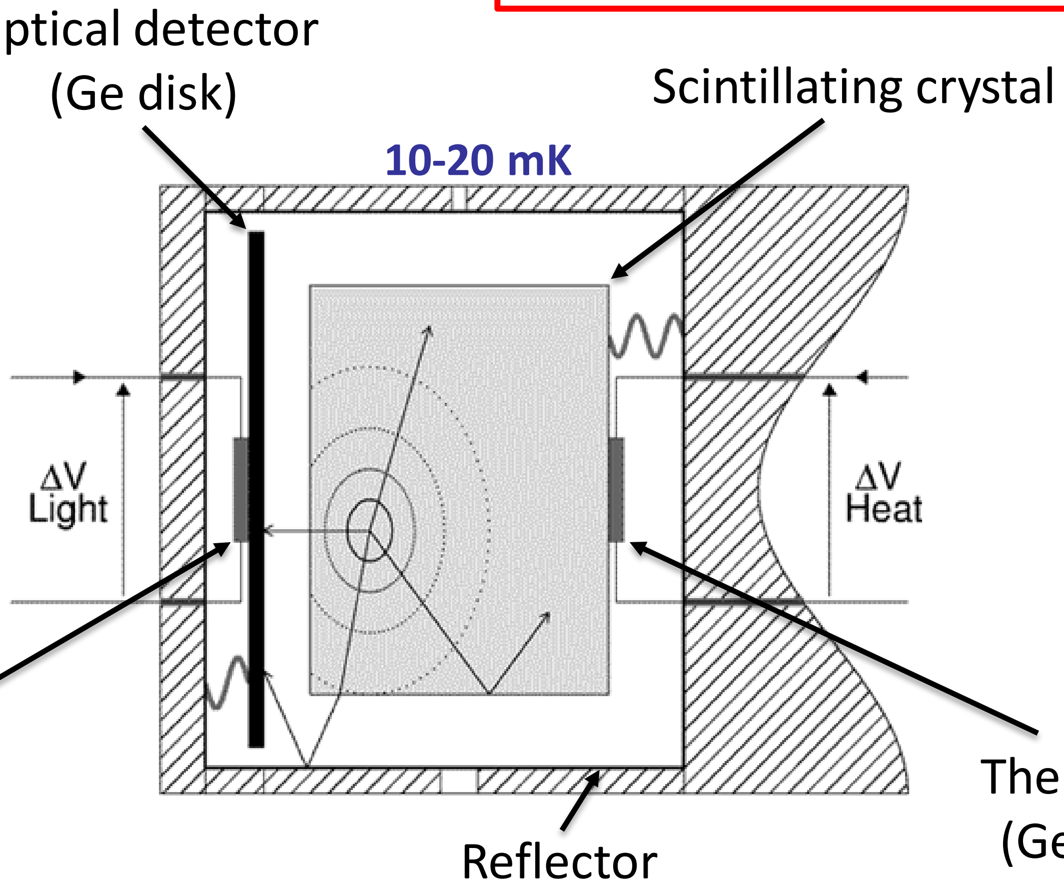

(figure from presentation of Pierre de Marcillac)

$ZnMoO_4$ cryogenic scintillating bolometers

- **High energy resolution** (≈ 6-10 keV @ 2615 keV [1, 2])
- **High detection efficiency** (80–85)%
- **Excellent α/β discrimination** (10-20 sigma)
- **High percentage of Mo** (43% in weight)

Energy resolution 5.6 keV at 2615 keV [3]

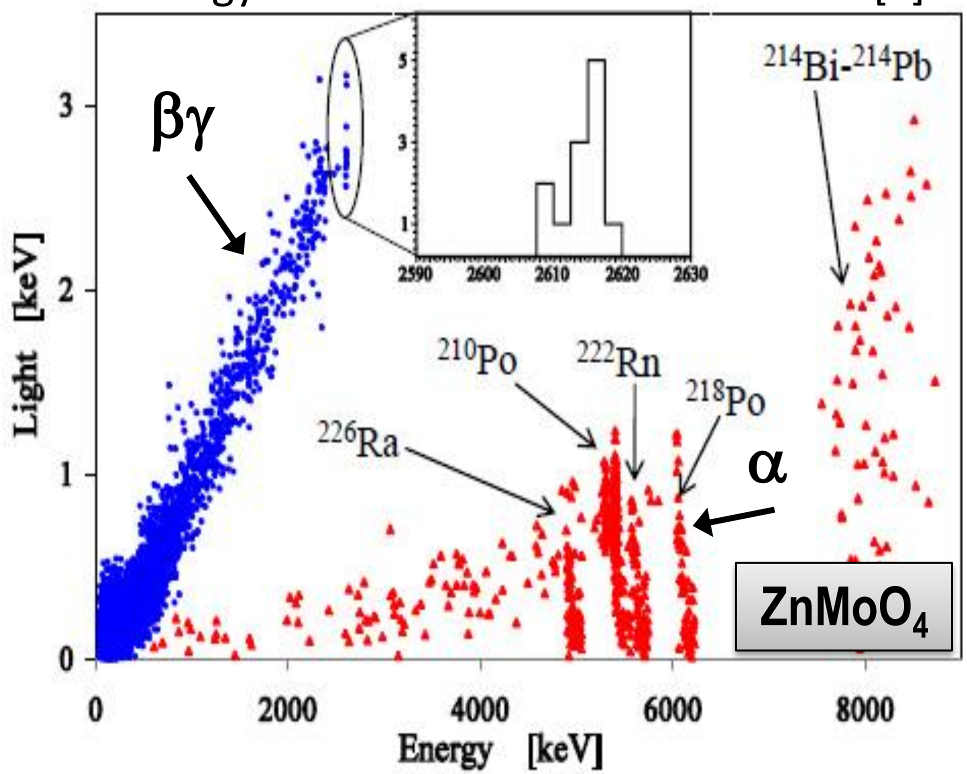

[1] E. Armengaud et al., JINST 10 (2015) 007 [2] J.W. Beeman et al., Eur. Phys. J. C 72 (2012) 2142 [3] L. Gironi et al., JINST 5 (2010) 11007

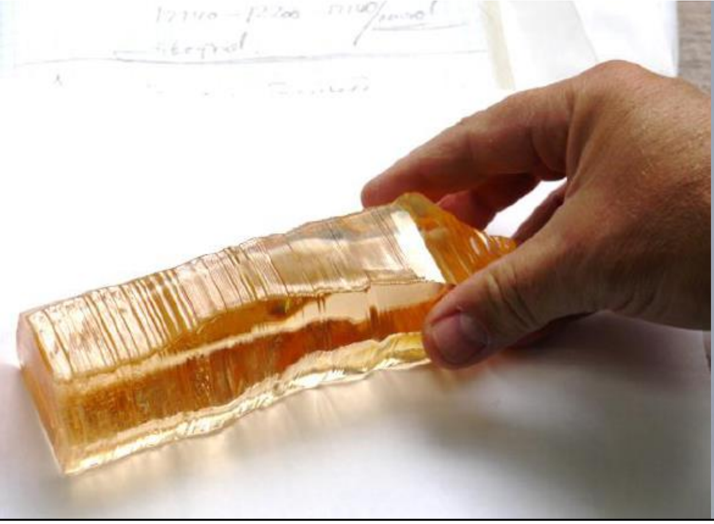

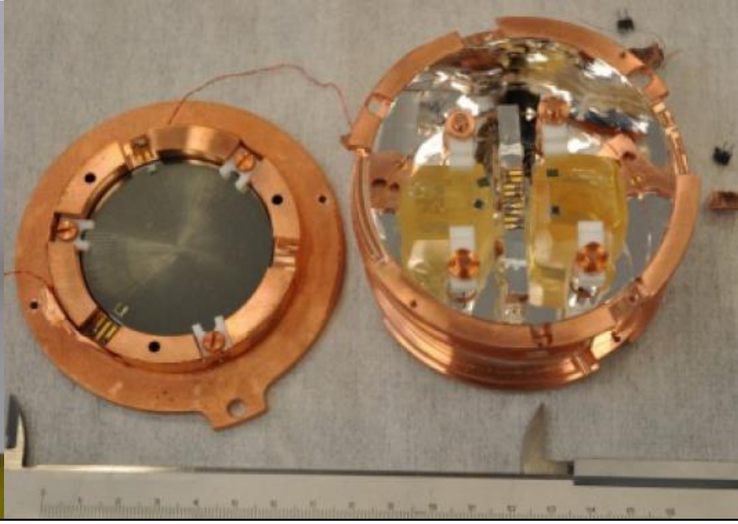

DEVELOPMENT OF ZINC MOLYBDATE CRYOGENIC SCINTILLATING BOLOMETERS

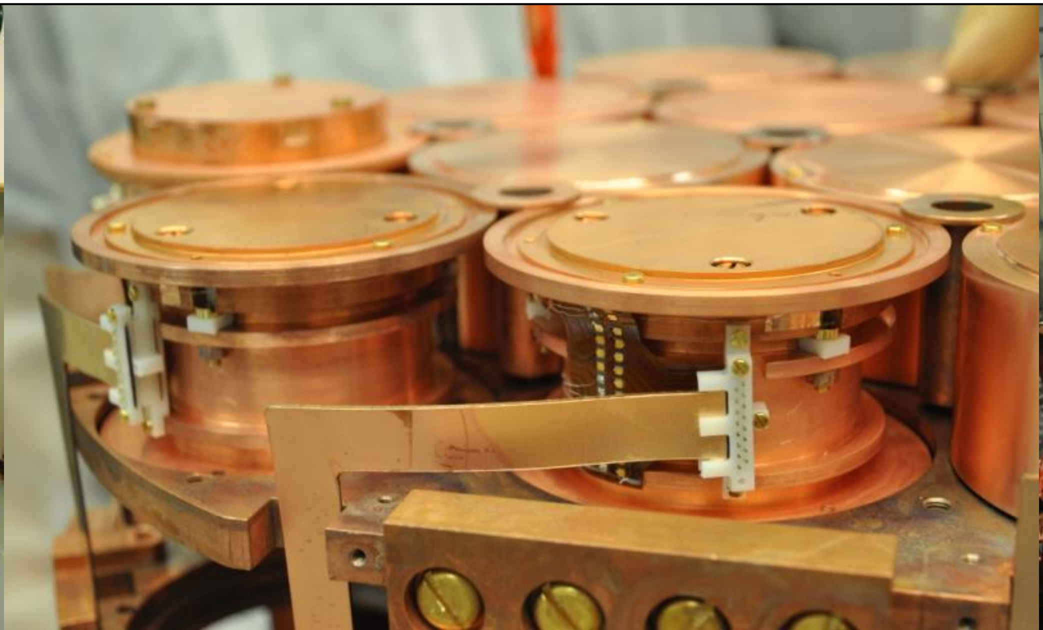

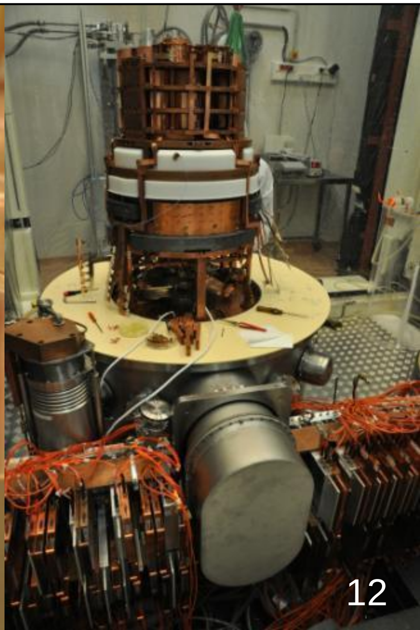

Development of $ZnMoO_4$ crystals

2008

Czochralski (a) and Kyropoulos (b) methods

(IGP, Moscow, Russia)

Ø 15 × 40 mm
Ø 30 × 15 mm

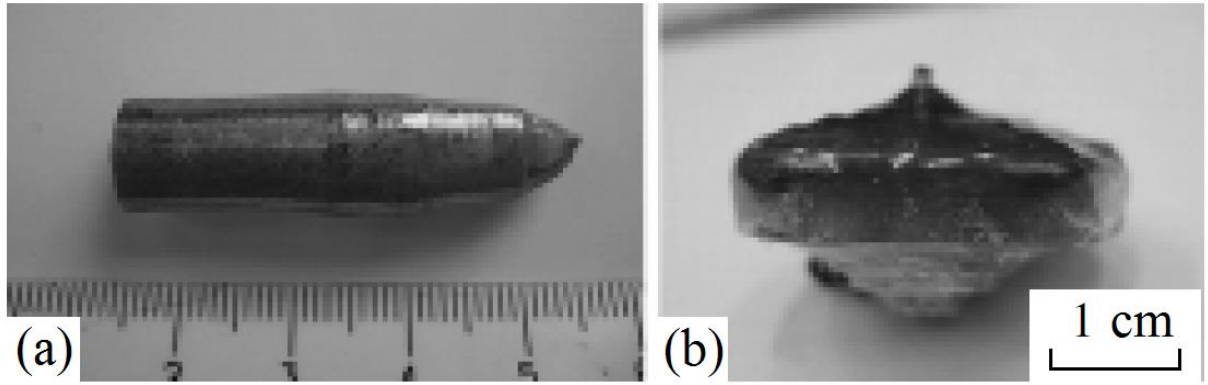

2009

Czochralski technique

(ISMA, Kharkiv, Ukraine)

Ø 25 × 50 mm

2010

Low-thermal-gradient Czochralski technique

(NIIC, Novosibirsk, Russia)

Ø 25 × 60 mm

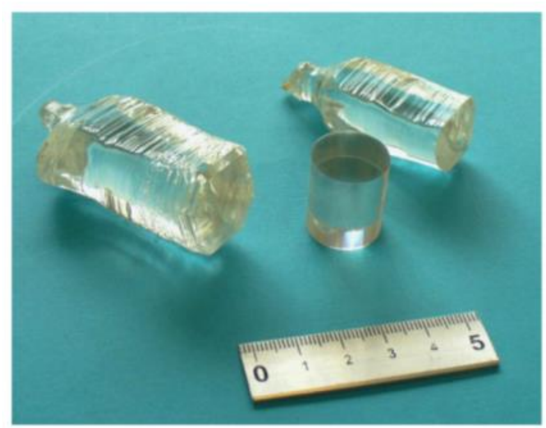

Advanced large volume $ZnMoO_4$ and $Zn^{100}MoO_4$ crystals

Zinc molybdate scintillating crystals were produced in Nikolaev Institute of Inorganic Chemistry by using **low-thermal-gradient Czochralski technique** and **two-stage molybdenum purification technique** (double sublimation with addition of zinc molybdate and recrystallization from aqueous solution of ammonium para-molybdate).

2013

$ZnMoO_4$

crystal boule

~ 1.5 kg

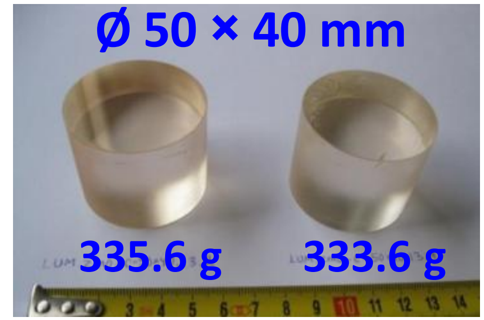

$Zn^{100}MoO_4$ crystals enriched in isotope ^{100}Mo to 99.5% were developed

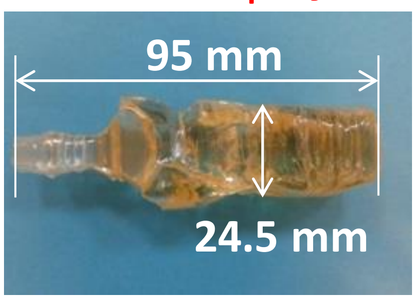

2014

$Zn^{100}MoO_4$

crystal boule

170.7 g

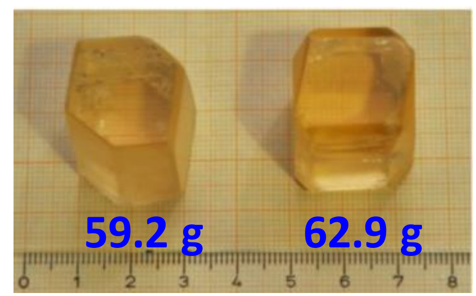

2015

$Zn^{100}MoO_4$

crystal boule

~ 1.4 kg

High crystal yield (> 80%) and low irrecoverable loses of ^{100}Mo (< 4%)

Characterization of $ZnMoO_4$ crystals

Ø15×40 mm Ø30×15 mm
2008 Czochralski and Kyropoulos methods

Ø25×11 mm
2009 Czochralski technique

Ø25×60 mm
2010 Low-thermal-gradient Czochralski technique

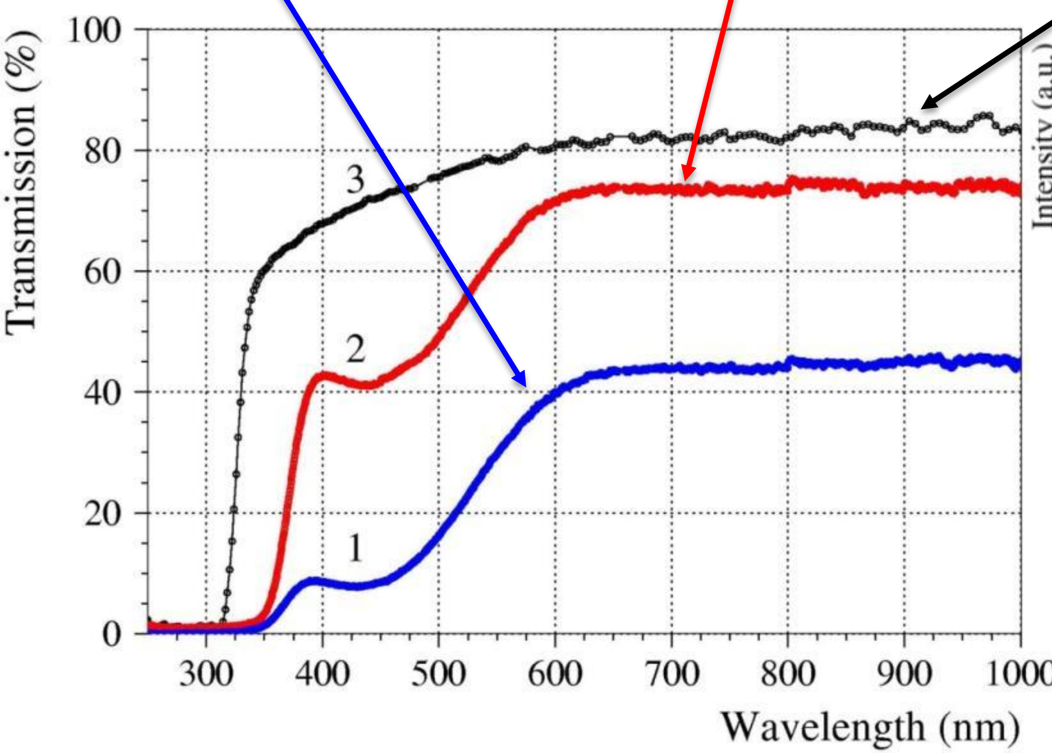

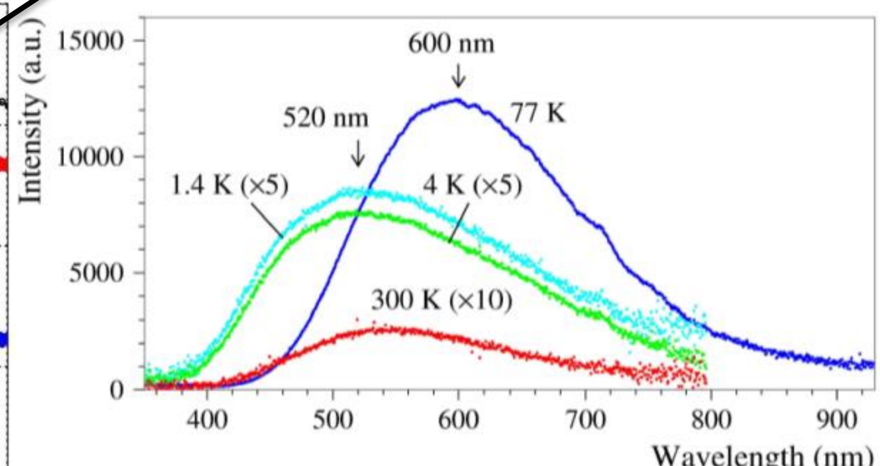

Emission spectra of the $ZnMoO_4$ crystal under the X-ray excitation

Aboveground low-temperature measurements with precursor 313 g $ZnMoO_4$ crystal

$ZnMoO_4$ crystal

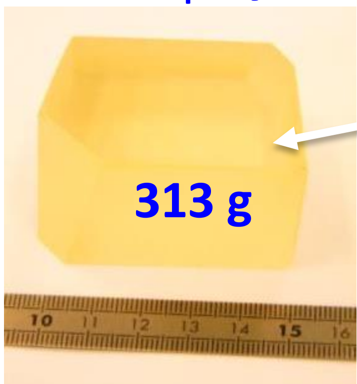

$ZnMoO_4$ scintillating bolometer

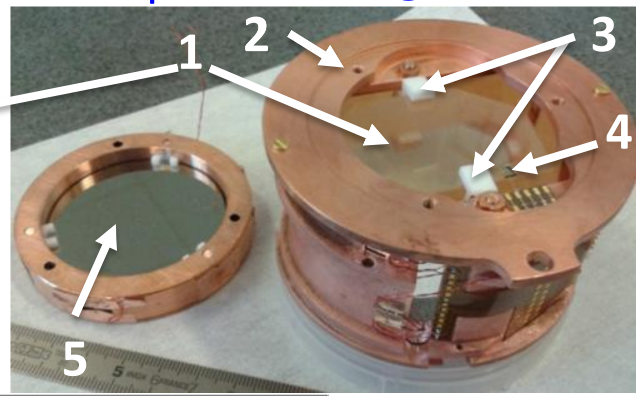

(1) 313 g precursor $ZnMoO_4$ crystal
(2) Cu holder of the detector
(3) PTFE supporting elements
(4) Two NTD thermistors
(5) Two Ge light detectors

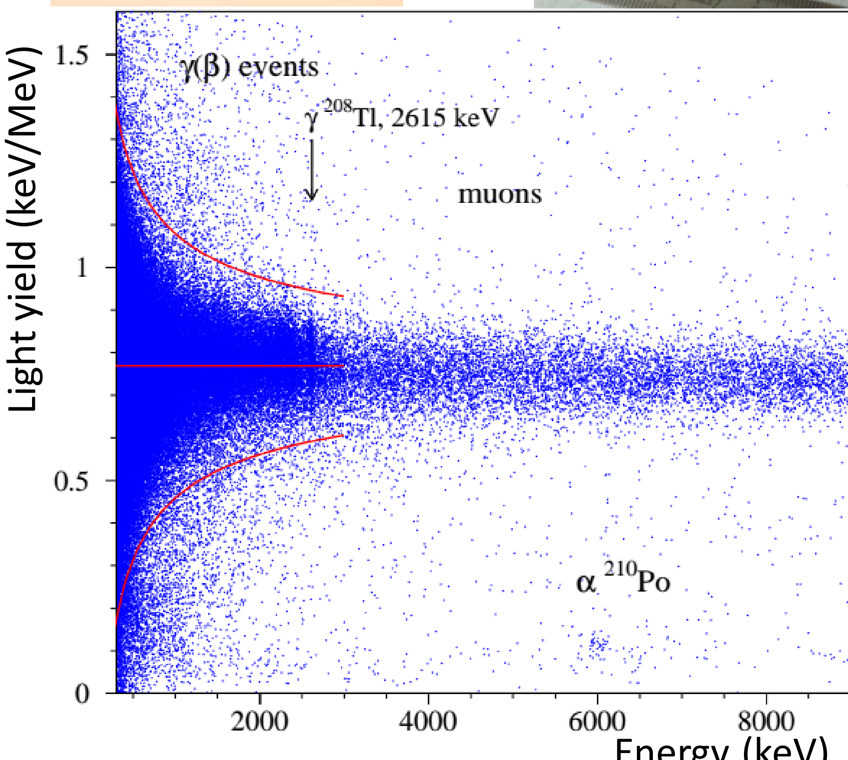

Centre de Sciences Nucléaires et de Sciences de la Matière (Orsay, France)

Data taking

16 bit ADC, 30 kHz sampling rate
Pulse profile ≈ 2 s
Working *T* was 17 mK
FWHM = 24(2) keV at 2615 keV

The detector performance was deteriorated by the pile-up effects due to the high counting rate ≈ 2.5 Hz

Underground low-temperature test of precursor 313 g $ZnMoO_4$ crystal

EDELWEISS set-up, Laboratoire Souterrain de Modane (LSM, France)

1.7 km rock overburden (4800 m.w.e.)
~5 μ/day/m^2; 10^{-6} n/day/cm^2 (>1 MeV)
Deradonized air supply (~30 mBq/m^3)

Cryostat (~50 liters)
15 Ge bolometers
1 $ZnMoO_4$ bolometer

Data taking
14 bit ADC, 2 kHz sampling rate
Pulse profile ≈ 2 s
Working *T* was 19 mK

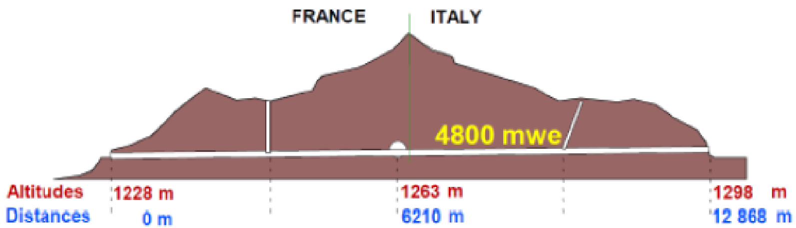

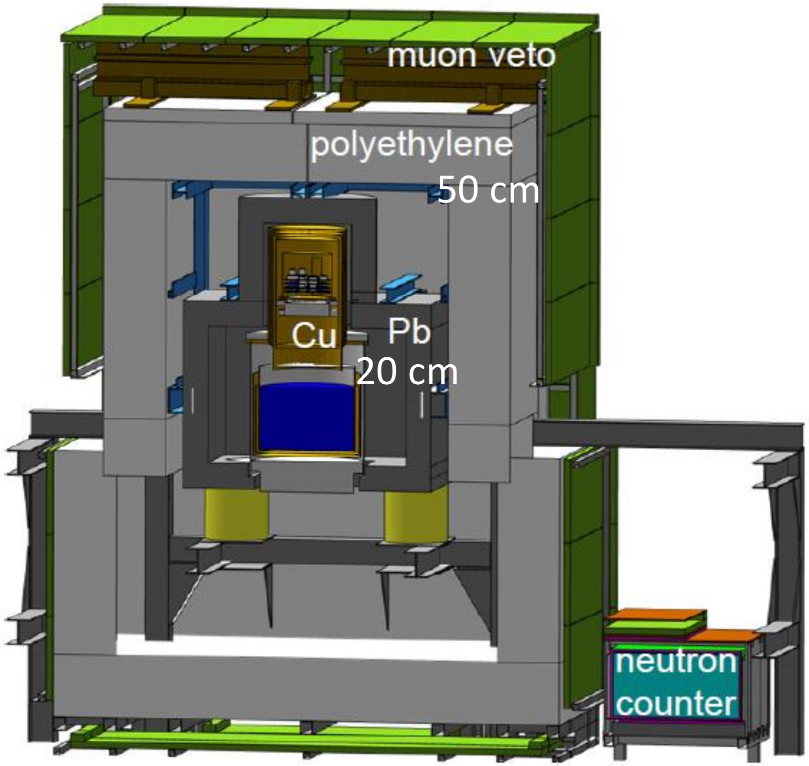

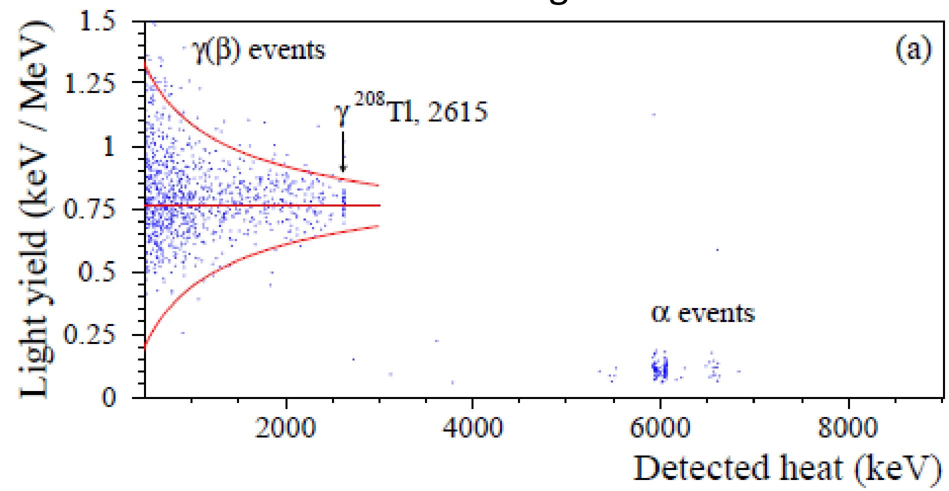

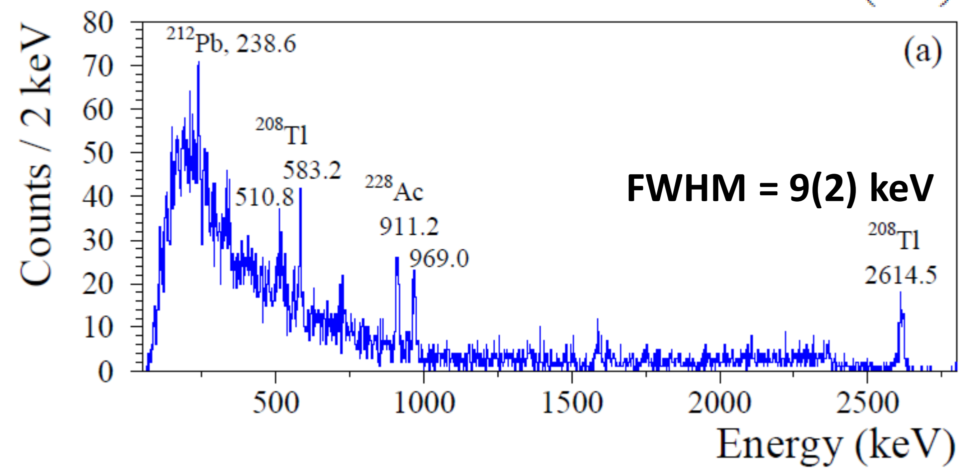

Scintillating bolometers based on two advanced quality $ZnMoO_4$ crystals

EDELWEISS set-up (LSM, Modane, France)

$ZnMoO_4$
Ø50×40 mm

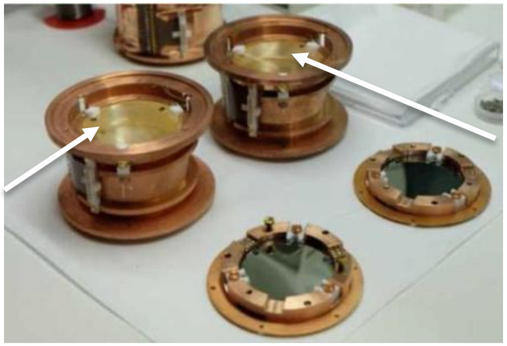

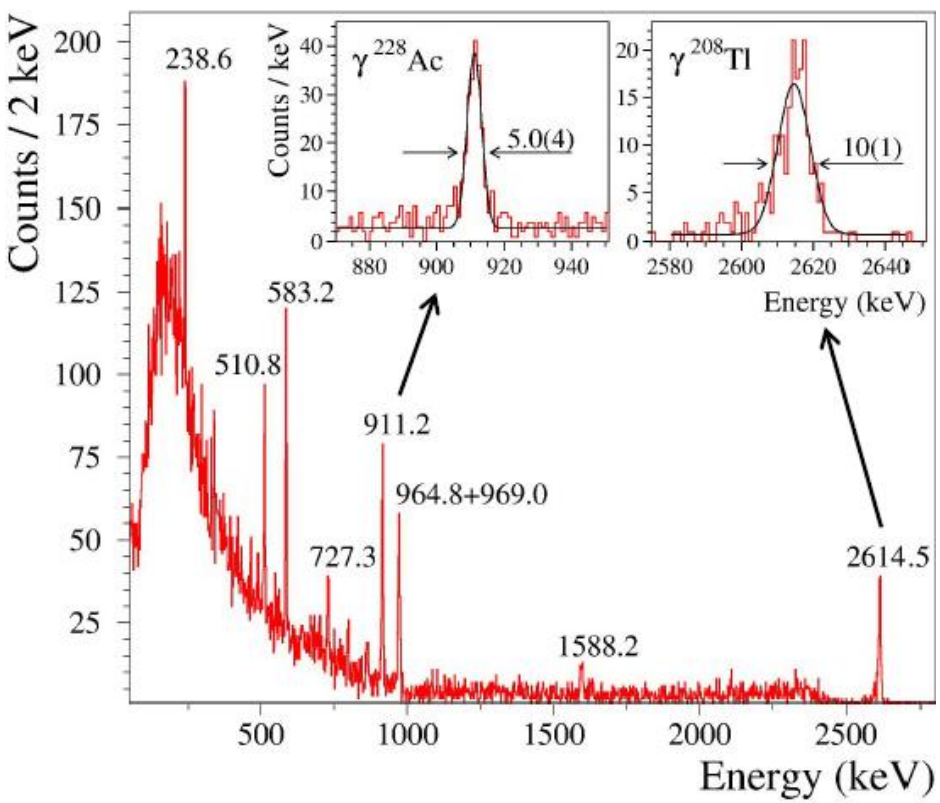

Excellent spectrometric performance and α/γ(β) discrimination capability

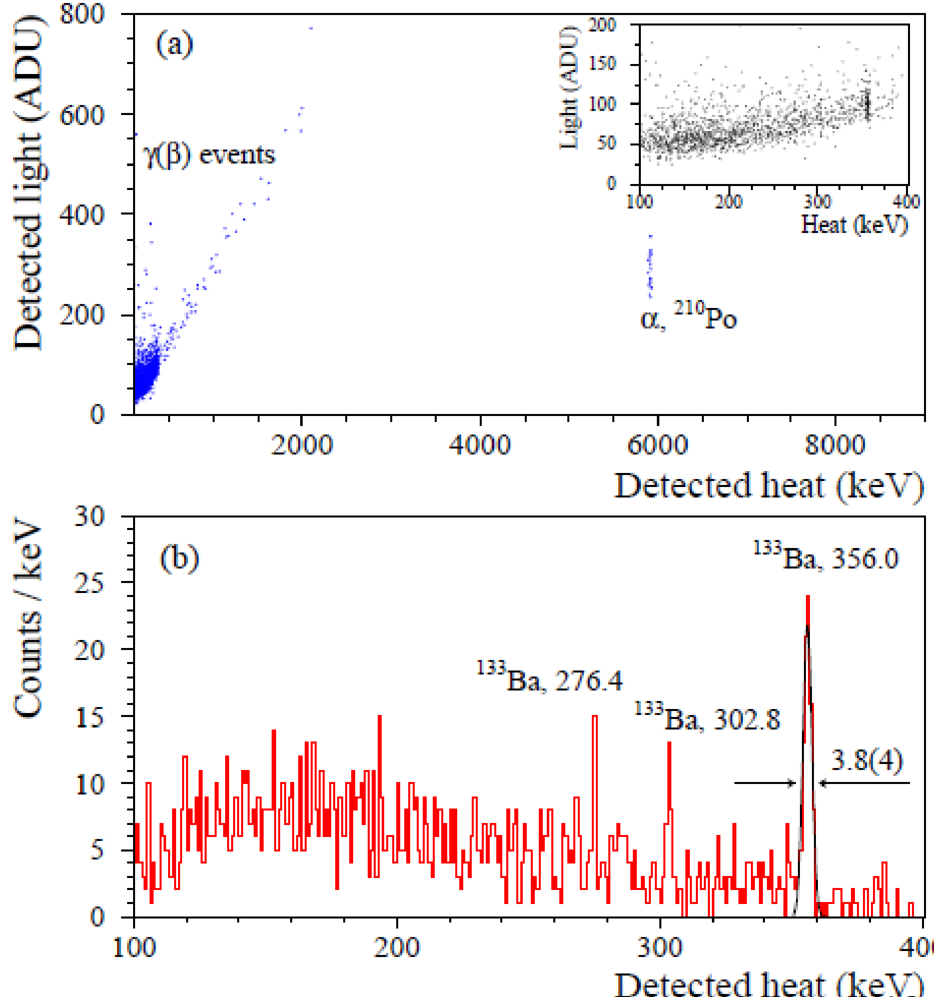

First bolometric test of two enriched $Zn^{100}MoO_4$ crystal scintillators

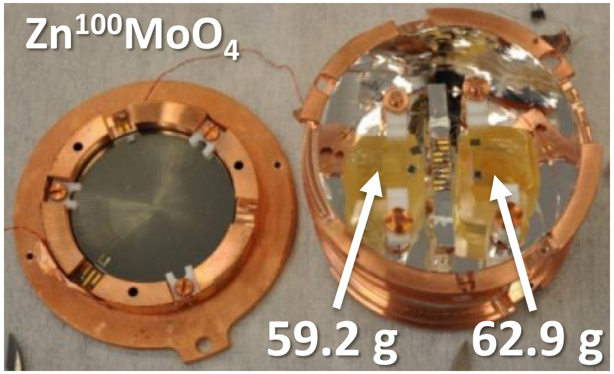

The energy spectra were accumulated in **aboveground measurements** at CSNSM for over 18.3 h.

The detector was operated at 13.7 mK and irradiated by gamma quanta from low activity ^{232}Th source.

Promising bolometric and scintillation characteristics

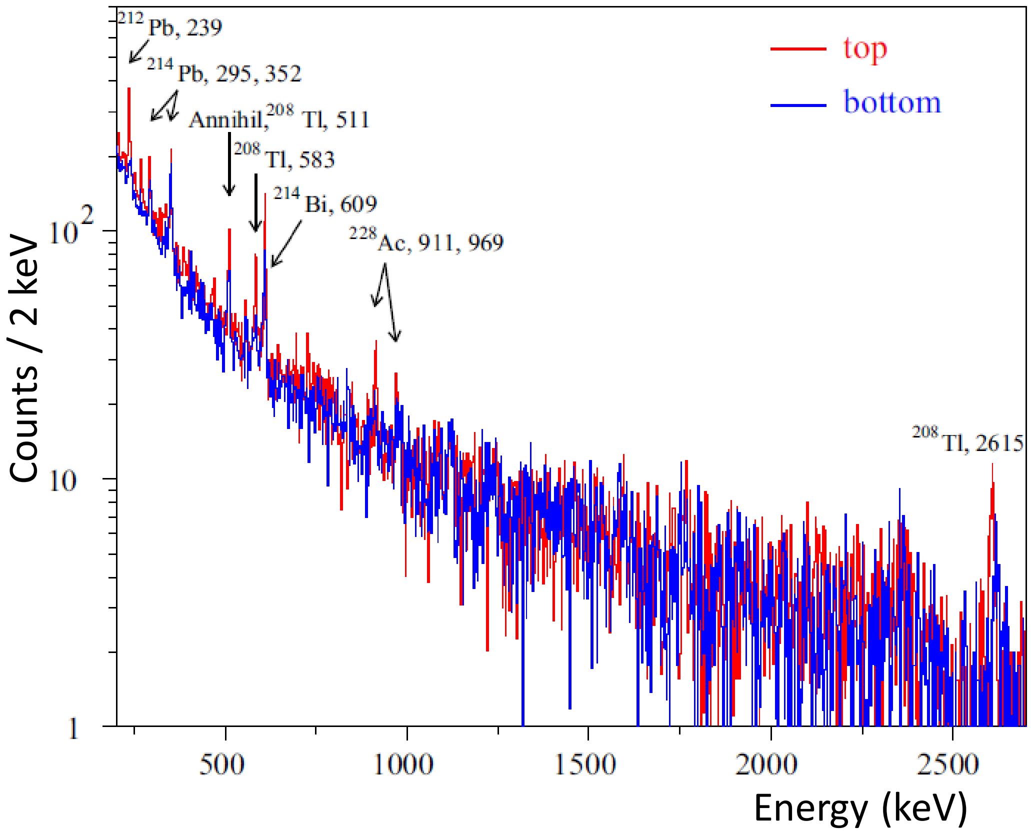

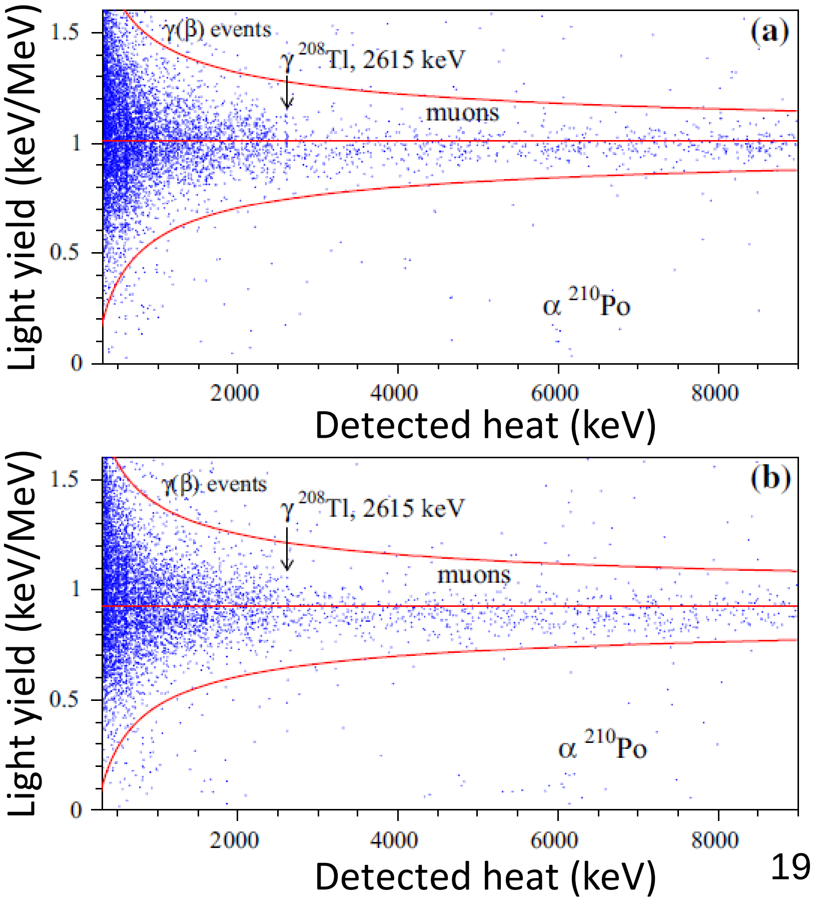

Main properties of the $ZnMoO_4$ and $Zn^{100}MoO_4$ cryogenic scintillating bolometers

Detector		FWHM, keV					$LY_{\gamma(\beta)}$, keV/MeV	QF_{α}
Crystal	Mass, g	Baseline	^{133}Ba 356 keV	^{214}Bi 609 keV	^{208}Tl 2615 keV	^{210}Po 5407 keV		
$ZnMoO_4$	313	1.4(1)	6.4(1)	6(1)*	24(2)*/9(2)	19(1)	0.77(11)*	0.15(2)*/0.14(1)
	336	1.5(2)	6(1)	—	—	29(4)	—	—
	334	1.06(3)	3.8(4)	—	10(1)	15(1)	—	0.19(2)
$Zn^{100}MoO_4$	59.2	1.4(1)	—	5.0(5)*	11(3)*	—	1.01(11)*	≈ 0.15*
	62.9	1.8(1)	—	10(1)*	15(3)*	—	0.93(11)*	≈ 0.15*

* — aboveground measurements

The low-temperature tests of the zinc molybdate crystals (produced from natural and enriched molybdenum) demonstrated high performance of the detectors

Radioactive contamination of zinc molybdate crystals

Nuclide	Activity, μBq/kg		
	LUMINEU crystal	Precursor crystals	
	334 g	313 g	329 g
	2216 h	803 h	524 h
^{232}Th	≤ 2.3	≤ 5.5	≤ 8
^{228}Th	≤ 5.3	12 ± 4	≤ 6
^{238}U	≤ 1.8	8 ± 3	≤ 6
^{234}U	≤ 2.5	≤ 8.1	≤ 11
^{230}Th	≤ 1.8	≤ 8.4	≤ 6
^{226}Ra	≤ 4.8	22 ± 5	27 ± 6
^{210}Po	1271 ± 22	703 ± 28	700 ± 30
Unidentified (on surface)	—	134 ± 12	—

E.Armengaud et al., JINST 10 (2015) P05007

The radioactive contamination of the advanced $ZnMoO_4$ crystals by ^{228}Th and ^{226}Ra is on the level of ≤ 0.005 mBq/kg thanks to the developed methods of molybdenum deep purification and improved crystallization technique

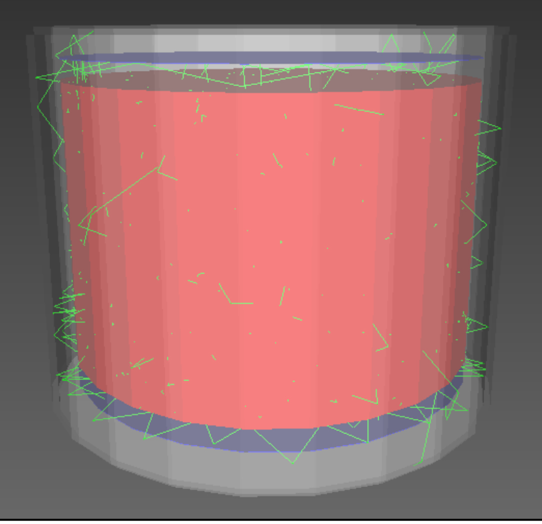

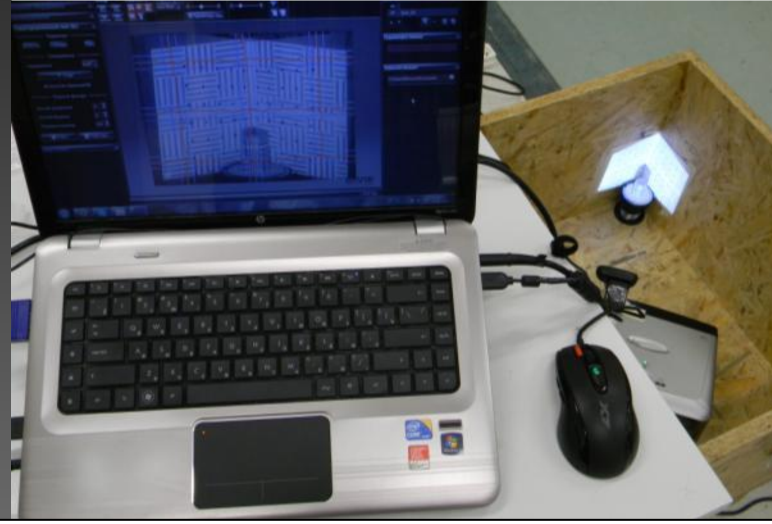

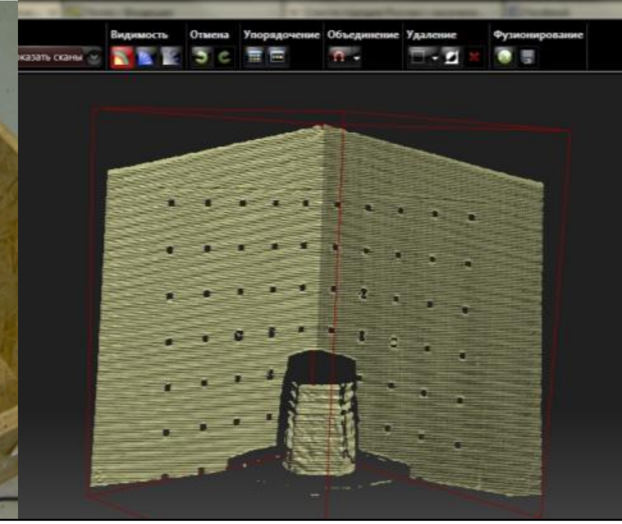

MONTE CARLO SIMULATION OF ZINC MOLYBDATE CRYOGENIC SCINTILLATING BOLOMETERS

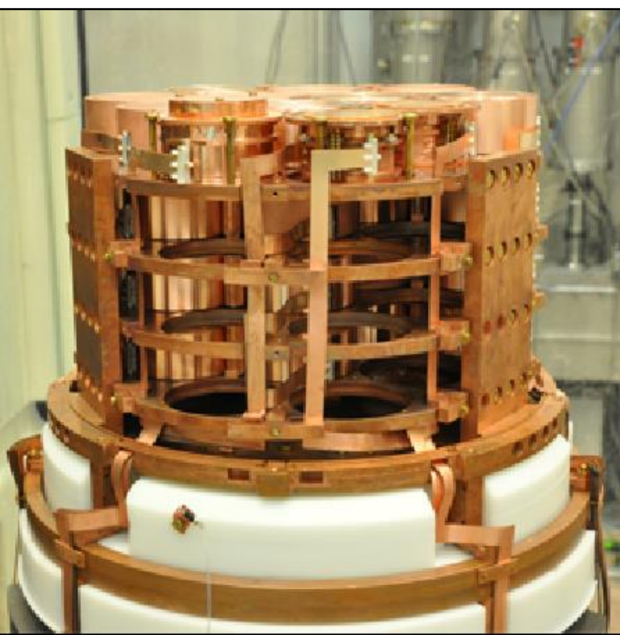

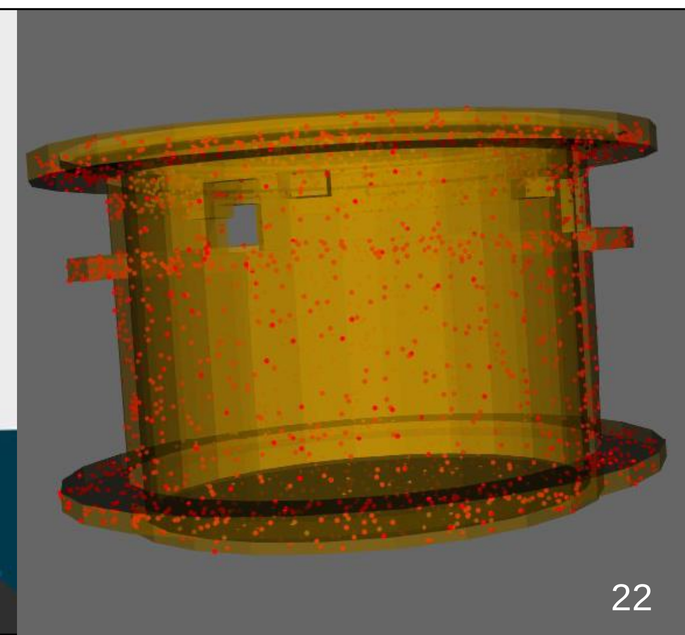

Simulation of the light collection from $ZnMoO_4$ crystal scintillators

We simulated the collection of scintillation photons in $ZnMoO_4$ cryogenic scintillating bolometers in different geometry using GEANT4 package:

- Three shapes of the $ZnMoO_4$ crystal: cylinder, hexagonal prism, octagonal prism
- Two sizes of $ZnMoO_4$ crystal: Ø60 × 20 mm and Ø60 × 40 mm
- Three diameters of cylindrical Ge detector: 20 mm, 40 mm and 60mm
- Two types of the crystal surface: polished and diffused

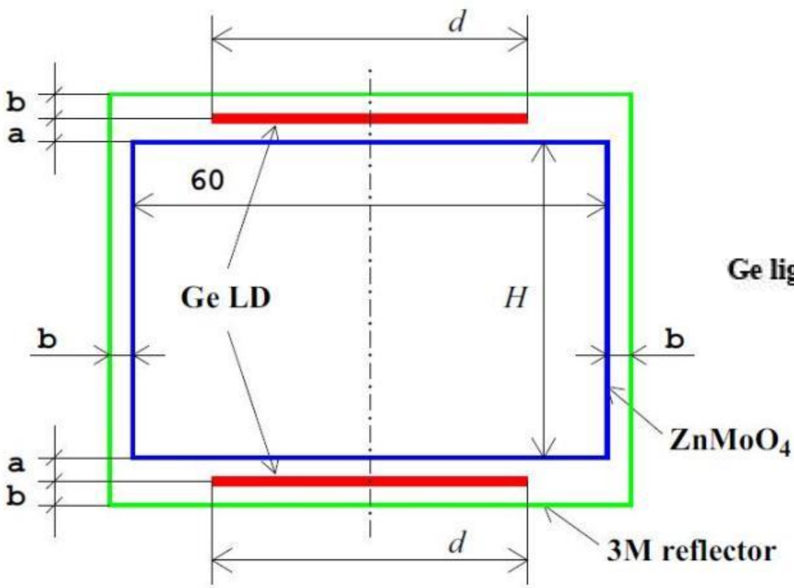

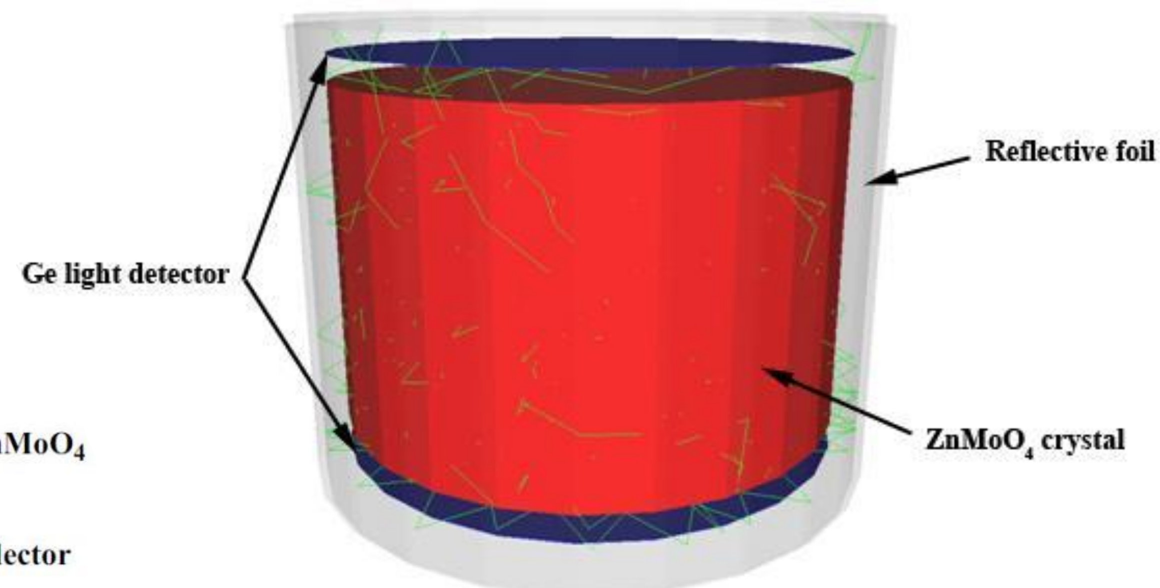

Light collection from $ZnMoO_4$ crystal scintillators

Shape of $ZnMoO_4$ crystal	Size of crystal	Surface Condition	Part of photons (%) reaching photodetectors with diameter (mm)		
			20	40	60
Cylinder	Ø60 × 40	Polished	2.6	6.7	11.8
		Diffused	3.6	11.0	20.5
	Ø60 × 20	Polished	4.3	10.6	16.8
		Diffused	**7.7**	**21.9**	**36.5**
Octahedron	60 × 40	Polished	3.5	8.4	14.3
		Diffused	3.9	11.9	22.6
	60 × 20	Polished	6.0	14.0	21.4
		Diffused	**8.3**	**23.5**	**38.8**
Hexagonal	60 × 40	Polished	3.8	9.1	15.3
		Diffused	4.2	12.7	24.0
	60 × 20	Polished	6.6	14.7	22.1
		Diffused	**8.8**	**24.7**	**40.3**

Best light collection was achieved for hexagonal crystal shape with a diffused surface

Simulation results were confirmed by the experiment [1]

[1] F.A.Danevich et al., Nucl. Instrum. Meth. A 744(2014)41.

Dependence of light collection on distance between the reflector and side surface of $ZnMoO_4$ crystal

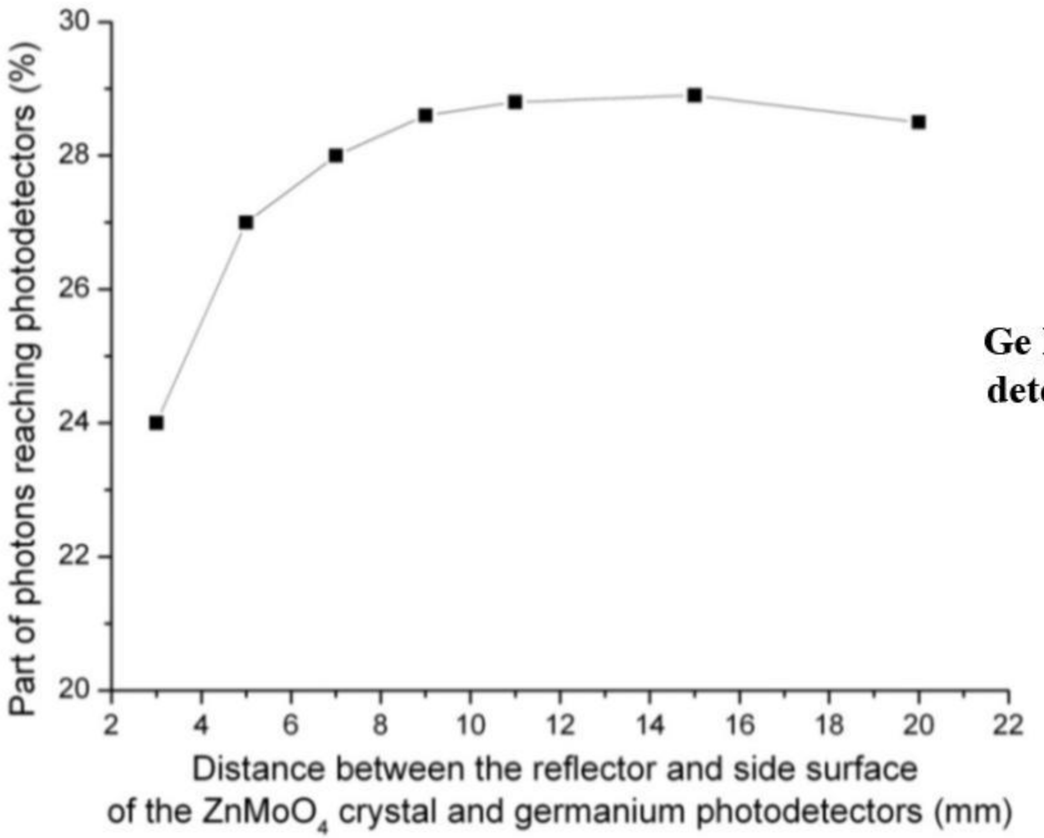

60 × 40 mm hexagonal crystal with diffused surface

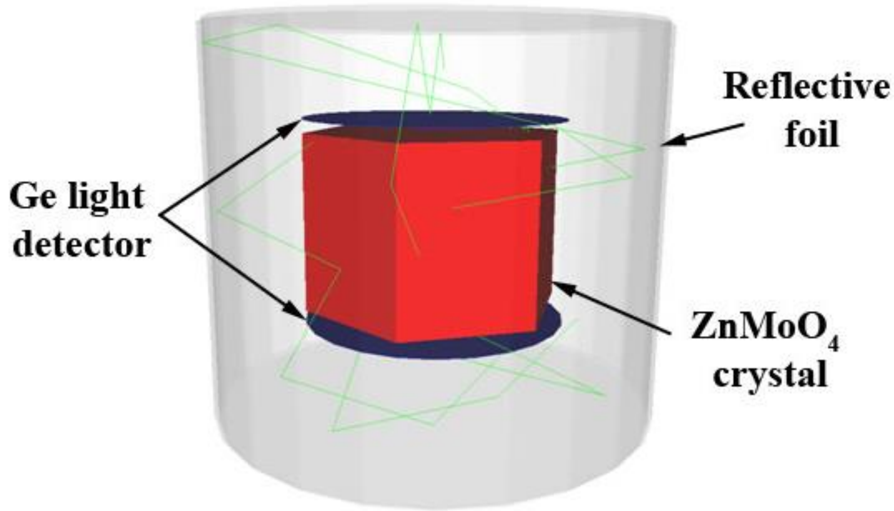

Light detectors 60 mm in diameter

Optimal distance between the light reflector and side surface of $ZnMoO_4$ crystal is 11–15 mm

Reconstruction of $Zn^{100}MoO_4$ crystals shape

To reproduce crystal shape as precise as possible we tried to build a 3D model and integrate the obtained geometry into the GEANT4 code. We applied 3D scanning of the crystals using structured light technique.

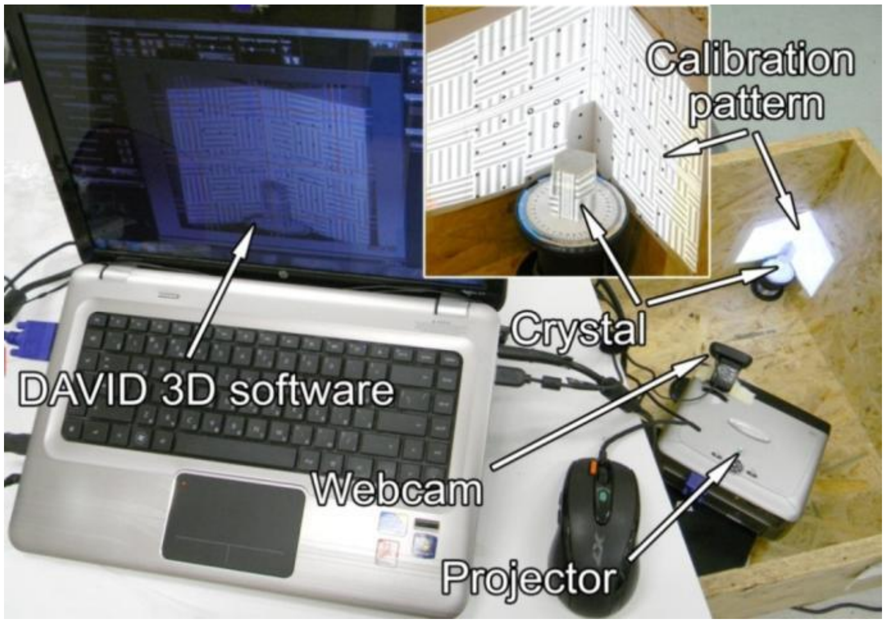

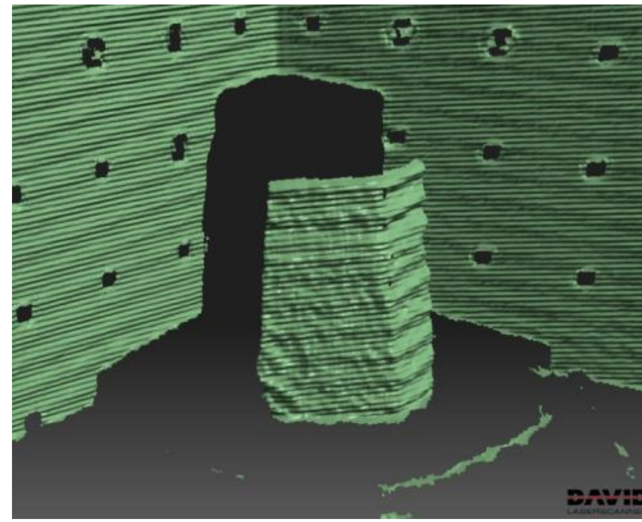

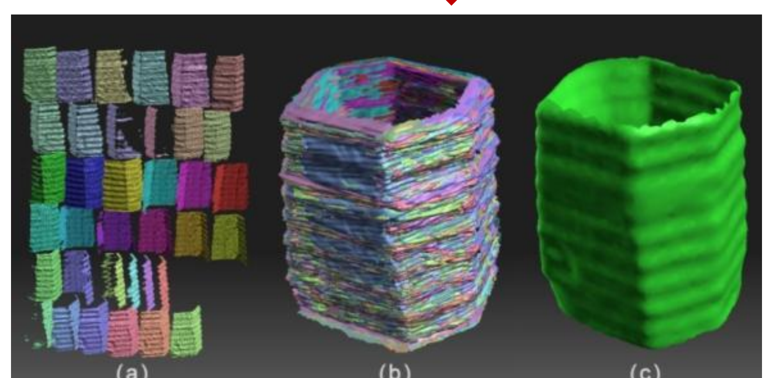

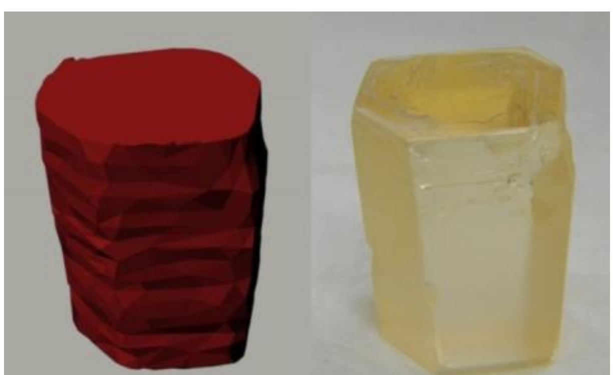

The final result of 3D scanning and $Zn^{100}MoO_4$ scintillator has visible shape differences

Comparison of $2\nu2\beta$ decay distributions for different shapes of $Zn^{100}MoO_4$ crystals

$Zn^{100}MoO_4$

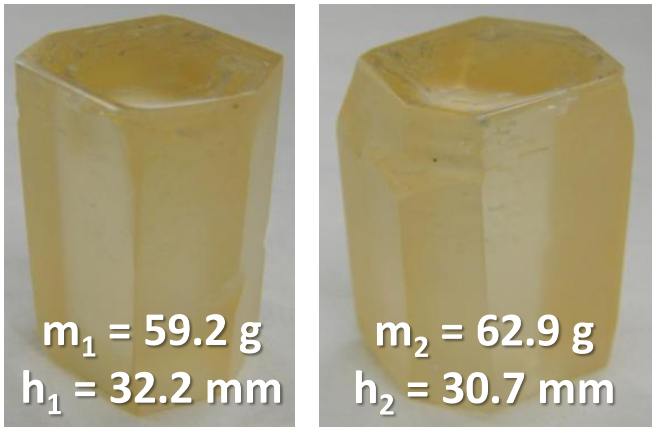

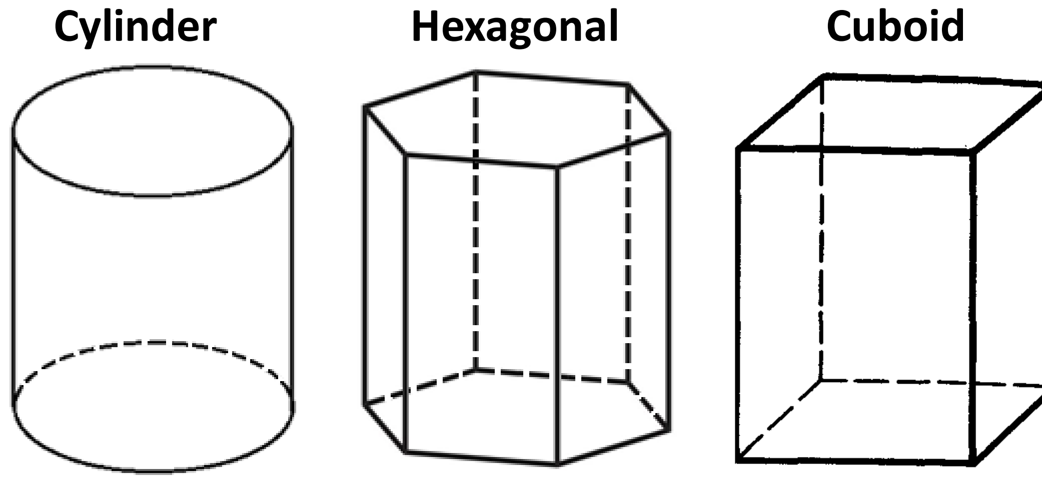

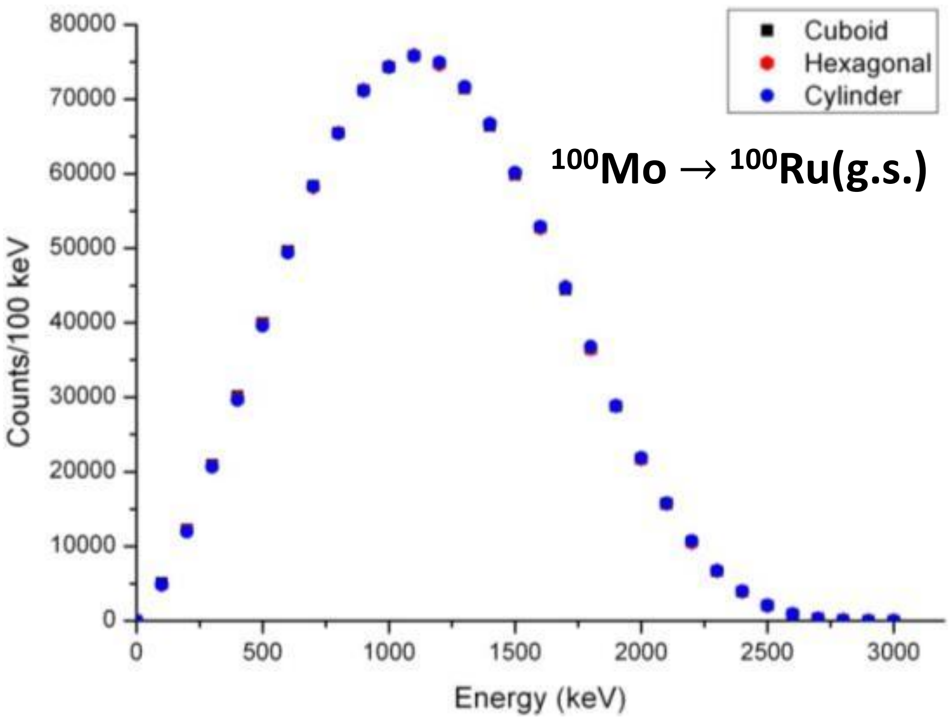

The **mass and height** of the scintillators were fixed with the two sets of values for all of the crystal shapes: **59.2 g, 32.2 mm**; and **495 g, 40 mm**.

Simulation have demonstrated no significant dependence of $2\nu2\beta$ decay processes in $Zn^{100}MoO_4$ scintillators on the crystal detector shape

^{232}Th calibration of $ZnMoO_4$ scintillating bolometer

GOAL: Check if background simulation for future experiment is reasonable

We have simulated response of the $ZnMoO_4$ scintillating bolometers installed in the EDELWEISS set-up to gamma quanta of ^{232}Th source aiming to compare simulated model with experimental spectrum.

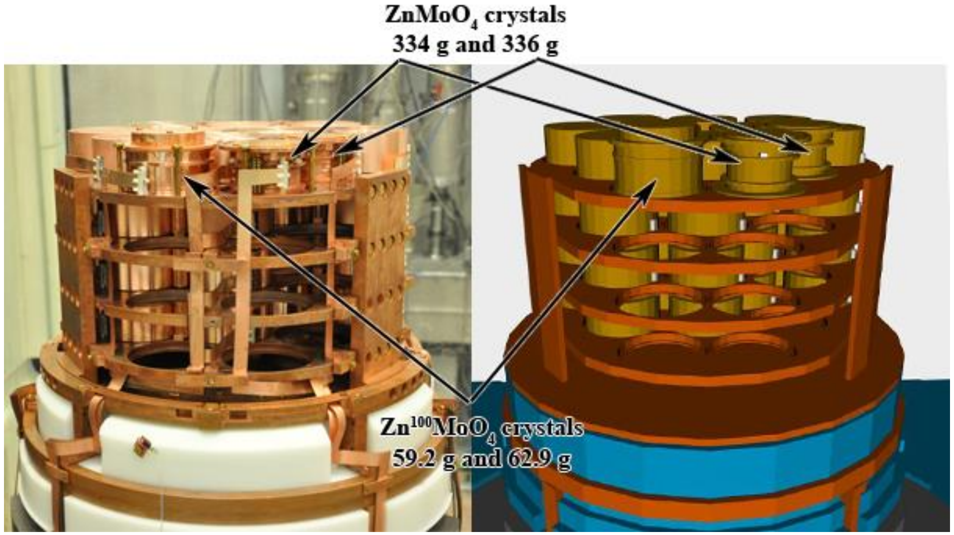

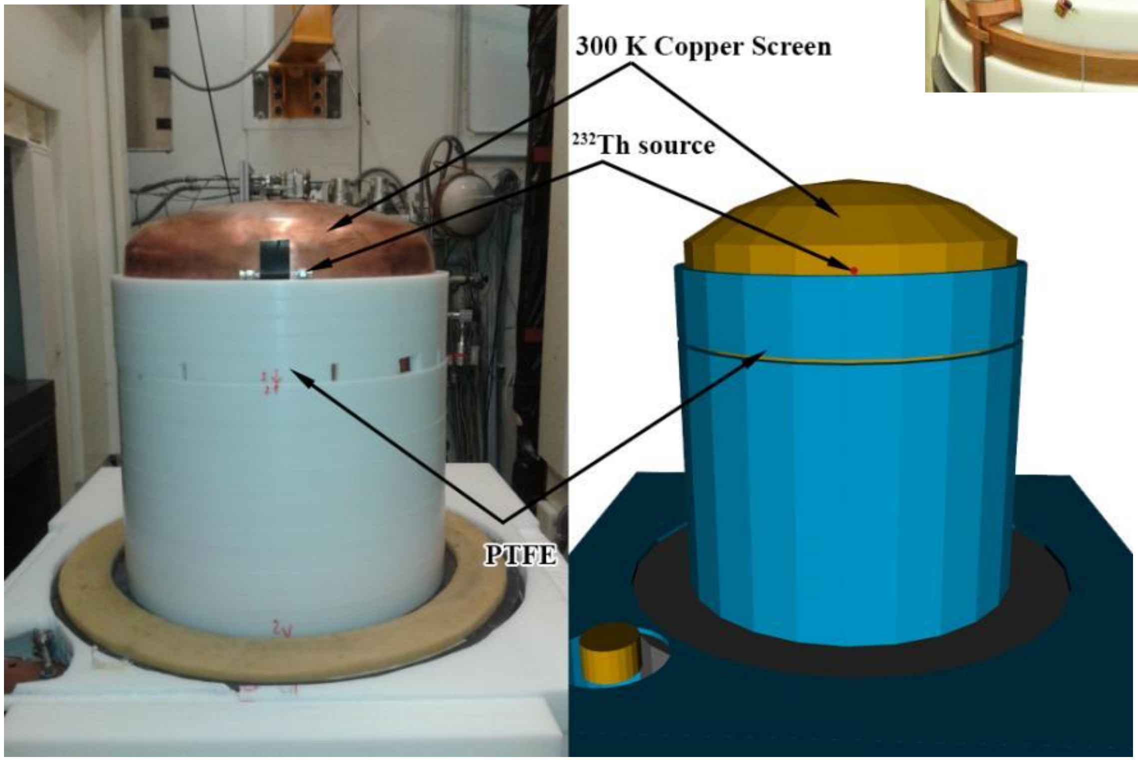

The isotropic ^{232}Th source was made of thoriated tungsten wires (1% of thorium in weight).

The source activity (≈ 600 Bq) was reduced twice by removing one half of wires.

Comparison of ^{232}Th simulated and experimental spectra

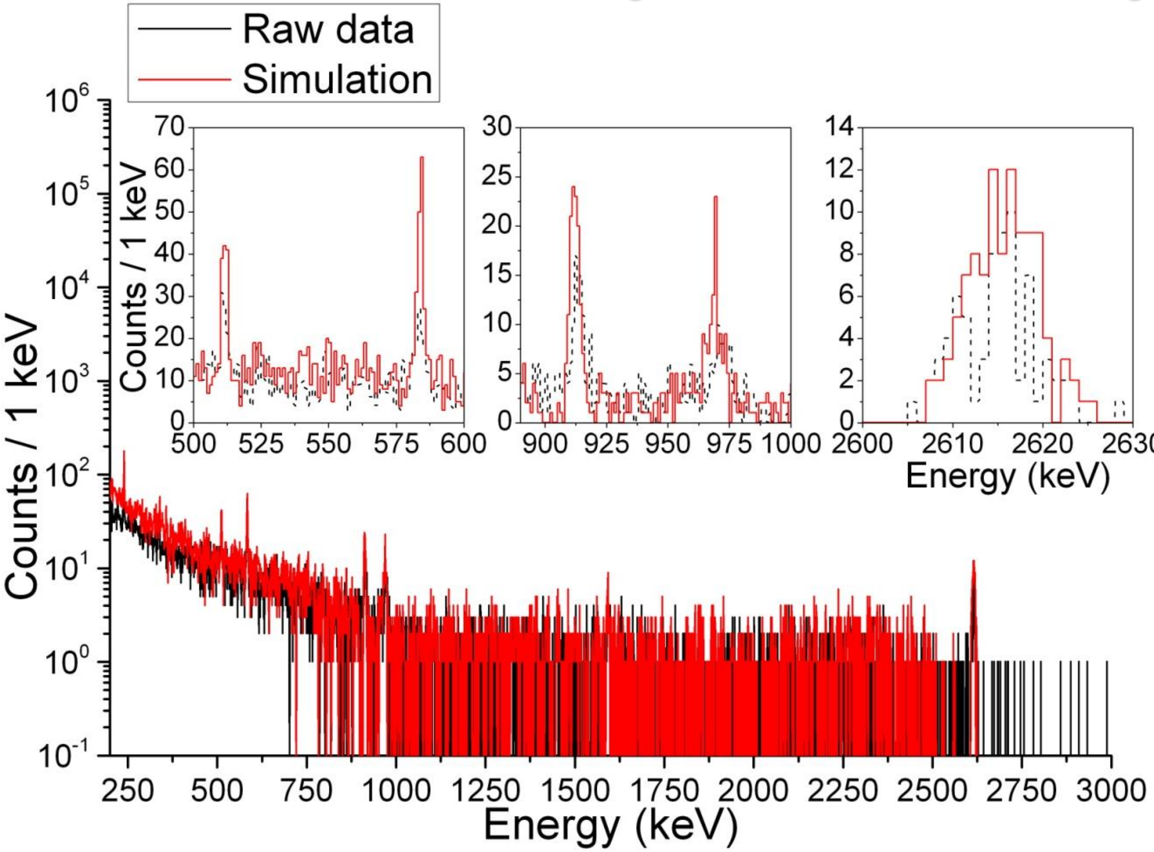

10^7 events of ^{232}Th source were generated by the event generator DECAY0 and used in the GEANT4 simulation.

Simulation reasonably reproduce the experiment

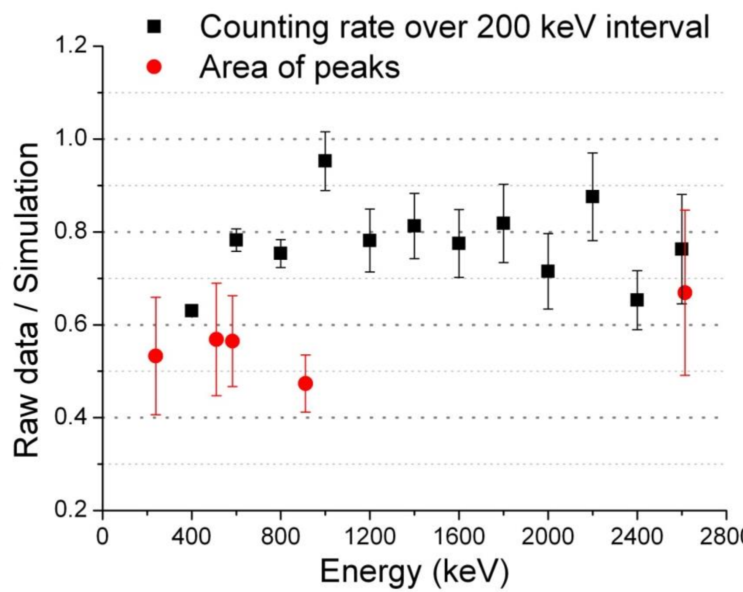

Difference between the simulated and measured data can be related to the **imprecise knowledge of the ^{232}Th source activity and position**, **difficulties to take into account pile-up of events**, and **simplified geometry of the GEANT4 model**.

Simulation of 48 $Zn^{100}MoO_4$ cryogenic scintillating bolometers in the EDELWEISS set-up

1) Internal contamination of $Zn^{100}MoO_4$ crystals by ^{232}Th and ^{226}Ra (bulk and surface contamination)
2) Cosmogenic activation of $Zn^{100}MoO_4$ crystals by ^{56}Co and ^{88}Y
3) 0ν2β of ^{100}Mo
4) Contamination of the set-up by ^{232}Th and ^{226}Ra
5) Cosmogenic activation of copper by ^{56}Co

23.8 kg of $Zn^{100}MoO_4$ crystals
10.2 kg of ^{100}Mo

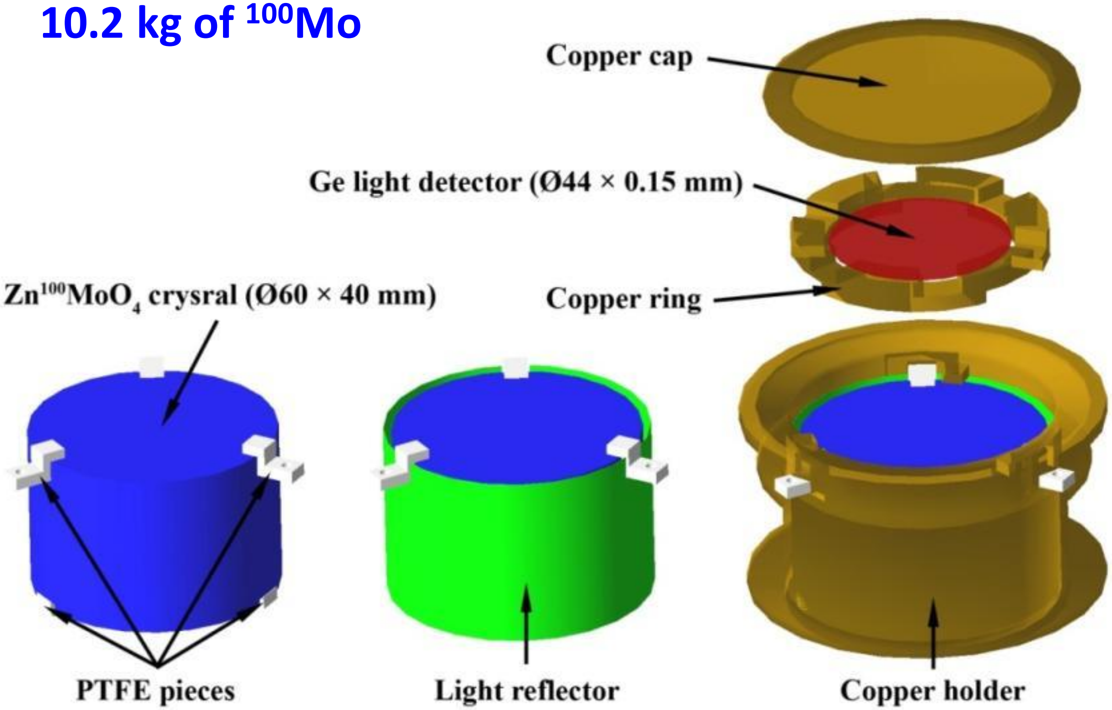

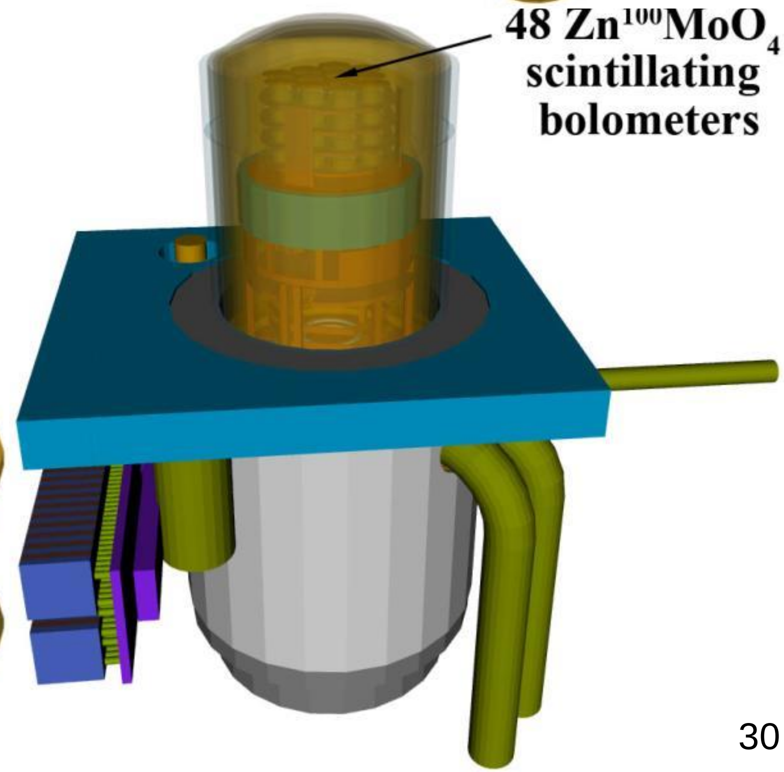

Simulation conditions

- 10^6 events uniformly distributed in material for bulk contamination, 10^5 events exponentially distributed with a mean depth of 5 µm for surface contamination
- 50 keV energy threshold of detectors working in anticoincidences
- Average cosmogenic activity was taken during 5 years of underground measurements, assuming 3 months of activation on the Earth surface and one year of cooling down underground
- 10^3 suppression factor of background from ^{208}Tl by delayed coincidences
- Background from α particles is suppressed by pulse-shape discrimination with efficiency 99.9%

$Zn^{100}MoO_4$ crystal

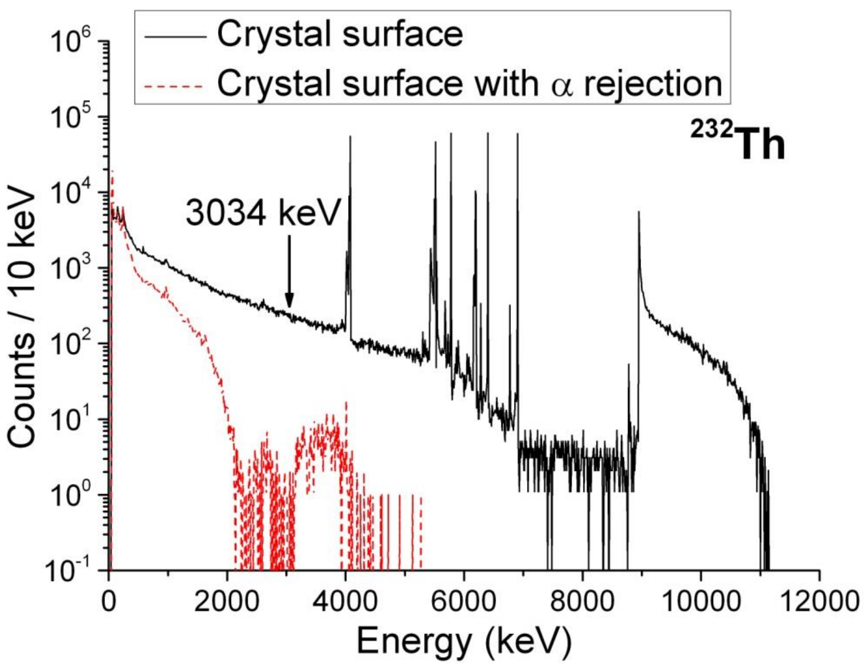

Copper holder

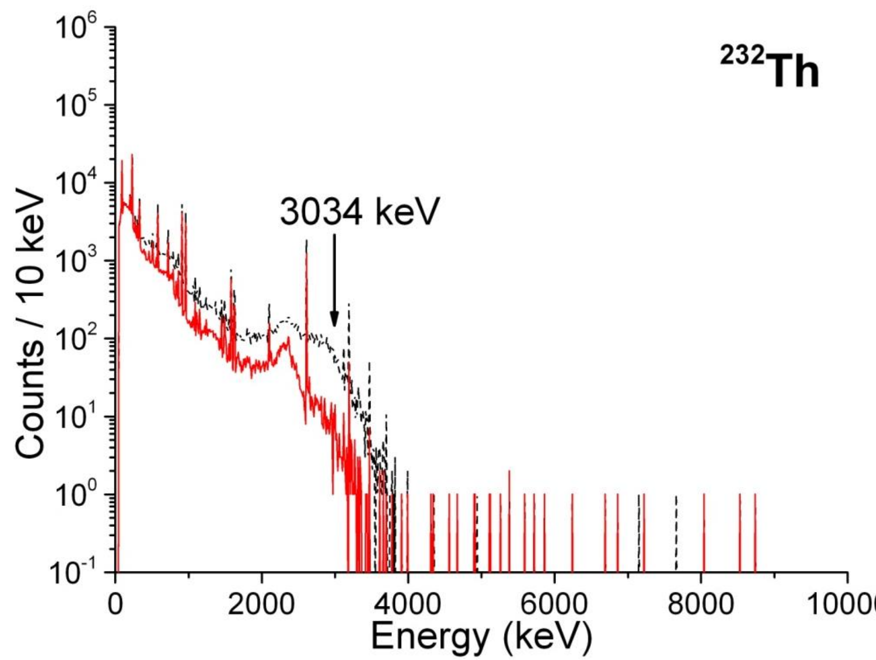

Total background spectra

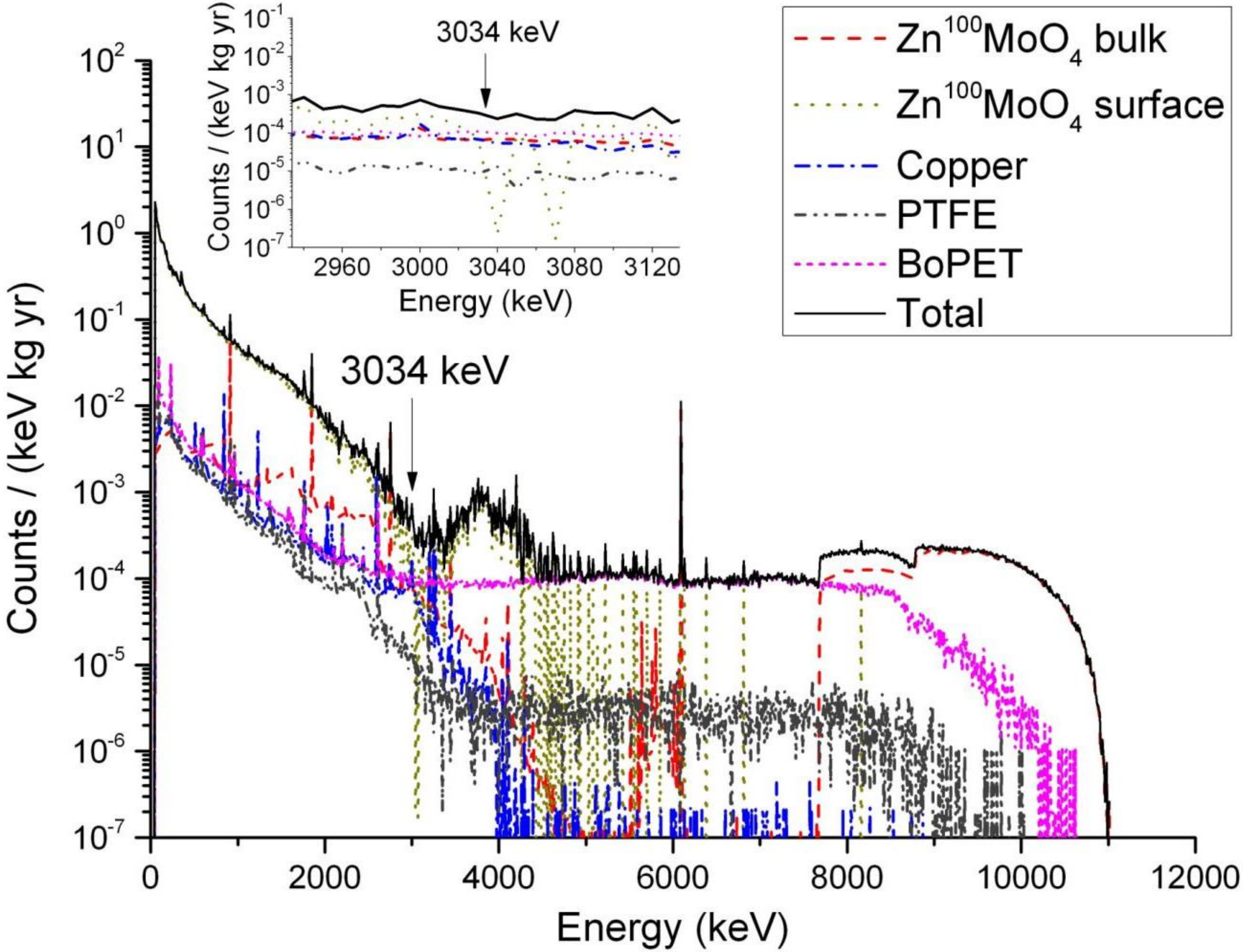

Total background evaluation

Position	Source of background	Activity (μBq/kg)	Background (counts/(keV·kg·yr))
$Zn^{100}MoO_4$ crystal bulk	^{208}Tl	10 (^{232}Th)	8.0×10^{-6}
	^{214}Bi	10	3.1×10^{-8}
	^{212}Bi	10 (^{232}Th)	5.1×10^{-8}
	^{88}Y	0.3	6.3×10^{-7}
	^{56}Co	0.06	6.2×10^{-5}
$Zn^{100}MoO_4$ crystal surface	^{232}Th	0.5	1.2×10^{-5}
	^{238}U	2.4	1.5×10^{-4}
Cu holder	^{232}Th	20	1.3×10^{-6}
	^{214}Bi	70	1.5×10^{-7}
	^{56}Co	0.2	6.6×10^{-5}
PTFE clamps	^{232}Th	100	9.6×10^{-6}
	^{214}Bi	60	7.5×10^{-7}
BoPET reflective foil	^{232}Th	100	7.5×10^{-5}
	^{214}Bi	60	2.1×10^{-5}
Total			4.1×10^{-4}

A **total background** rate in the region of interest is **4.1×10^{-4} counts/(keV·kg·yr)** for $Zn^{100}MoO_4$ crystal scintillators, which corresponds to **2.5 counts/(ton·yr)** in a 6 keV window centered at the 0ν2β peak position.

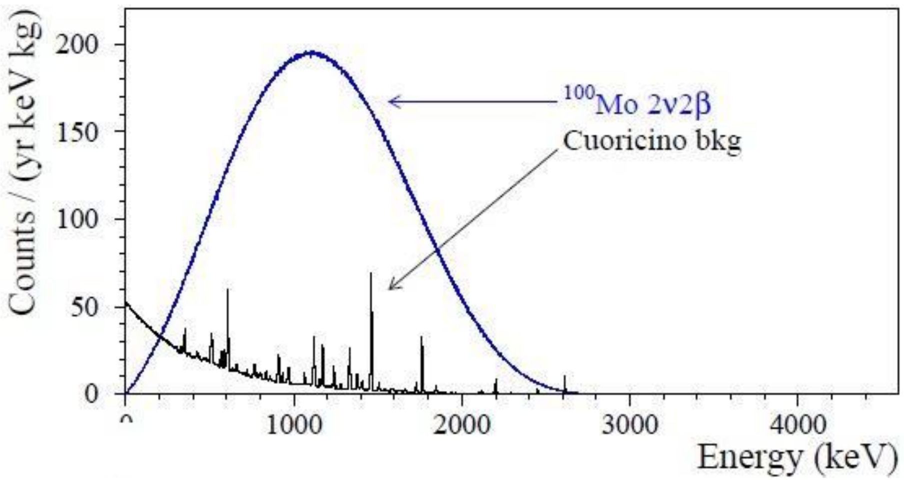

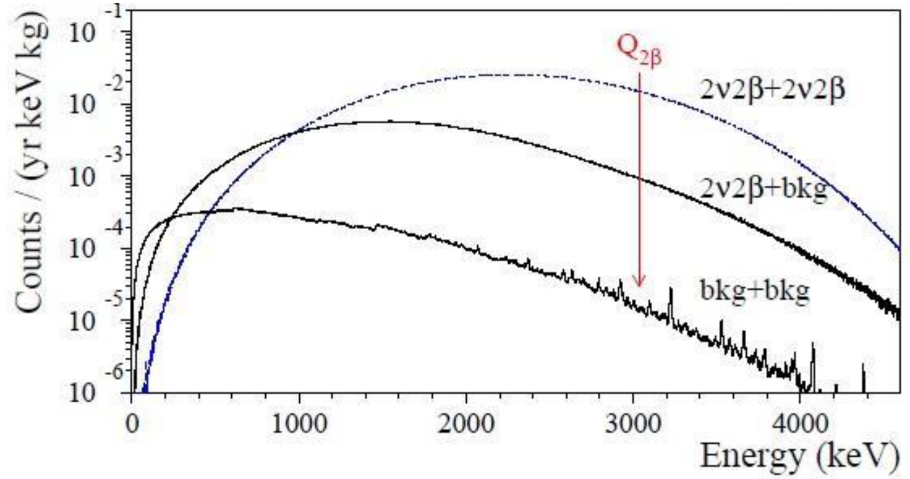

REJECTION OF RANDOMLY COINCIDENT EVENTS IN 0ν2β DECAY EXPERIMENTS WITH $ZnMoO_4$ CRYOGENIC BOLOMETERS

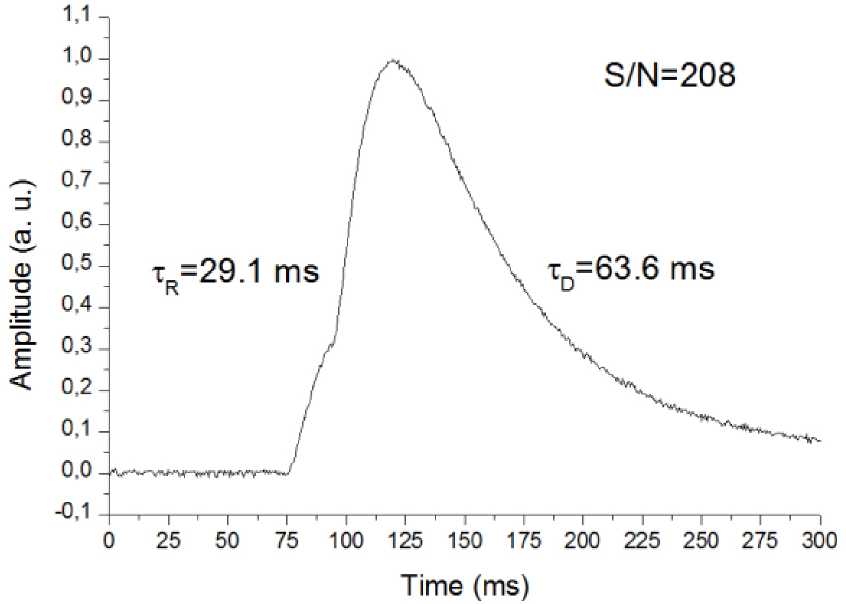

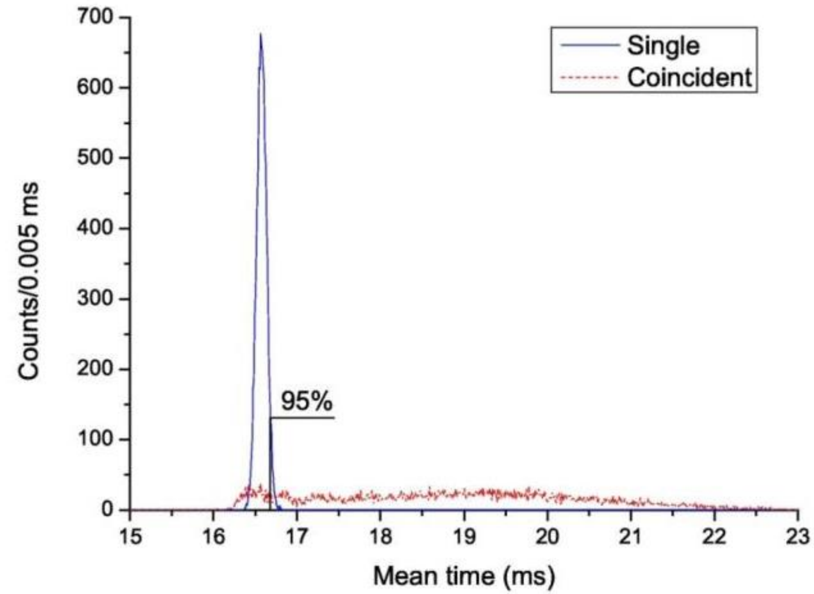

Random coincidence of 2ν2β events

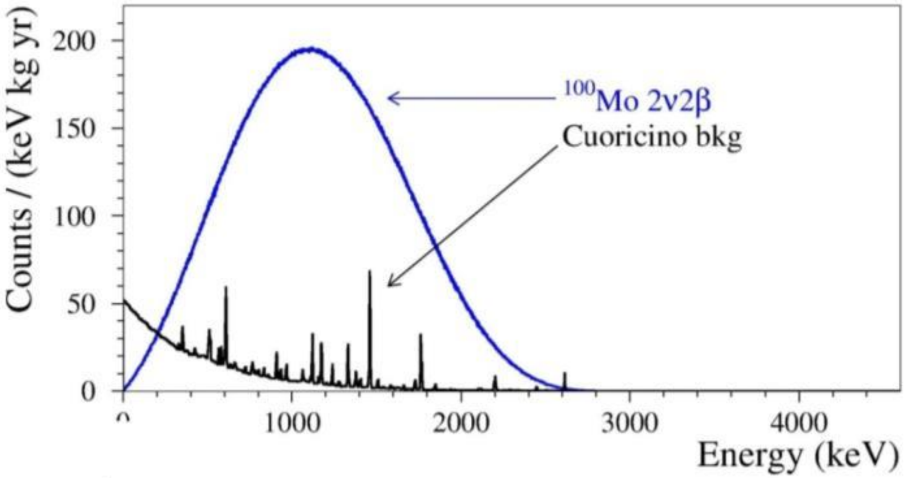

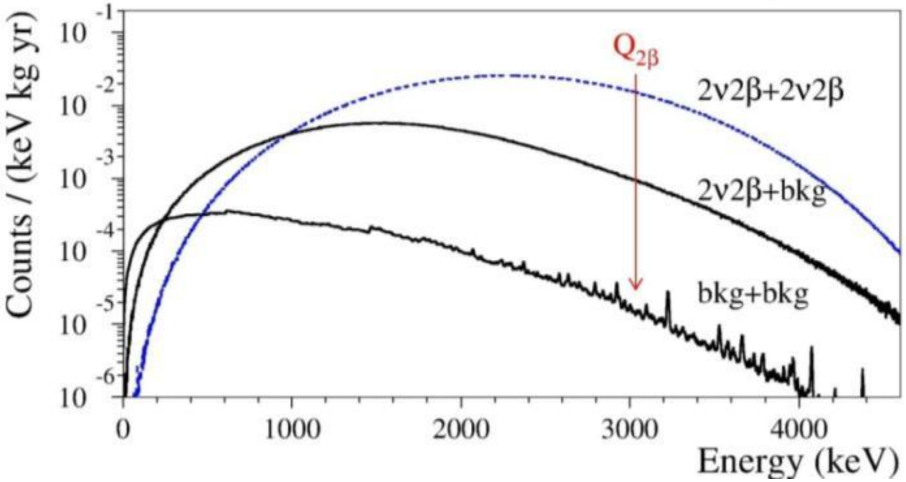

Poor time resolution of scintillating bolometers

Background from random coincidence of 2ν2β events and external gamma quanta

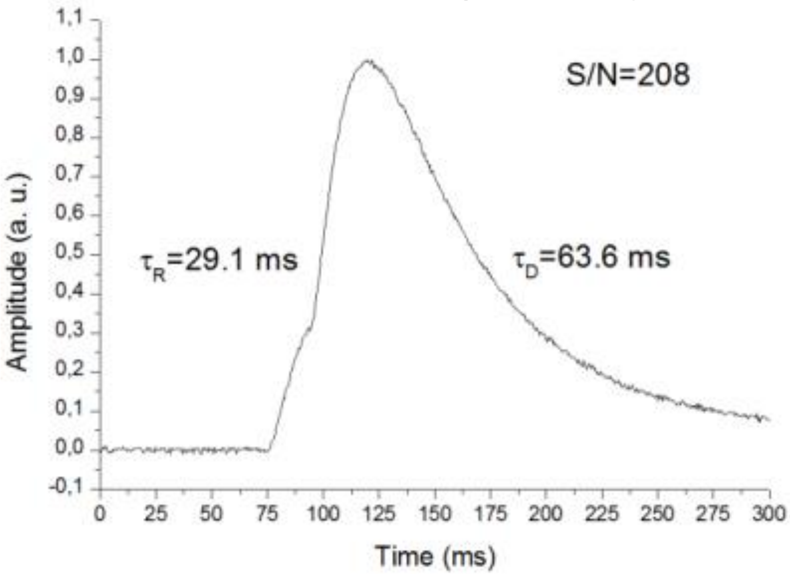

The total counting rate due to the randomly coinciding 2ν2β decay events and external gamma events in the region of interest is estimated as ≈ **0.016 counts/(keV·kg·yr)** for Ø60 × 40 mm $Zn^{100}MoO_4$ cryogenic bolometer with a time resolution 45 ms.

Random coincidence of events could be the main source of background in cryogenic bolometers to search for 0ν2β decay

Pulse profiles for scintillating bolometers

Single and randomly coincident signals were generated by using pulse profiles and noise baselines accumulated with 313 g $ZnMoO_4$ crystal scintillator operated as a cryogenic scintillating bolometer with Ge light detector.

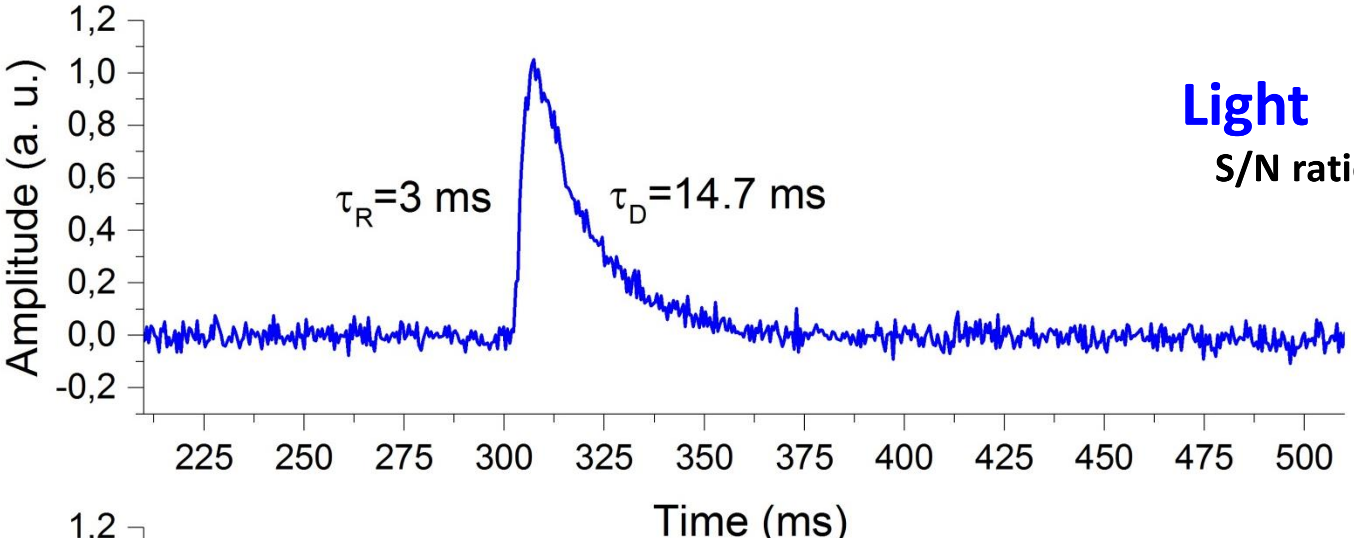

Light

S/N ratio = 30

$$\frac{\mathbf{S}}{\mathbf{N}} = \frac{\mathbf{max(signal)}}{\mathbf{std(noise)}^*}$$

* — standard deviation of noise baseline

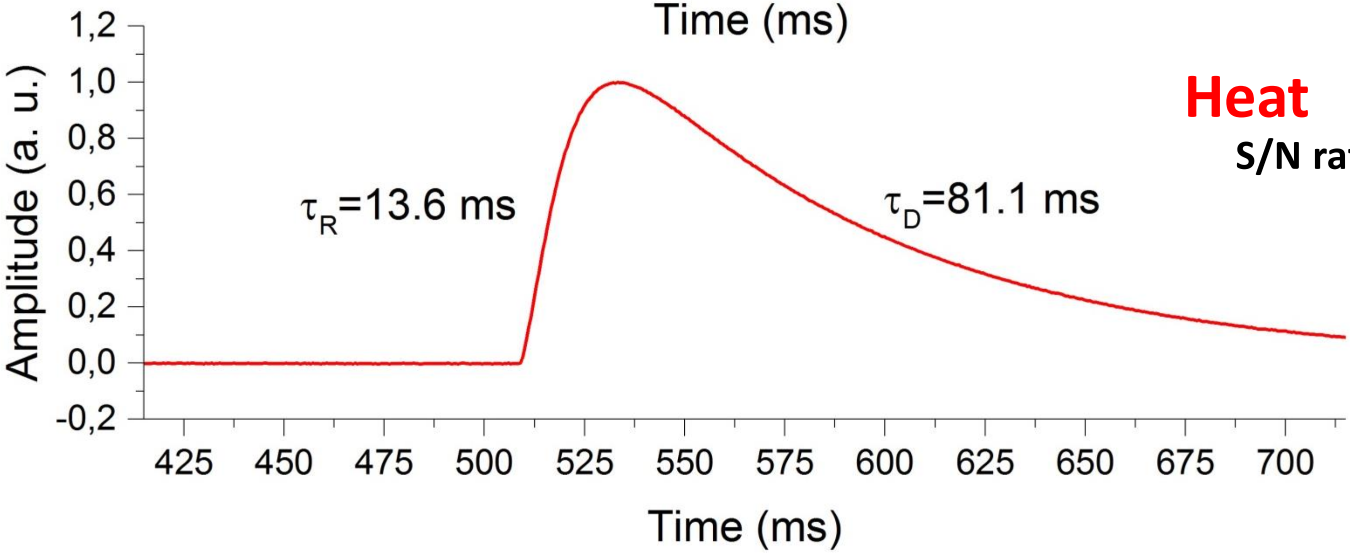

Heat

S/N ratio = 900

Generation of the pulse profiles

Amplitude of the first pulse $\boldsymbol{A_1}$ was obtained by sampling the 2ν2β distribution for ^{100}Mo

Amplitude of the second pulse $\boldsymbol{A_2}$ was chosen so that the total pulse amplitude was $Q_{2\beta}(^{100}\mathrm{Mo}) + \Delta E$, where ΔE is a random component in the energy interval [−5, +5] keV

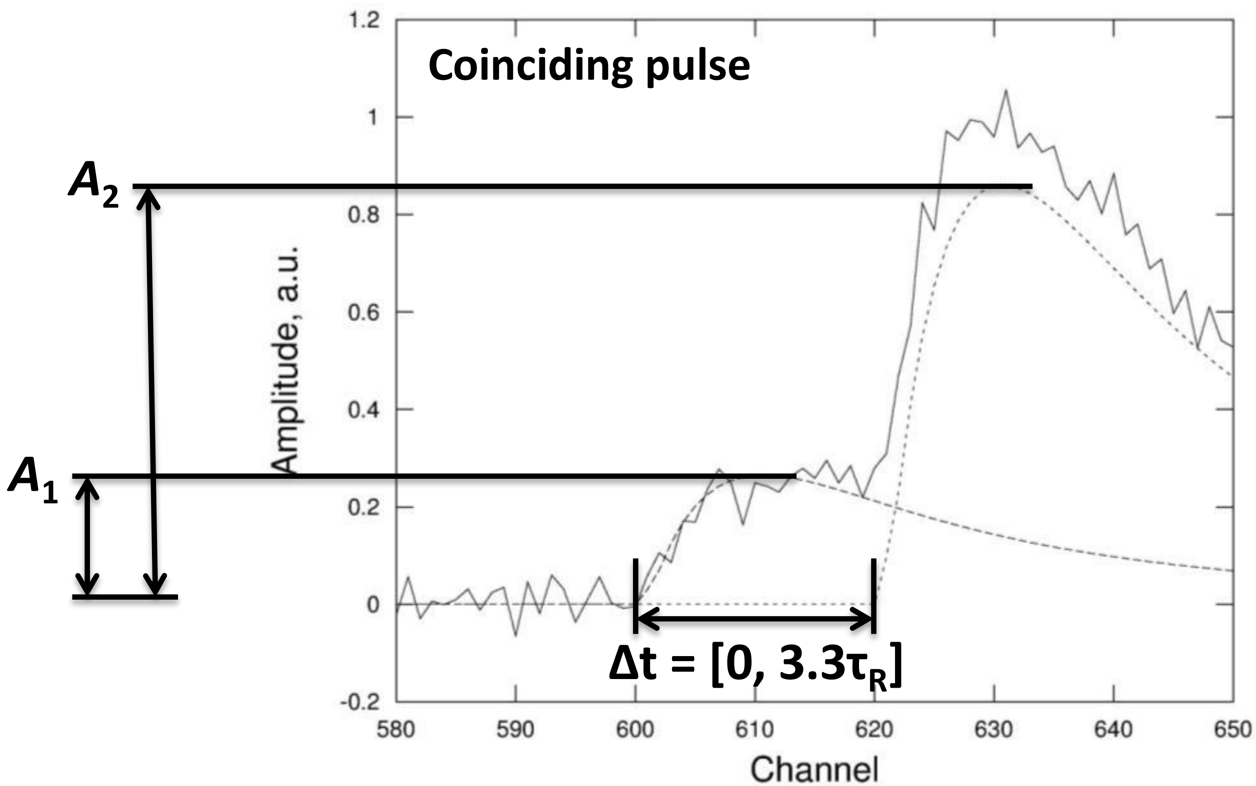

We generated 10000 single and 10000 coinciding pulses

Coinciding signals were randomly generated in the time interval from 0 to $3.3\tau_R$ ($\Delta t = [0, 3.3\tau_R]$), where τ_R is the rise-time of the signals

Reconstruction of the time origin of events

To reconstruct the time origin of each event from our data the following procedure was used:

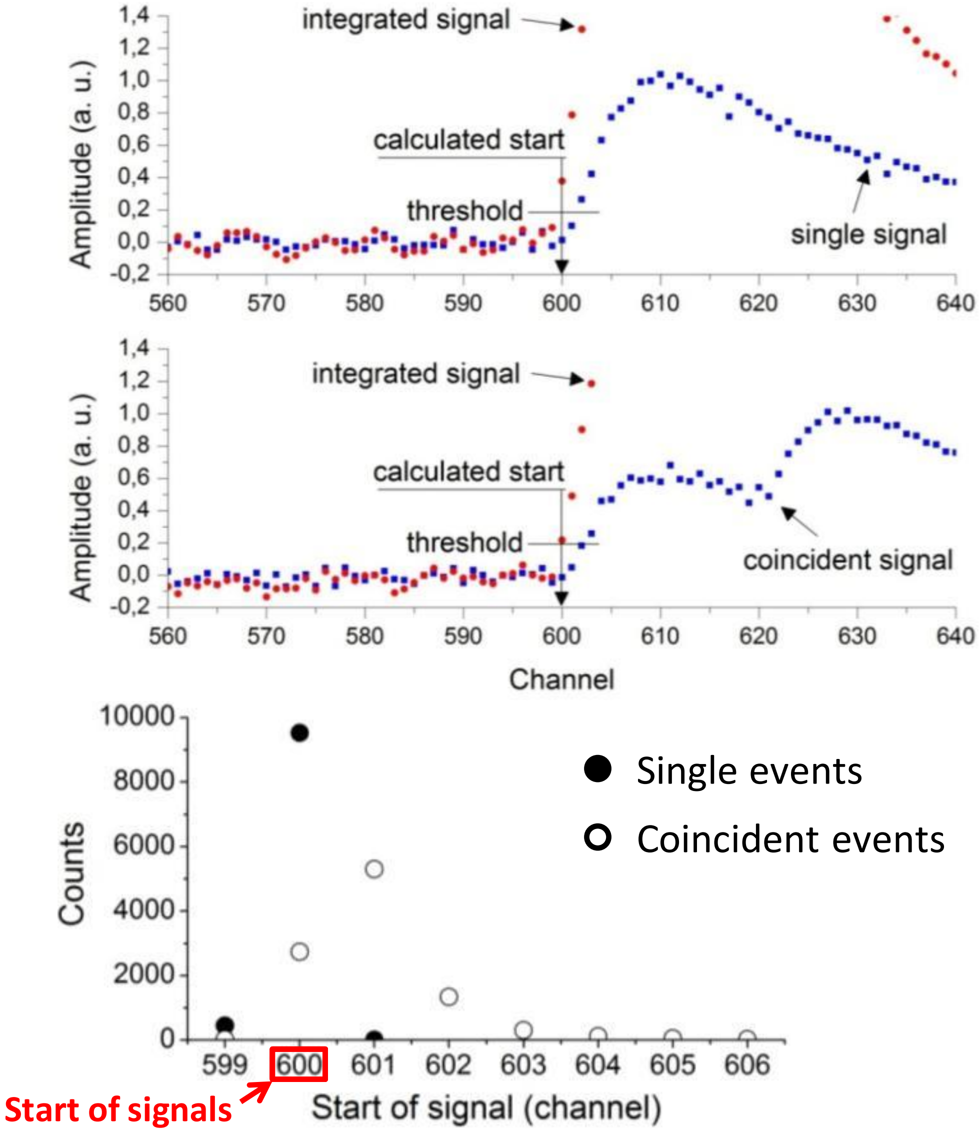

1. Preliminary search for the presence of a signal
2. Summation of the data over a certain number of channels depending on the time structure of signal and noise data
3. Calculation of the standard deviation of the integrated signal baseline fluctuations
4. Search for the pulse start under the request that the signal exceeds the threshold set on a certain number of standard deviations of the baseline

Methods of pulse-shape discrimination

We have applied three techniques to discriminate randomly coincident events:

1) Mean-time

For each pulse $f(t_k)$ we calculate parameter $\langle t \rangle$ (mean-time) with the following formula:

$$\langle t \rangle = \sum f(t_k) t_k / \sum f(t_k),$$

where sum is over time channels k, starting from origin of pulse and up to certain time.

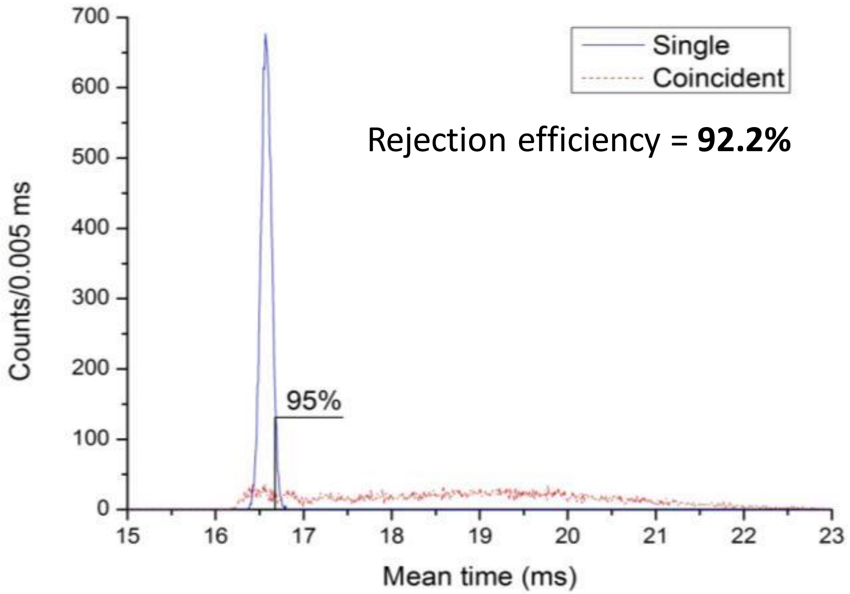

2) χ^2

$$\chi^2 = \sum (f(t_k) - f_S(t_k))^2,$$

where sum is over time channels k, starting from the origin of pulse and up to a certain time, $f_S(t)$ is shape of the reference single signal

3) Front edge analysis

Front edge parameter was defined as time between two points on the pulse front edge with amplitudes Y_1% and Y_2% of the pulse amplitude.

We demanded a 95 % efficiency in accepting single signals

Optimization of pulse-shape discrimination methods

All of the pulse-shape discrimination methods were optimized to find a maximum rejection efficiency.

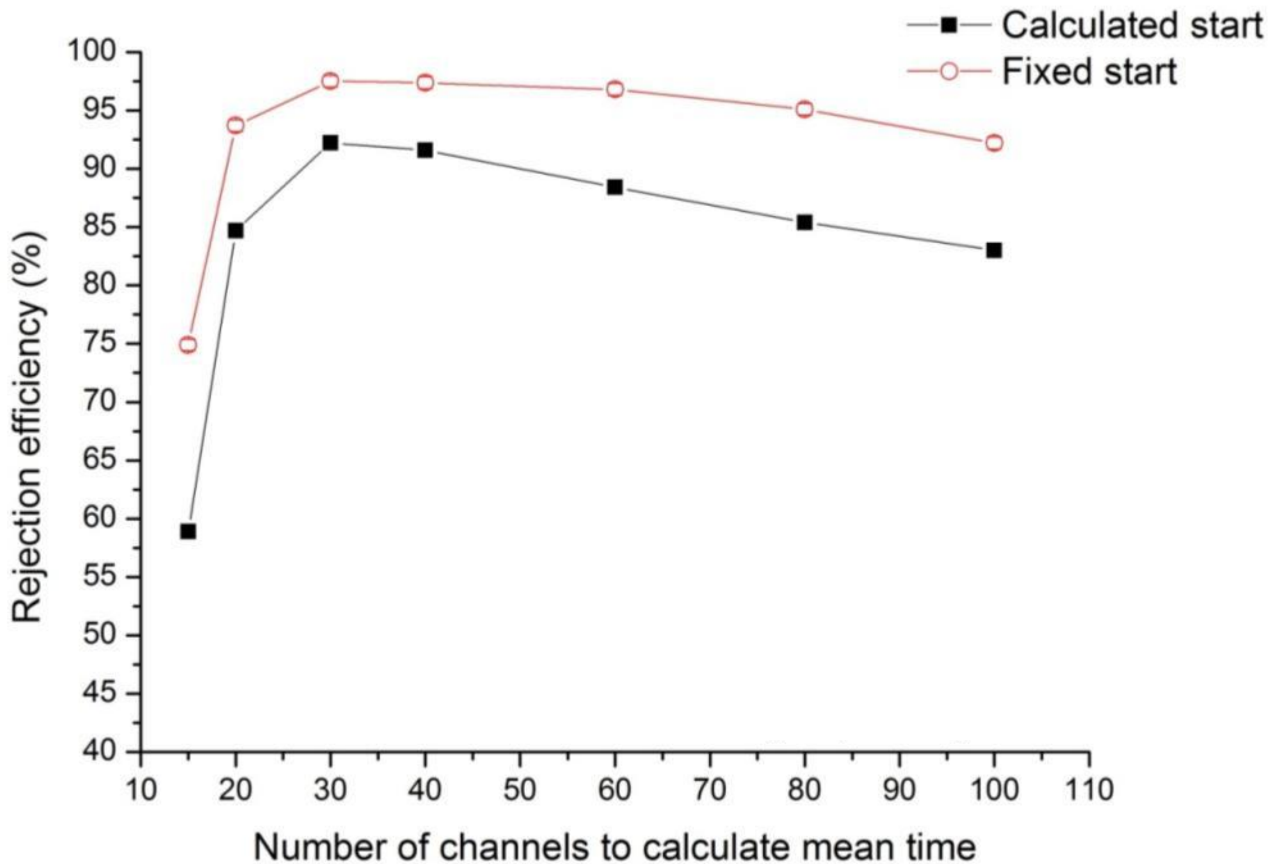

Optimization for mean-time and χ^2 methods was performed by choosing number of channels to calculate parameters mean-time and χ^2 respectively, while for front edge analysis the parameter Y_1 was varied.

Rejection efficiency of randomly coinciding events

The rejection efficiency of the methods was calculated with pulses start positions found by our algorithms, and using the known start positions from the generation procedure.

Channel, rise-time	Start position	Mean-time method, %	Front edge analysis, %	χ^2 method, %
Light, 3 ms	Known	97.5 ± 0.5	96.4 ± 0.5	97.4 ± 0.5
	Found	**92.2 ± 0.5**	**88.1 ± 0.5**	**92.3 ± 0.5**
Heat, 13.6 ms	Known	99.4 ± 0.2	99.4 ± 0.2	99.4 ± 0.2
	Found	**99.3 ± 0.2**	**99.3 ± 0.2**	**99.3 ± 0.2**

All the methods give rejection efficiency 88%–92% for the light signals with a rise-time of 3 ms and signal-to-noise ratio 30, and at the level of 99% for the heat signals with the rise-time of 13.6 ms and the signal-to-noise ratio 900.

Background from random coincidence of events can be reduced to the level of ≈ 10^{-4} counts/(keV·kg·yr) at $Q_{2\beta}$

Dependence of rejection efficiency on signal-to-noise ratio for heat signals

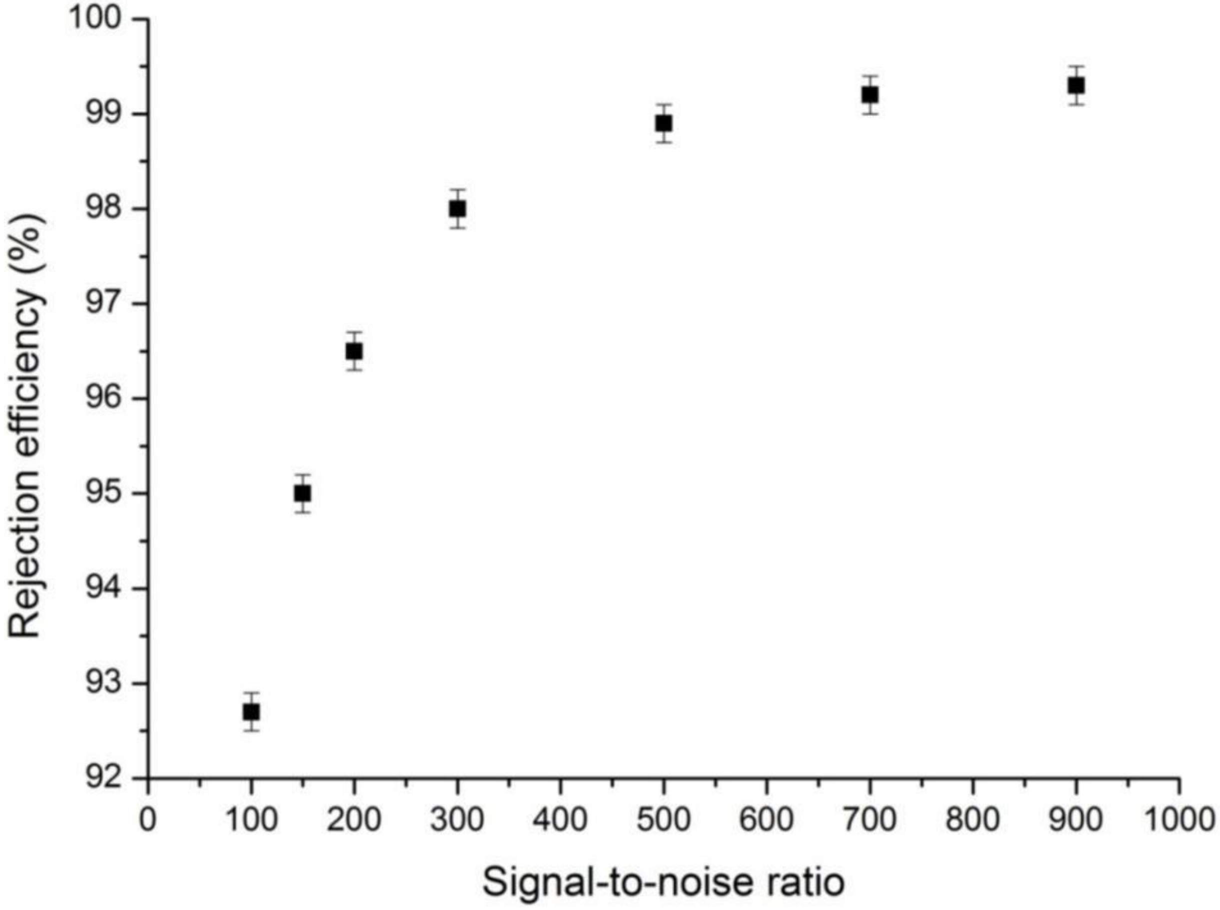

Analysis of slower heat signals with lower level of noise allows to reach a much higher rejection efficiency than that of fast but noisy light signals

Dependence of rejection efficiency on rise-time, signal-to-noise ratio and data acquisition sampling rate

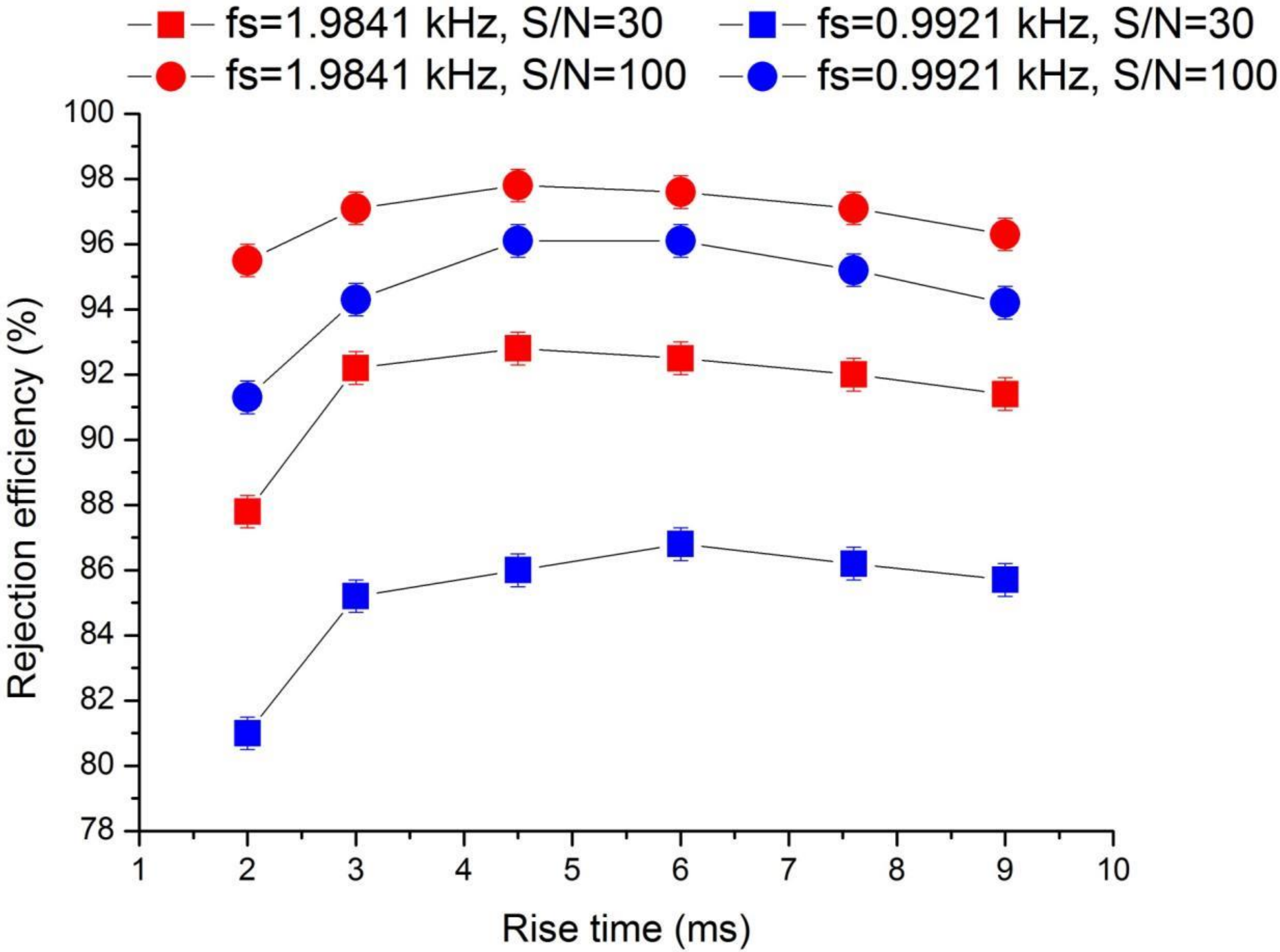

Application of the analysis to the real data

We found 6 coinciding events in the energy interval 2.8–3.2 MeV accumulated with 313 g $ZnMoO_4$ scintillating bolometer operated at the LSM. We also selected 59 single pulses with the energy 2.6 MeV, and 1000 noise baselines from the same run.

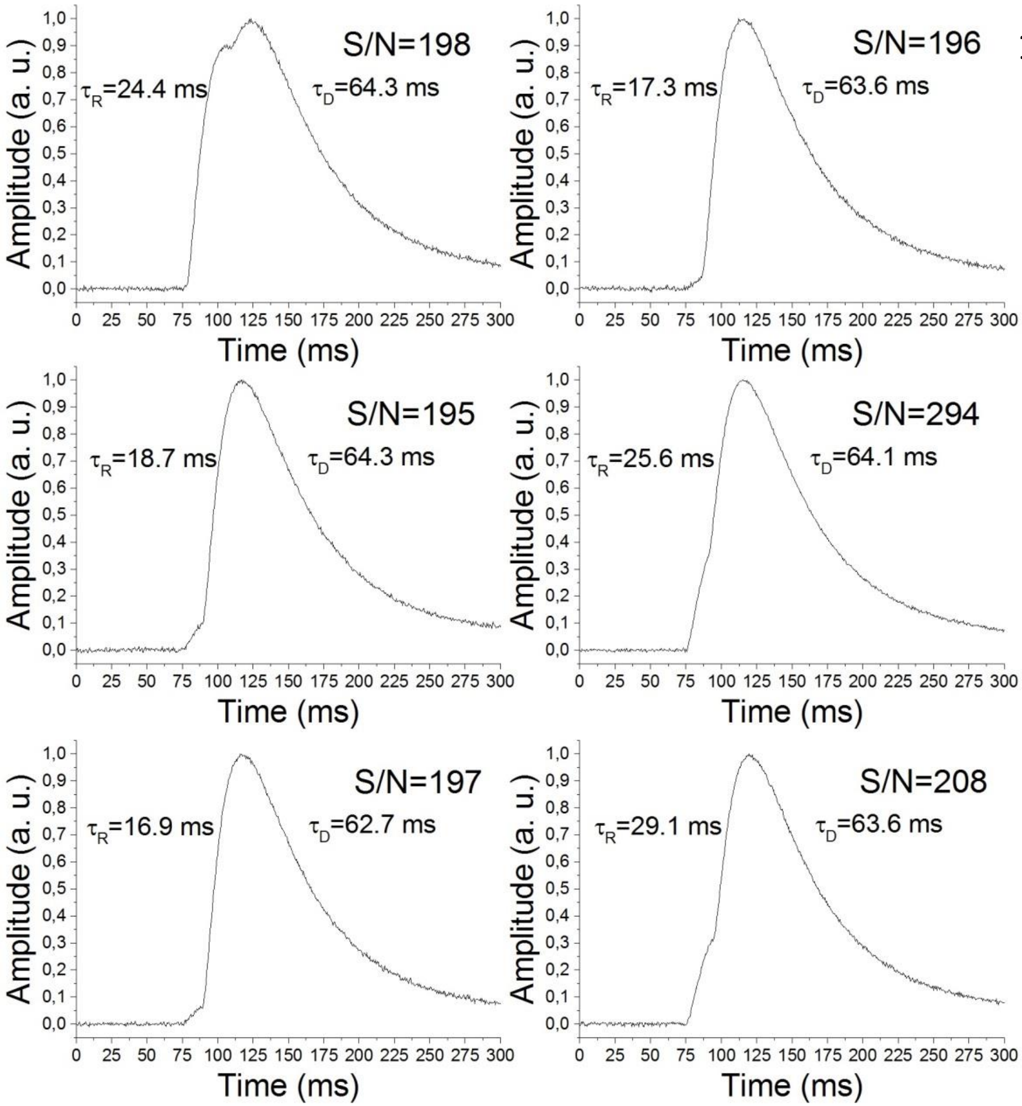

1000 single and 1000 coincident heat pulses were generated to optimize the mean-time method

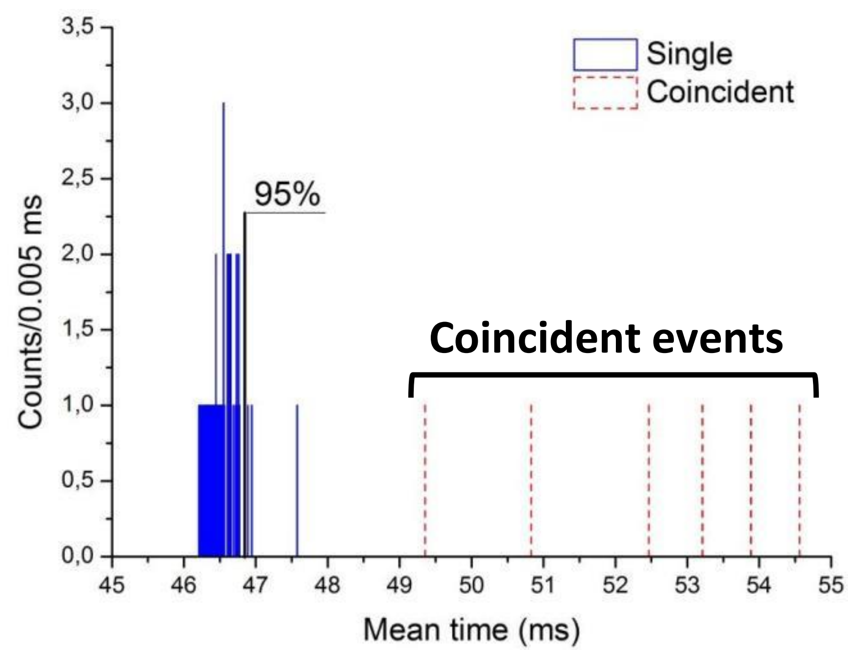

All of the six pile-up pulses selected "by eye" were rejected using the developed algorithm

Conclusions (1)

- The **developed purification method** combined with the **low-thermal-gradient Czochralski technique** gave a **significant improvement of zinc molybdate crystals quality, high crystal yield (≈80%)** and **low irrecoverable losses of ^{100}Mo (≈4%). The optical and luminescence properties of the produced $ZnMoO_4$ crystals confirmed improved quality of the detectors**. Finally, **large volume (~1.4 kg) $Zn^{100}MoO_4$ crystal boule enriched in ^{100}Mo was produced recently**.

- **Low-temperature aboveground and underground measurements with the natural and enriched zinc molybdate crystals demonstrated their excellent characteristics.** The **radioactive contamination of $ZnMoO_4$ crystals by ^{228}Th and ^{226}Ra is on the level of < 0.005 mBq/kg**.

- **Simulation of the light collection from $ZnMoO_4$ crystals has shown the advantages of hexagonal (octahedral) crystal shape with diffused surface** in comparison to polished cylindrical scintillators.

- Monte Carlo **simulation of 2ν2β decay processes in $Zn^{100}MoO_4$ crystals of different shape** (cylinder, hexagonal and cuboid) **demonstrated no significant dependence of 2ν2β decay distributions from the crystal shape**.

Conclusions (2)

- Monte Carlo **simulation of 48 $Zn^{100}MoO_4$ scintillating bolometers (Ø60 × 40 mm) in the EDELWEISS set-up was performed**. The contamination of $Zn^{100}MoO_4$ crystal and nearest materials by ^{238}U and ^{232}Th daughters, and cosmogenic activation by ^{56}Co and ^{88}Y were simulated. A **total background rate in the region of interest is 4.1 × 10^{-4} counts/(keV·kg·yr)**.

- **Random coincidence of events in cryogenic bolometers could be the main source of background** due to the poor time resolution. The **developed pulse-shape discrimination methods allow to reduce the background from ≈ 0.02 counts/(keV·kg·yr) to the level of ≈ 10^{-4} counts/(keV·kg·yr) at $Q_{2\beta}$**.

- **Total background rate of $Zn^{100}MoO_4$ scintillating bolometers is estimated as ≈ 5 × 10^{-4} counts/(keV·kg·yr) at $Q_{2\beta}$**, including ≈ 4 × 10^{-4} counts/(keV·kg·yr) from radioactive sources and ≈ 10^{-4} counts/(keV·kg·yr) from random coincidence of events.

- The current progress on the zinc molybdate crystal production, the low-temperature bolometric tests and Monte Carlo simulation shows that **$Zn^{100}MoO_4$ scintillating bolometers are excellent candidates for the next-generation large-scale experiment to search for 0ν2β of ^{100}Mo to explore the inverted hierarchy region of neutrino mass pattern.**

Search for double beta decay of ^{116}Cd with enriched $^{116}CdWO_4$ crystal scintillators (Aurora experiment)

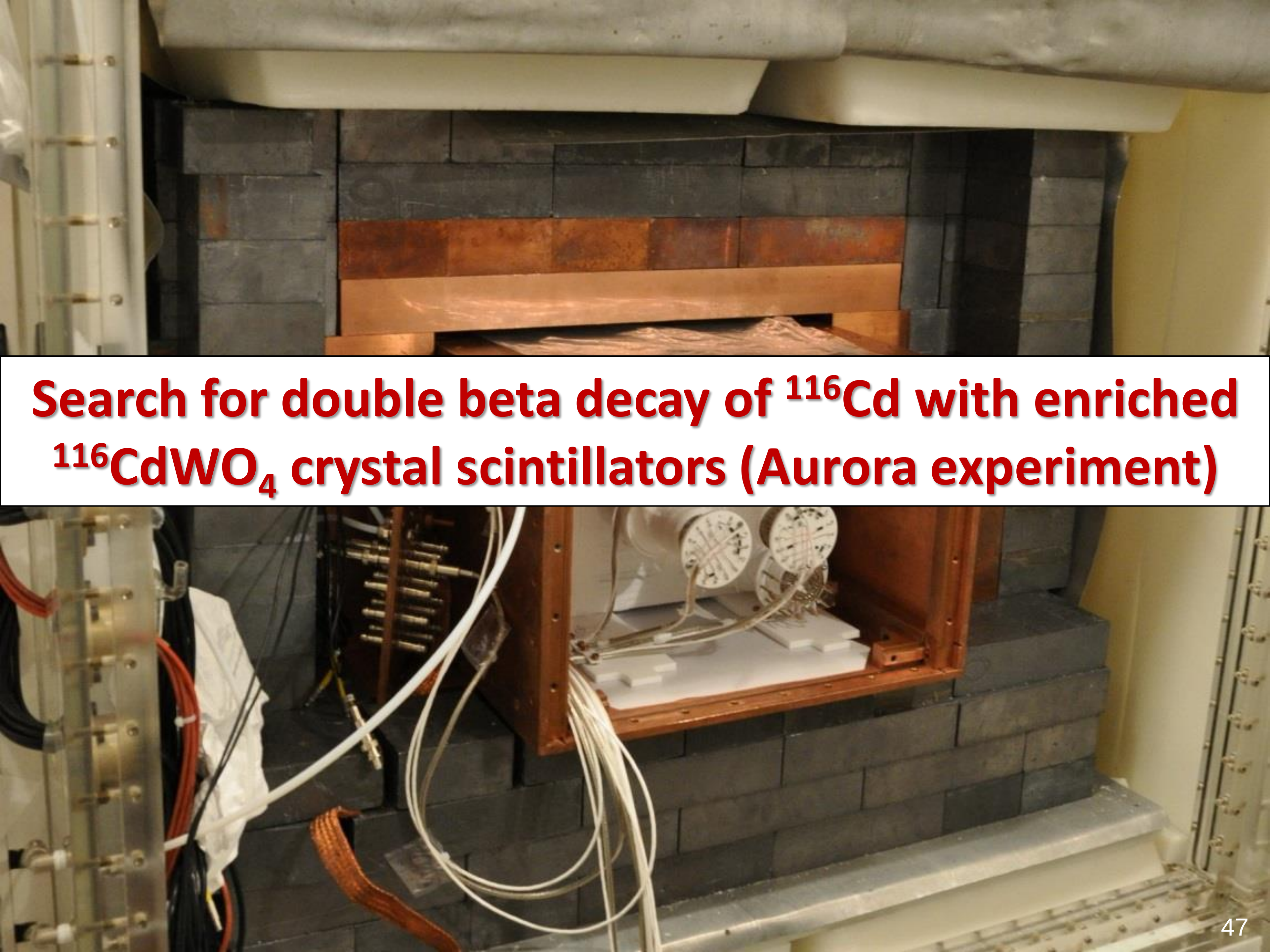

2β decay of ^{116}Cd

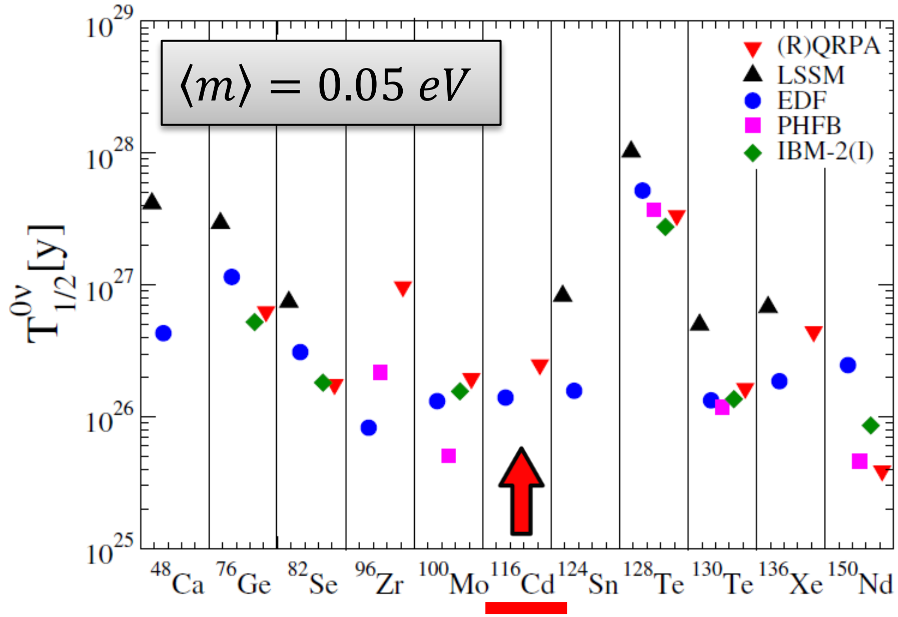

J.D.Vergados, H.Ejiri, F.Simkovic, Rep. Prog. Phys. 75 (2012) 106301

- **Large transition energy :**
  $Q_{2\beta}$ = 2813.44(13) keV
- **Considerable natural isotopic abundance δ = 7.49(18)% and possibility of enrichment by centrifugation**
- **Favorable theoretical estimations of the decay probability**

$CdWO_4$ crystals

- good scintillation properties
- source = detector approach
- low levels of internal contamination
- particle discrimination ability (↓ background)

$CdWO_4$ were successfully used in low-background experiments to search for 2β decay of Cd and W [1], as well as for the study of rare α [2] and β [3] decays

[1] ZPA 355(1996)433, PRC 68(2003)035501, EPJA 36(2008)167;
[2] PRC 67(2003)014310;
[3] PAN 59(1996)1, PRC 76(2007)064603

$^{116}CdWO_4$ crystal scintillators

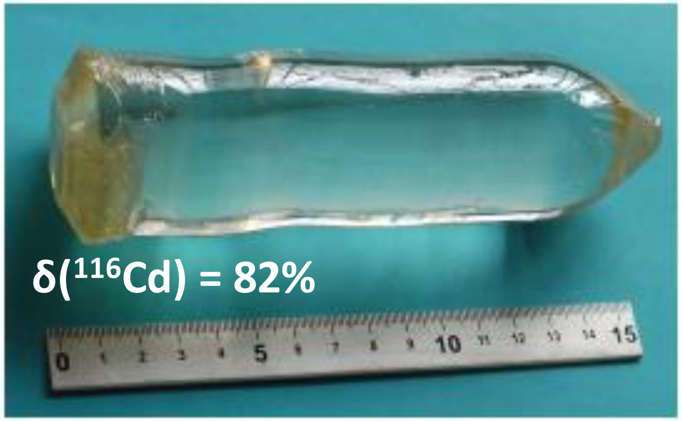

2011
$^{116}CdWO_4$
crystal boule
1868 g

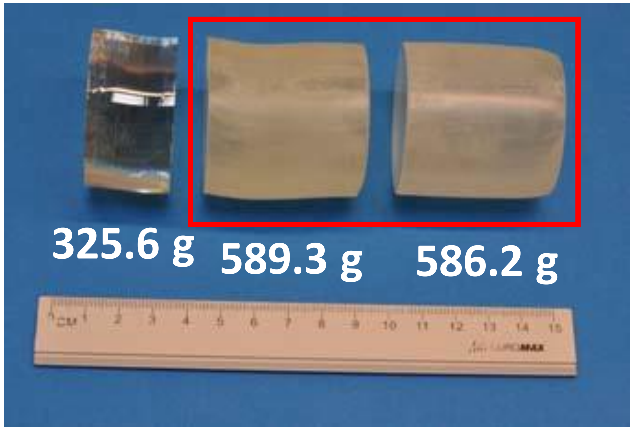

High crystal yield (87%) and low irrecoverable loses of ^{116}Cd (≈ 2%)

Excellent optical and scintillation properties of the crystal were obtained thanks to the **deep purification of ^{116}Cd and W**, and the advantage of the **low-thermal-gradient Czochralski technique** to grow the crystal [1]

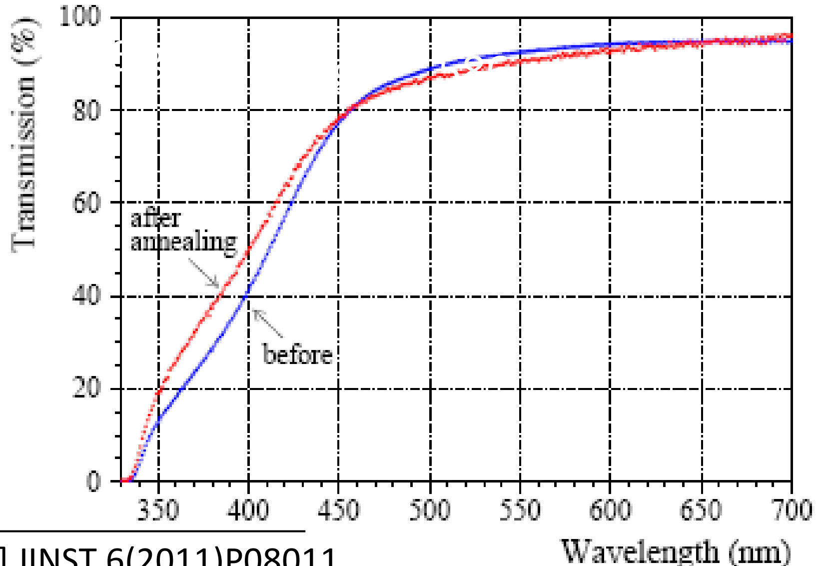

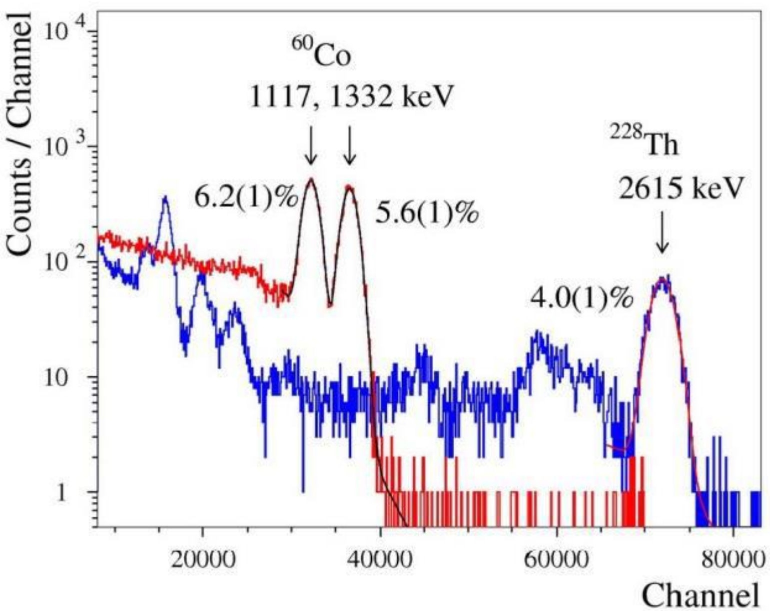

[1] JINST 6(2011)P08011

$^{116}CdWO_4$ scintillation detector

Constructed in 2011

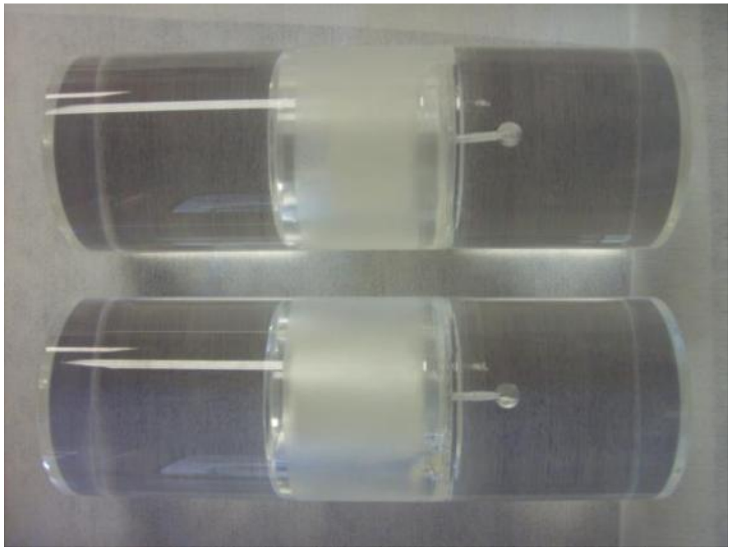

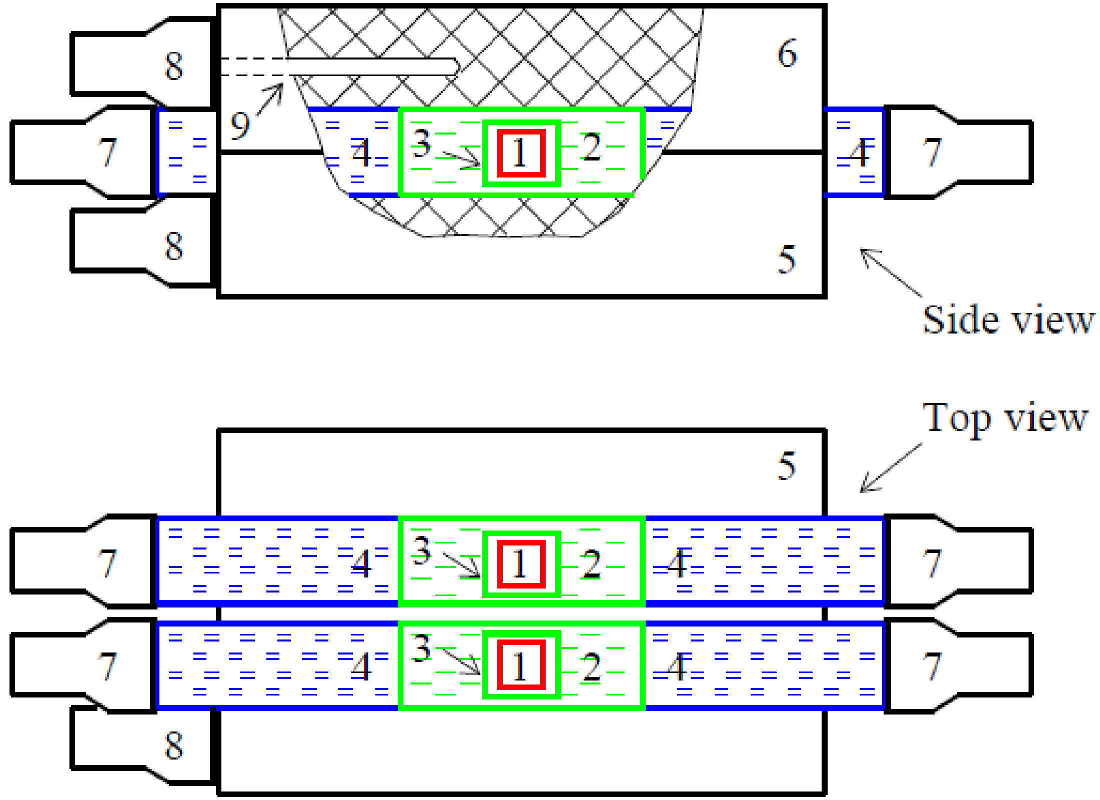

(1) $^{116}CdWO_4$ crystals, **(2)** plastic light-guides, **(3)** cavities in the light-guides filled by liquid scintillator, **(4)** quartz light guides, **(5, 6)** plastic scintillators, **(7)** four PMTs Hamamatsu R6233MOD, **(8)** two PMTs ETL 9302FLA, **(9)** calibration channel in the plastic scintillator 6.

$^{116}CdWO_4$ scintillation detector

The detector was several times upgraded

($^{116}CdWO_4$ crystals were annealed; reflective foils were changed; different liquid scintillators were used; plastic veto was removed; additional Cu shield was added; one PMT for each detector was removed; two quartz light-guides were glued together for each detector...)

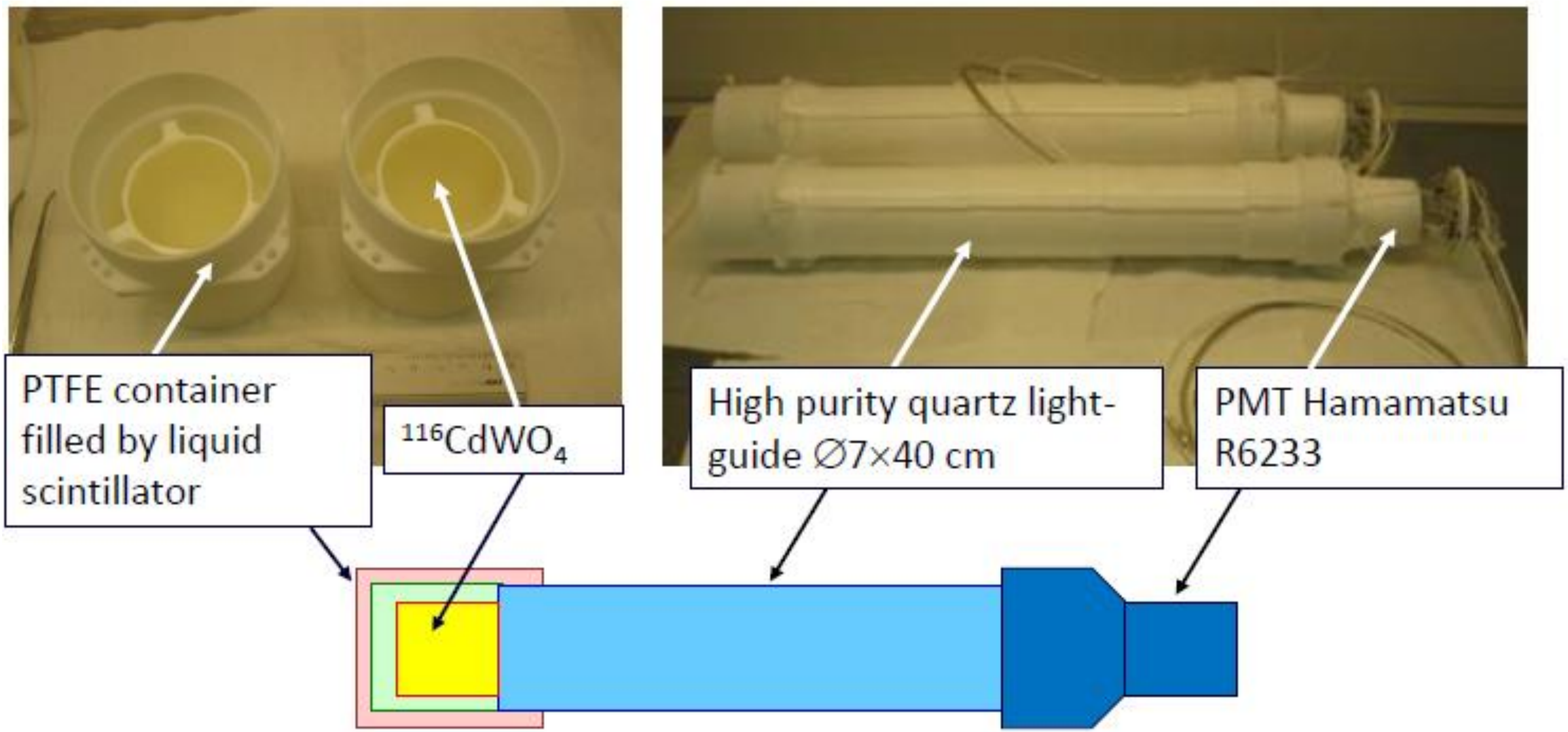

FWHM ≈ 5% at 2615 keV

Low background DAMA R&D set-up at LNGS

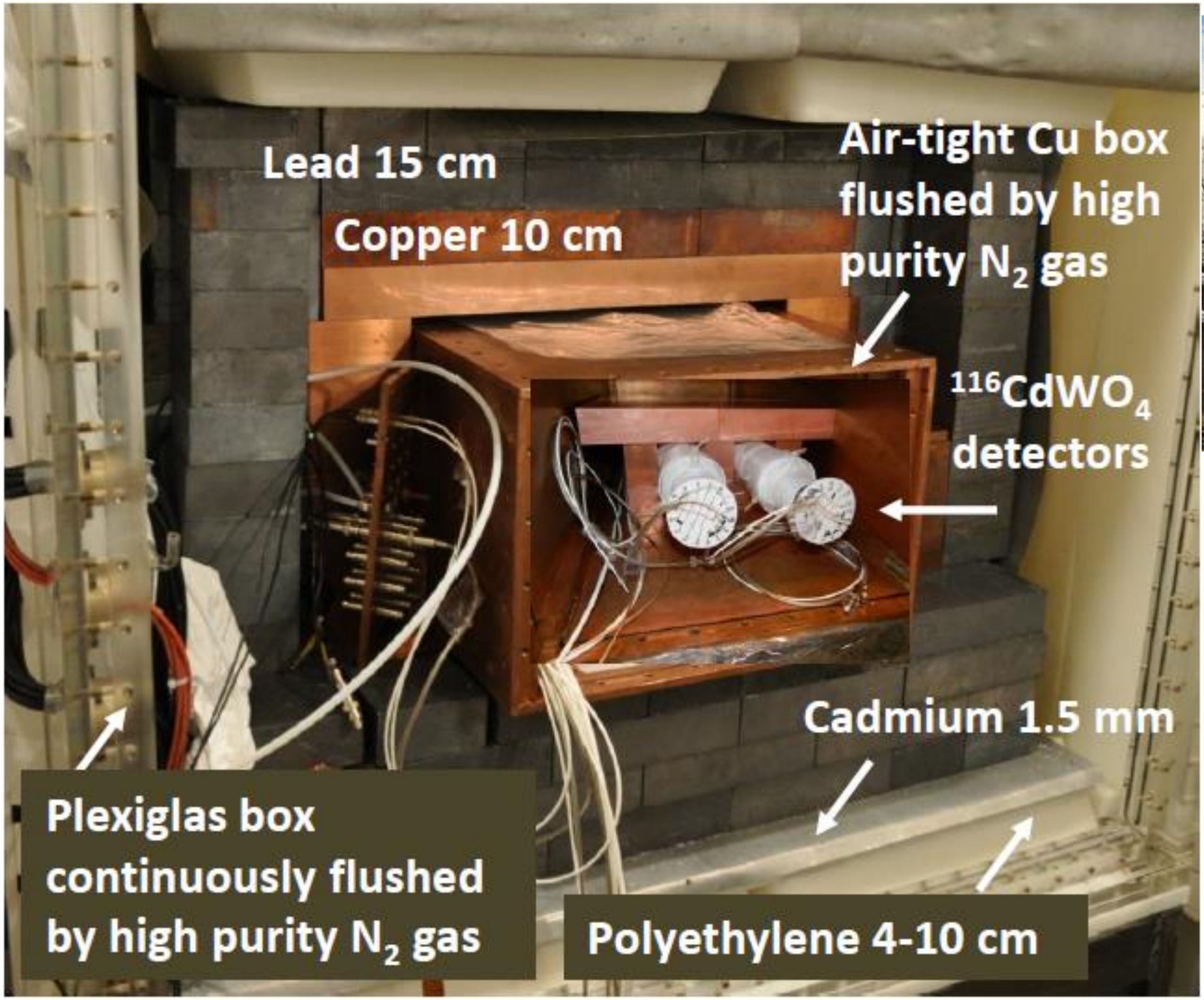

An event-by-event data acquisition system based on a 1 GS/s 8 bit transient digitizer (operated at 50 MS/s) records the time of each event and the pulse shape over a time window of ≈ 100 μs from the $^{116}CdWO_4$ detectors

The **background rate** in the region of interest 2.7 − 2.9 MeV (after pulse-shape discrimination) is on the level of **≈ 0.1 counts/(keV kg yr)**

Pulse-shape discrimination

The background exposure:
(12015 h × 1.162 kg)

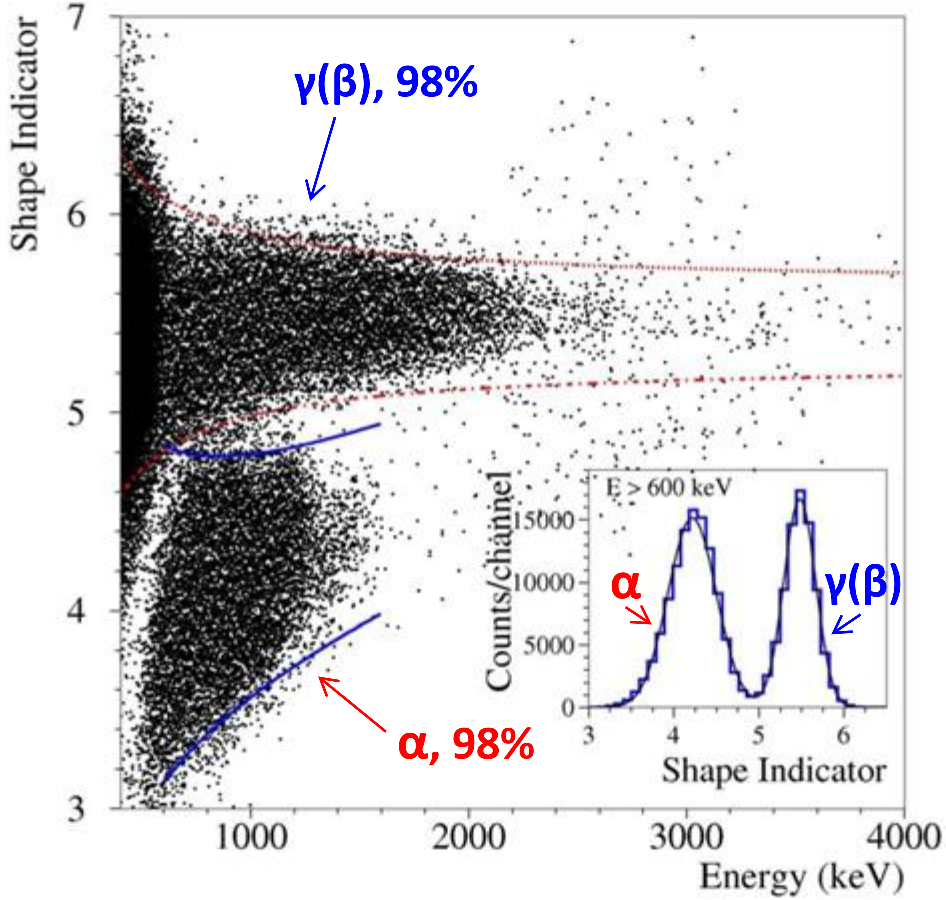

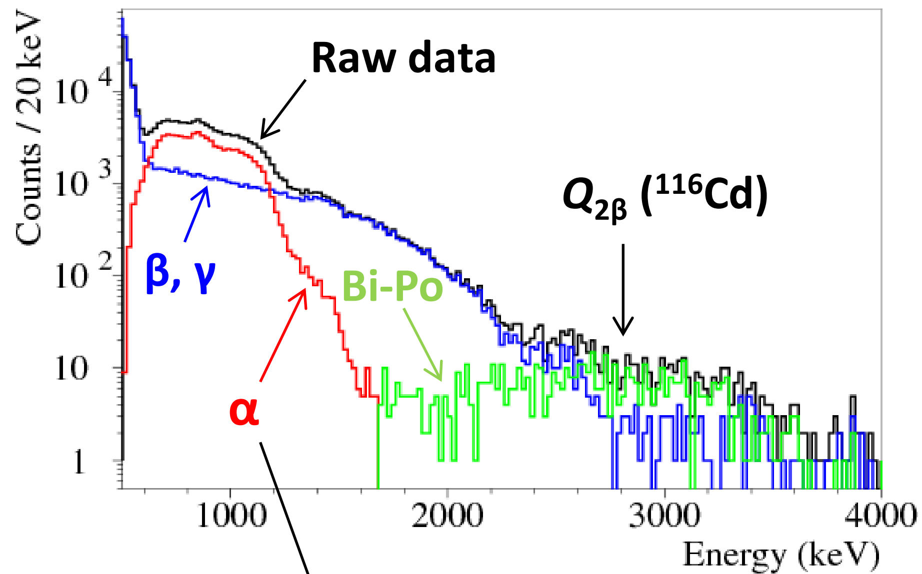

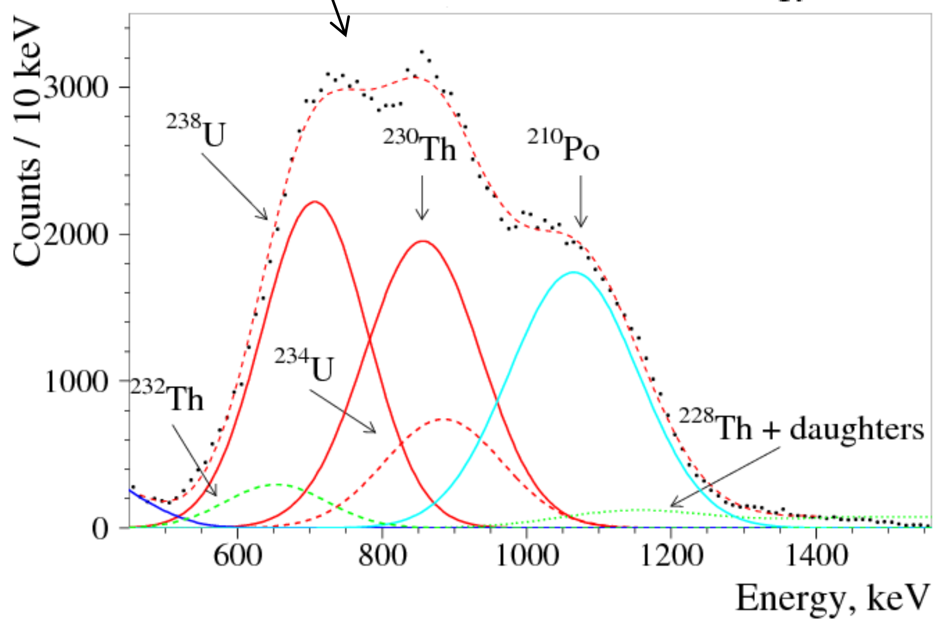

Activity of **^{238}U: 0.63(2) mBq/kg**
^{210}Po: 0.57(3) mBq/kg

Front edge and time-amplitude analyses

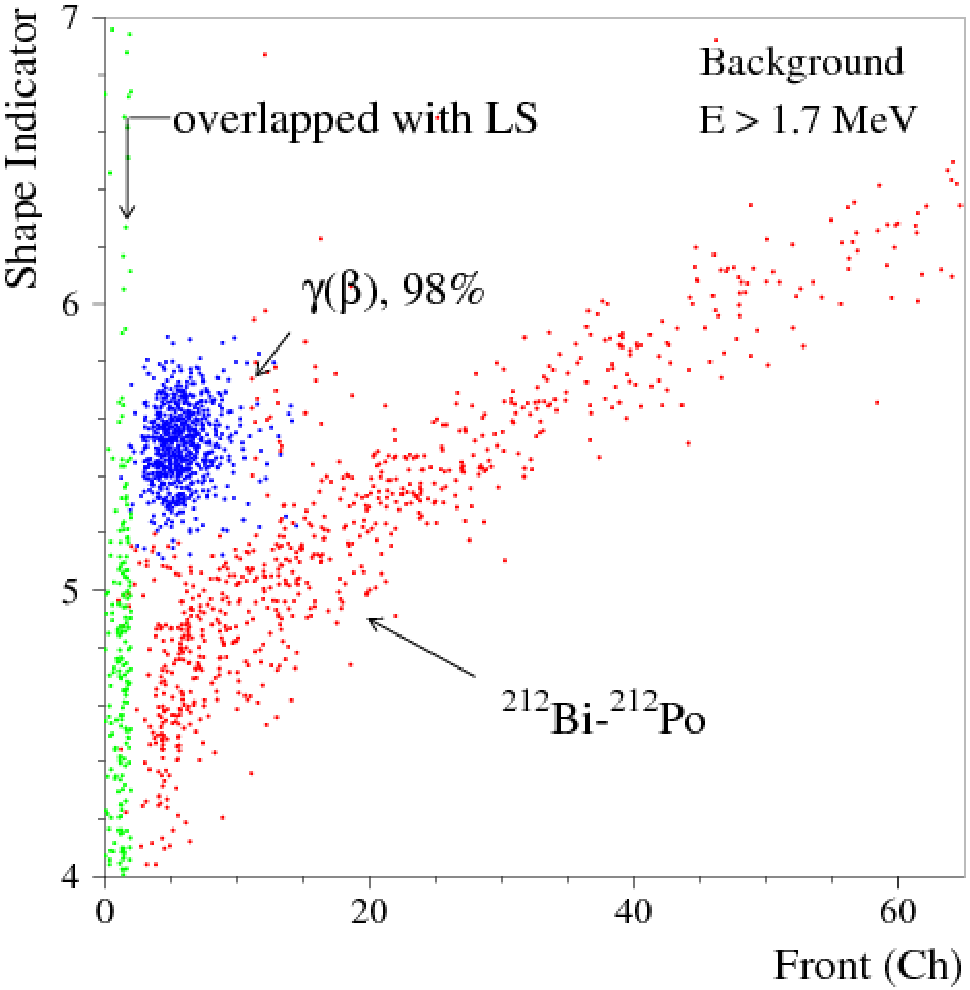

Activity ^{228}Th: 0.027(3) mBq/kg

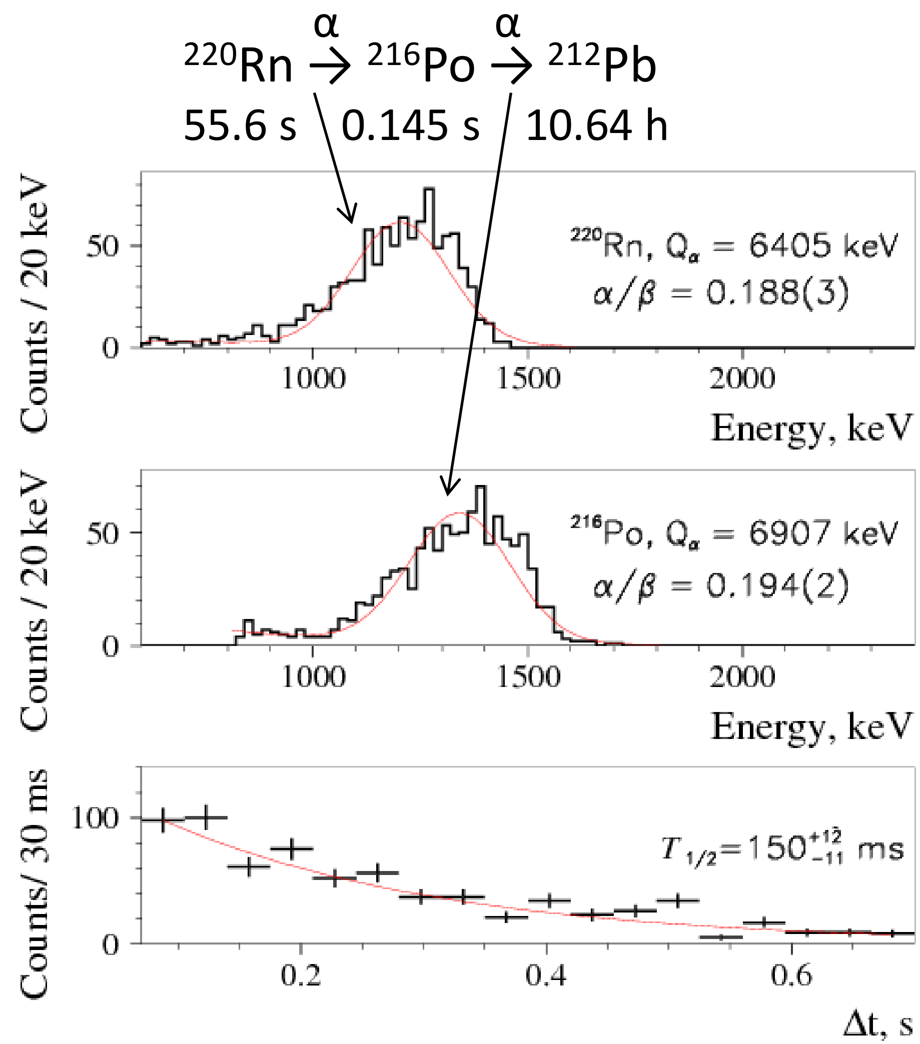

Activity ^{228}Th: 0.027(3) mBq/kg

Radioactive contamination of $^{116}CdWO_4$

Chain	Nuclide	Activity, mBq/kg
^{232}Th	^{232}Th	0.08
	^{228}Th	0.027(3)
^{238}U	^{238}U-^{234}Th	0.63(2)
	^{226}Ra	$\leq$ 0.005
	^{210}Pb	0.6(1)
	^{40}K	$\leq$ 0.9
	^{110m}Ag	$\leq$ 0.02

Total α activity = 2.25 mBq/kg

Two neutrino 2β decay of ^{116}Cd

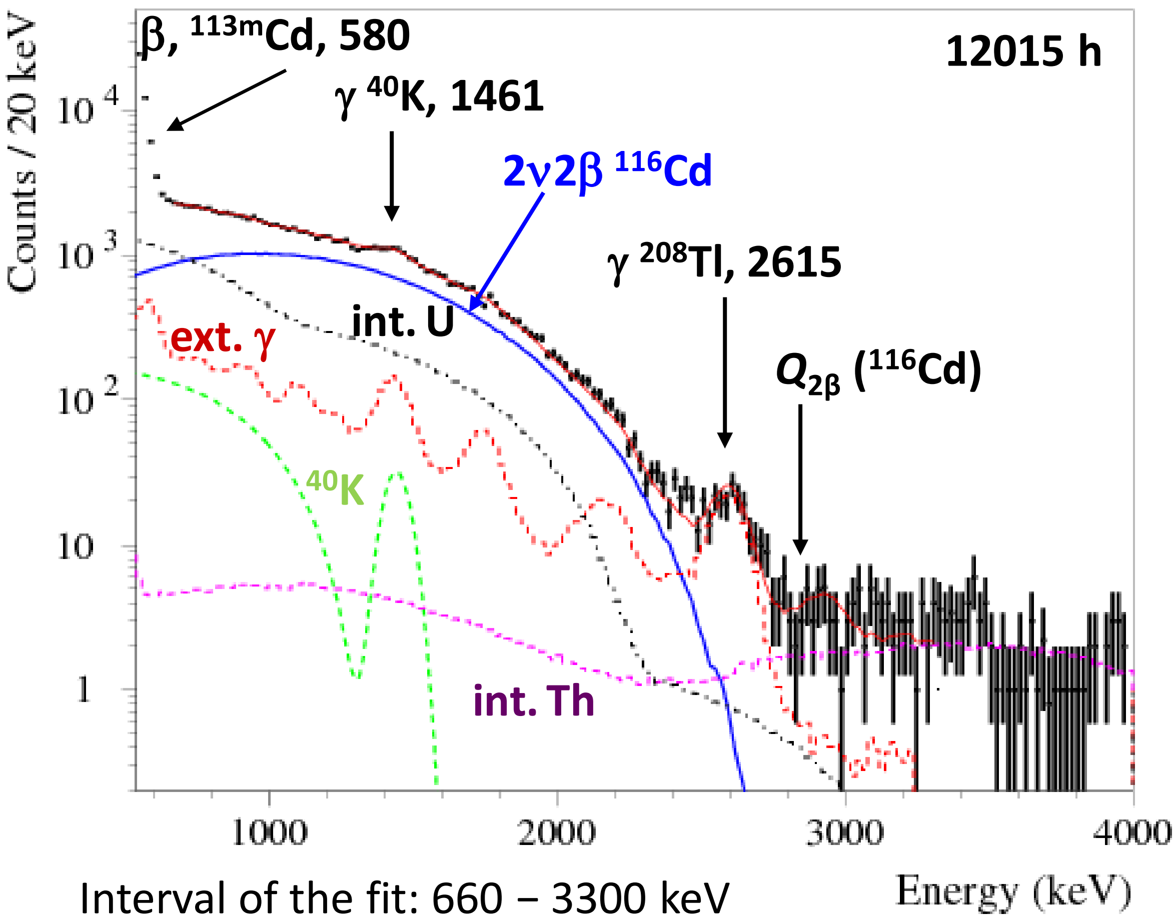

Interval of the fit: 660 – 3300 keV

Systematic errors

Source	Contribution ×10^{19} yr
Number of nuclei	0.002
Live time	< 0.002
Efficiency PSD	0.012
Fit	0.1
Simulation	0.025

$$T^{2\nu}_{1/2} = [2.69 \pm 0.14(\text{syst.}) \pm 0.02(\text{stat.})] \times 10^{19}\ \text{yr}$$

Comparison with other experiments

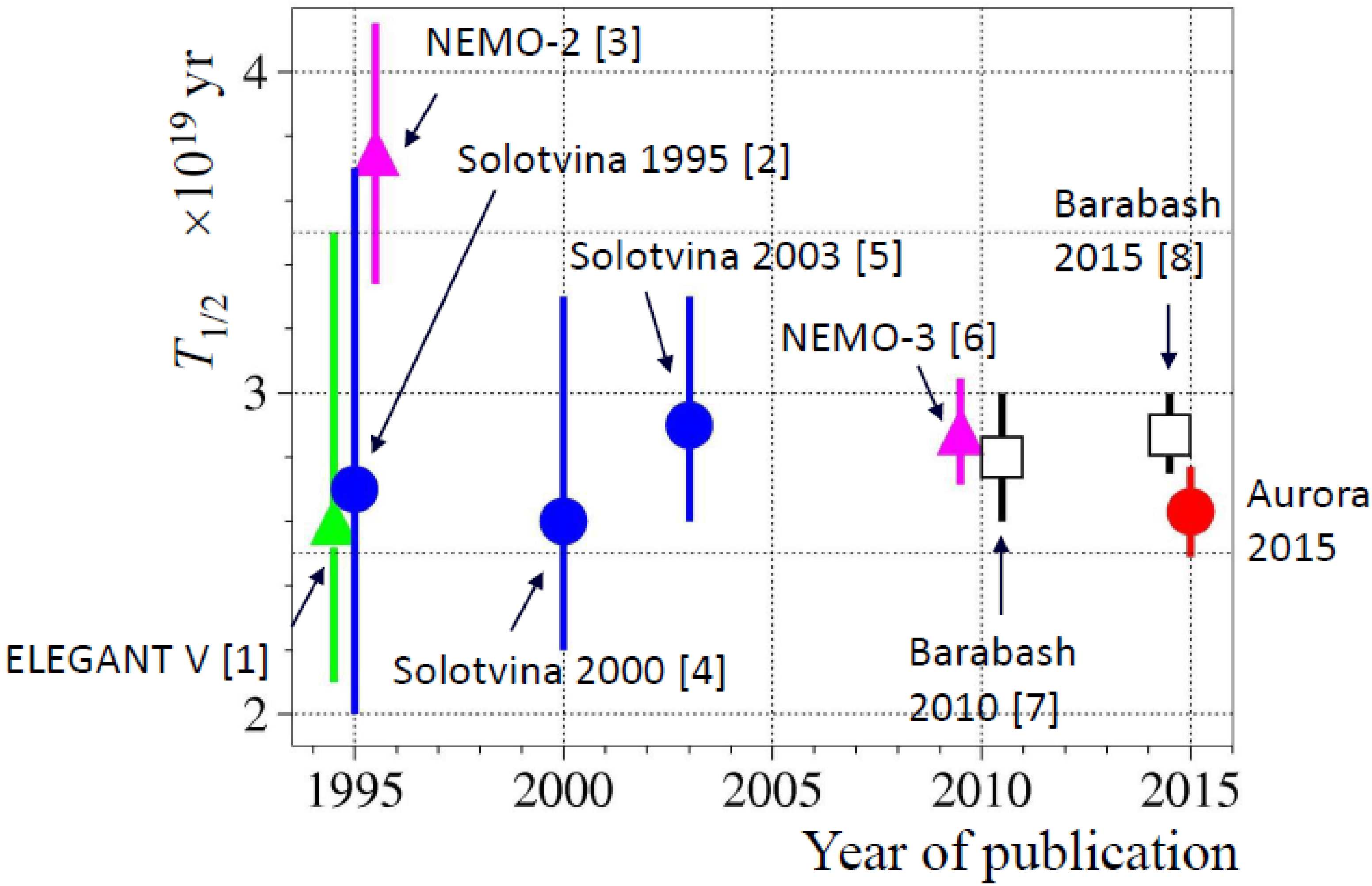

[1] H. Ejiri et al., J. Phys. Soc. Japan 64 (1995) 339
[2] F.A. Danevich et al., Phys. Lett. B 344 (1995) 72
[3]R.Arnold et al., Z. Phys. C 72 (1996) 239
[4] F.A.Danevich et al., PRC 62 (2000) 045501
[5] F.A.Danevich et al., PRC 68 (2003) 035501
[6] V.I. Tretyak et al., AIP Conf. Proc. 1572 (2013) 110
[7] A.S. Barabash, PRC 81 (2010) 035501
[8] A.S. Barabash, NPA 935 (2015) 52

Limit on $0\nu2\beta$ decay of ^{116}Cd

Fit in 2.5–3.1 MeV gives area of the effect S = -3.7 ± 10.2 counts
lim$S$ = 13.3 counts @ 90% C.L. by [1]

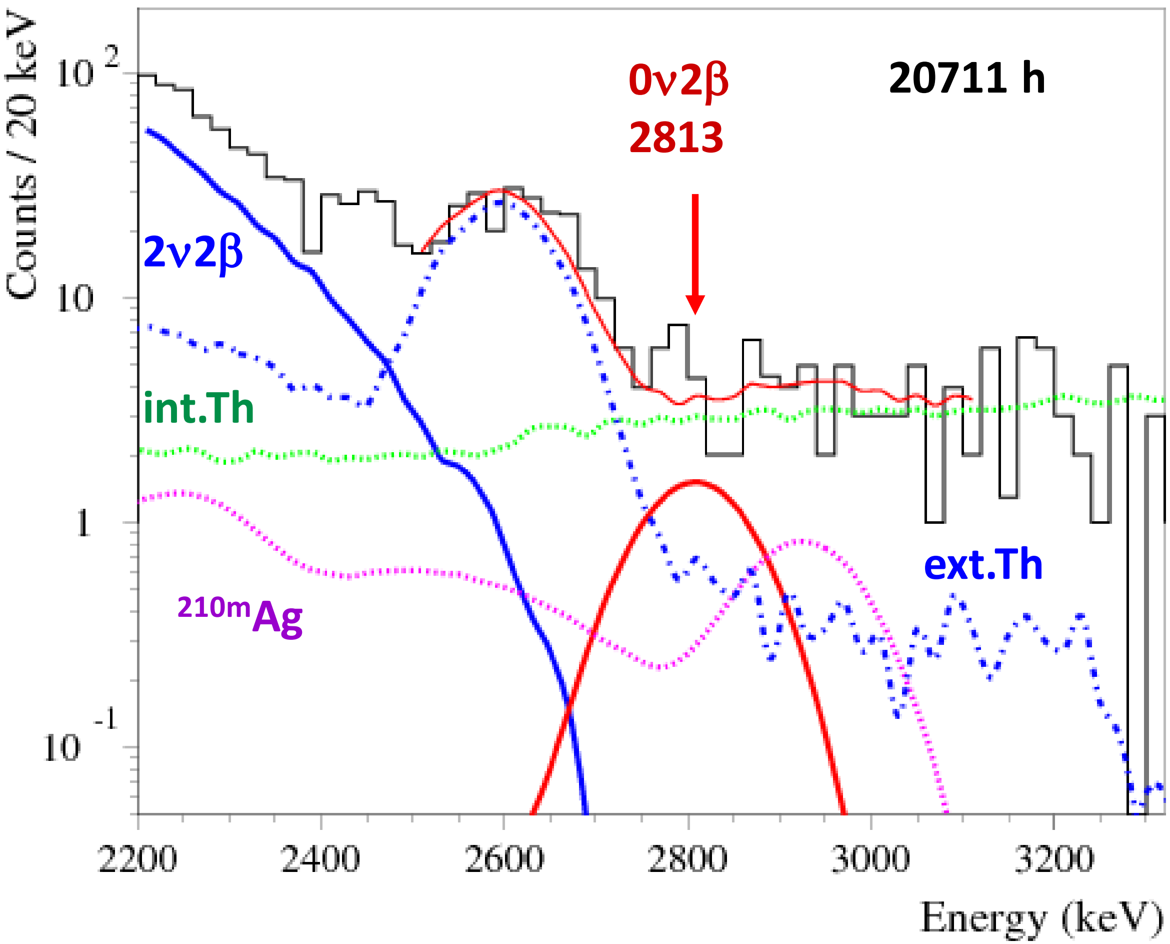

$$T_{1/2}^{0\nu} > 1.9 \times 10^{23} \text{ yr}$$

Effective Majorana neutrino mass

$\langle m_\nu \rangle \leq 1.7$ eV [2]

$\langle m_\nu \rangle \leq 1.2 - 1.8$ eV [3]

[1] G.J. Feldman and R. D. Cousins, Phys. Rev. D 57(1998)3873
[2] J. Barea, J. Kotila, and F. Iachello Phys. Rev. Lett. 109(2012)042501
[3] J.D. Vergados, H.Ejiri and F.Simkovic Rep. Prog. Phys. 75(2012)106301

Results

Decay mode	Transition, level of ^{116}Sn	*lim*$T_{1/2}$ (yr) 90% CL, present results	*lim*$T_{1/2}$, yr at 90% C.L. , best previous limit
0ν	g.s.- g.s.	**$\geq 1.9 \times 10^{23}$**	$\geq 1.7 \times 10^{23}$ [1]
0ν	g.s.- 2_1^+(1294 keV)	**$\geq 6.2 \times 10^{22}$**	$\geq 2.9 \times 10^{22}$ [1]
0ν	g.s.- 0_1^+(1757 keV)	**$\geq 6.3 \times 10^{22}$**	$\geq 1.4 \times 10^{22}$ [1]
0ν	g.s.- 0_2^+(2027 keV)	**$\geq 4.5 \times 10^{22}$**	$\geq 0.6 \times 10^{22}$ [1]
0ν	g.s.- 2_2^+ (2112 keV)	**$\geq 3.6 \times 10^{22}$**	$\geq 1.7 \times 10^{20}$[2] (at 68% CL)
0ν	g.s.- 2_3^+ (2225 keV)	**$\geq 4.1 \times 10^{22}$**	$\geq 1.0 \times 10^{20}$[2] (at 68% CL)
0ν*M*1	g.s.- g.s.	**$\geq 1.1 \times 10^{22}$**	$\geq 0.8 \times 10^{22}$ [1]
0ν*M*2	g.s.- g.s.	**$\geq 0.9 \times 10^{21}$**	$\geq 0.8 \times 10^{21}$ [1]
0ν*bM*	g.s.- g.s.	**$\geq 2.1 \times 10^{21}$**	$\geq 1.7 \times 10^{21}$ [1]
2ν	g.s.- g.s.	**[2.69±0.14(syst.)±0.02(stat.)]×10^{19}**	See slide 59
2ν	g.s.- 2_1^+(1294 keV)	$\geq 0.9 \times 10^{21}$	$\geq 2.3 \times 10^{21}$ [3]
2ν	g.s.- 0_1^+(1757 keV)	$\geq 1.0 \times 10^{21}$	$\geq 2.0 \times 10^{21}$ [3]
2ν	g.s.- 0_2^+(2027 keV)	$\geq 1.1 \times 10^{21}$	$\geq 2.0 \times 10^{21}$ [3]
2ν	g.s.- 2_2^+ (2112 keV)	**$\geq 2.3 \times 10^{21}$**	$\geq 1.7 \times 10^{20}$ [2] (at 68% CL)
2ν	g.s.- 2_3^+ (2225 keV)	**$\geq 2.5 \times 10^{21}$**	$\geq 1.0 \times 10^{20}$ [2] (at 68% CL)

[1] PRC 68(2003)035501 **[2]** Phys.Lett.B 249(1990)186 **[3]** NPA 577(1994)493

Conclusions

- The Aurora experiment to search for 2β decay processes in ^{116}Cd with the help of enriched radiopure $^{116}CdWO_4$ scintillators is running at the Gran Sasso underground laboratory

- The most precise measurement of 2ν2β decay of ^{116}Cd:

$$T^{2\nu}_{1/2} = [2.69 \pm 0.02(\text{stat.}) \pm 0.14(\text{syst.})] \times 10^{19}\ \text{yr}$$

- The new limit was set for the 0ν2β decay as

$$T^{0\nu}_{1/2} > 1.9 \times 10^{23}\ \text{yr},$$

which corresponds to $\langle m_\nu \rangle \sim (1.2 - 1.7)$ eV

- New improved limits are obtained for 2β decay of ^{116}Cd with emission of majorons and to the excited levels of ^{116}Sn:

$$\lim T_{1/2} \sim 10^{21}\text{–}10^{22}\ \text{yr}$$

Future plans

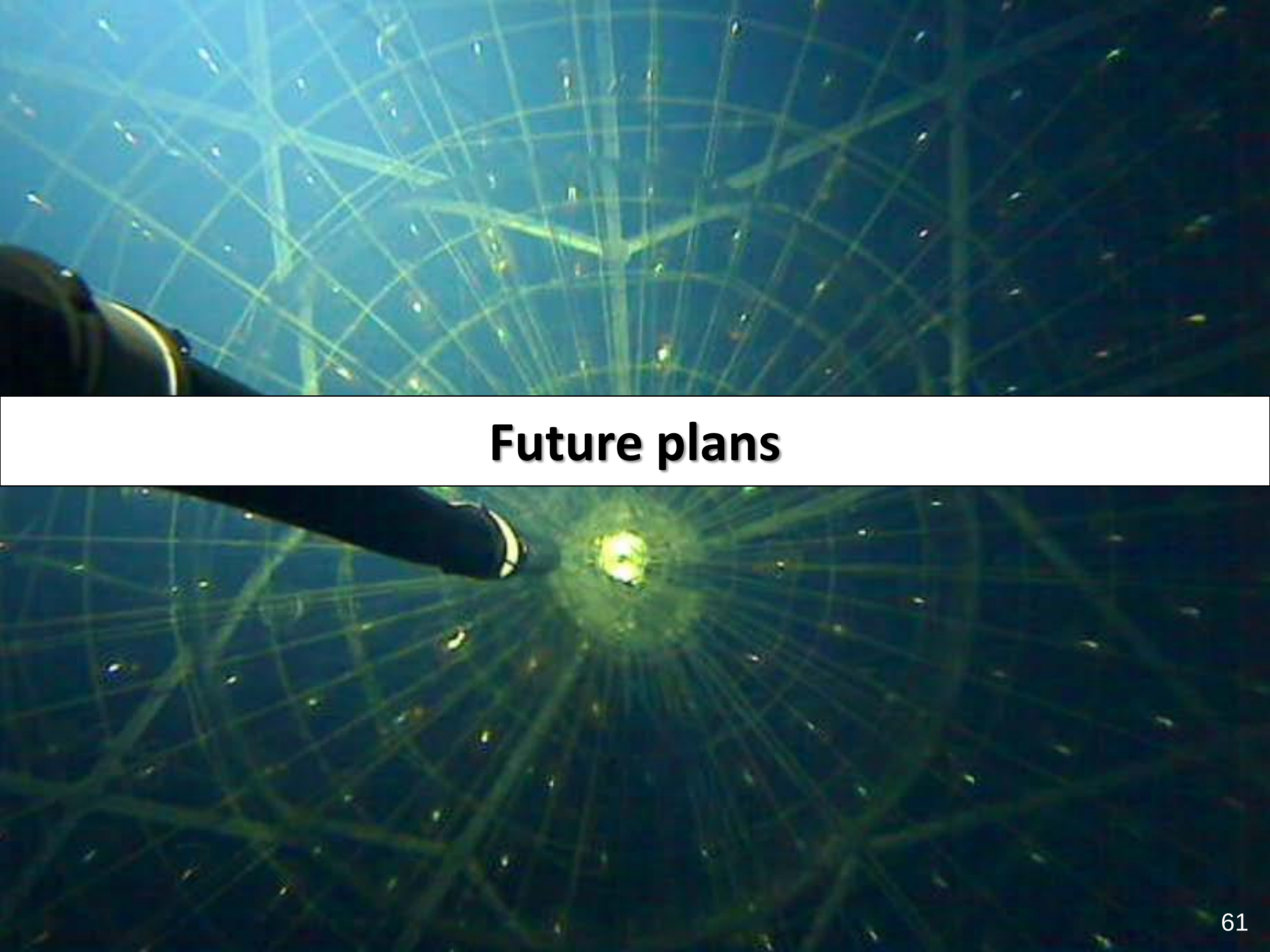

KamLAND-Zen2

KamLAND spherical tank inspection (~ May 2016) → **Improvement of Zen mini-balloon and OD**

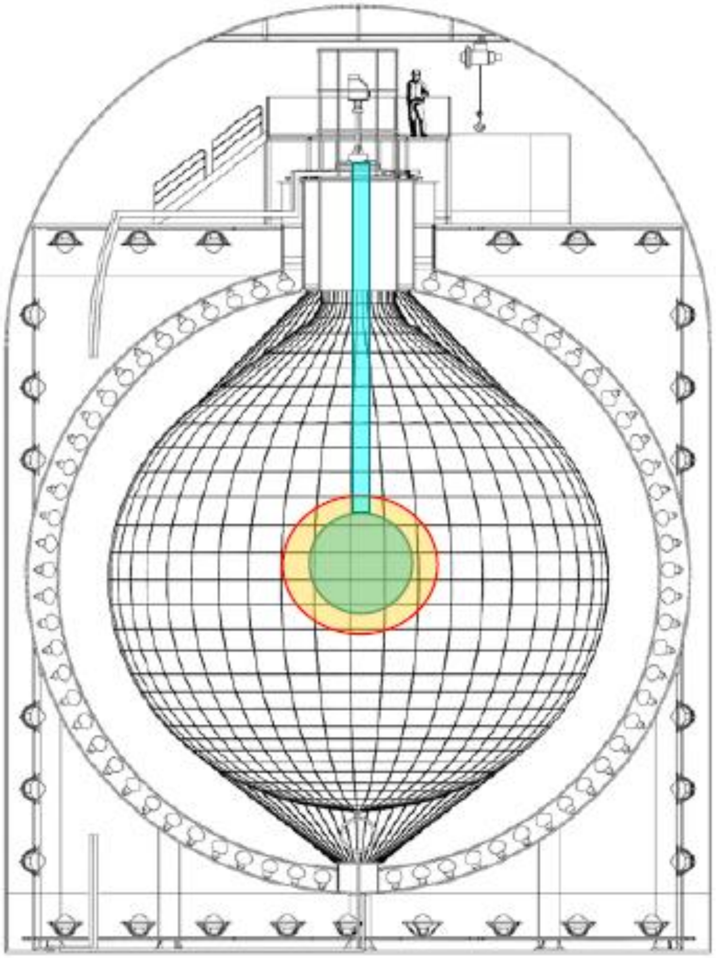

	KL-zen		KL-zen2
balloon size :	3.16mφ	=>	~4mφ
^{136}Xe amount :	383kg	=>	650~750kg
enlarge FV using ultra clean balloon			

Masayuki Koga , Particle Physics and Cosmology Workshop (PPC2015)

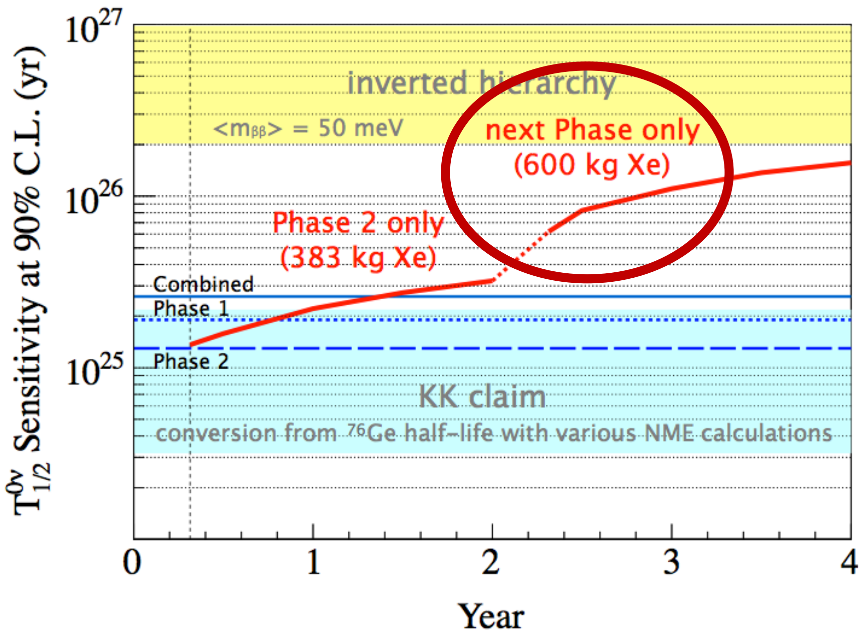

I would be happy to join the KamLAND-Zen experiment!

Surface contamination of the Inner Balloon

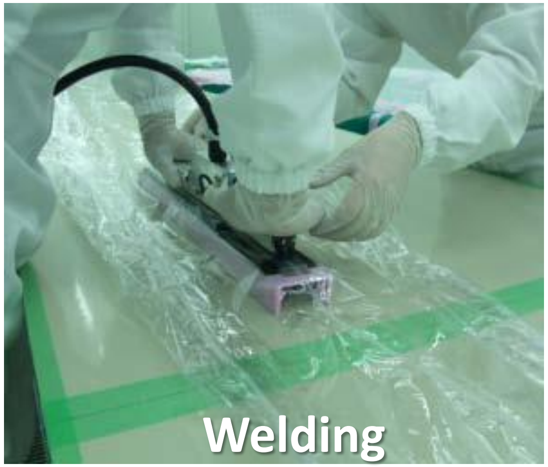

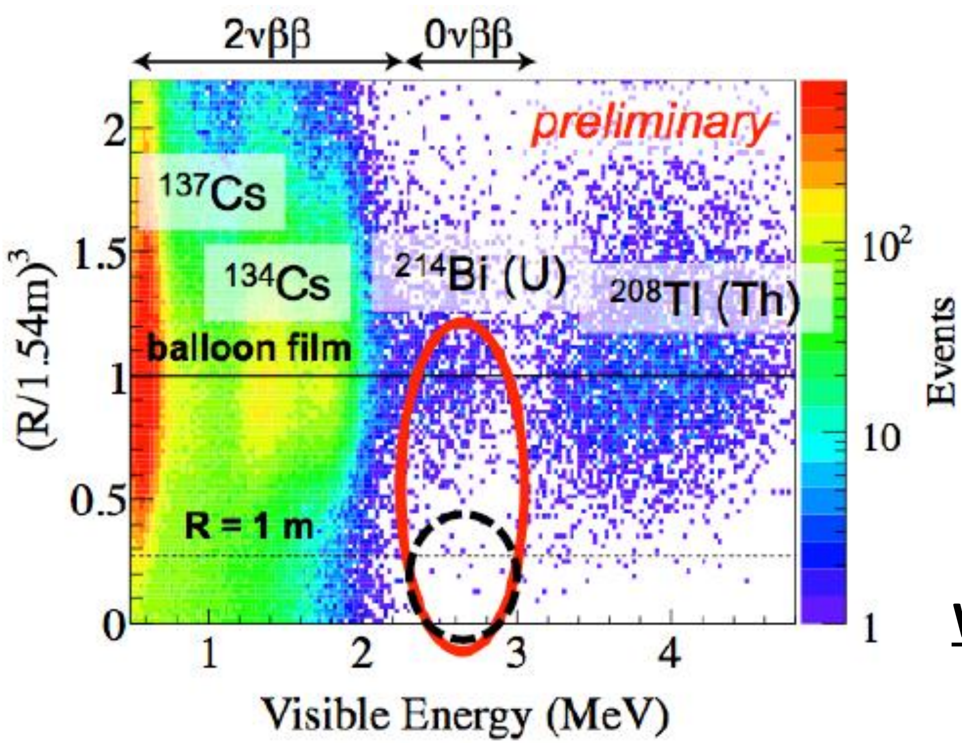

Expected contamination of the **past Inner Balloon (IB)** by ^{238}U was **2×10^{-12} g/g.** However, **on average IB contained 4.7×10^{-11} g/g of ^{238}U →**

Significant background from ^{214}Bi

Contamination of the new IB ???

We need to monitor surface contamination of the IB during its construction

Pictures from presentation of Masayuki Koga at Particle Physics and Cosmology Workshop (PPC2015)

Control of the surface contamination

I've received an offer to join the **development of an ultra-sensitive α-particle detector based on the existing Ion Pulse Ionization Chamber prototype** constructed at the Baksan Neutrino Observatory (Russia). The main features of the detector are:

- it can use various gases including air or nitrogen regardless of their purity
- it has a high energy resolution and can be used to determine tracking parameters of α-particles making possible background suppression to a level of 10^{-5} events/h/cm^2 or less
- it has a sensitivity to ^{238}U on the level of 10^{-10} g/g using a 1000 cm^2 sample

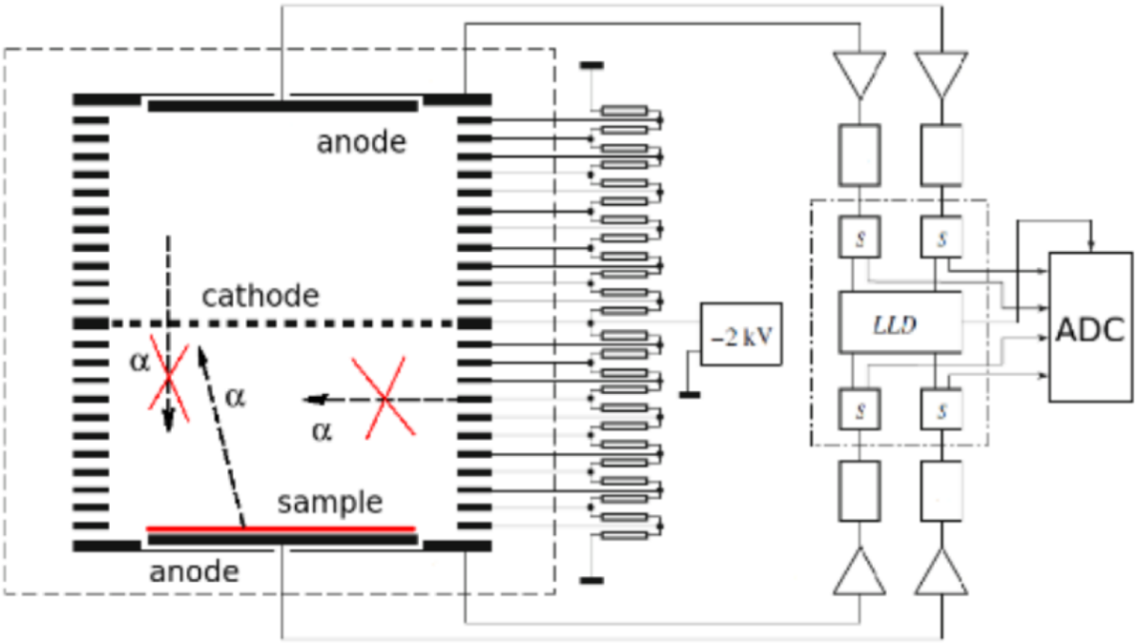

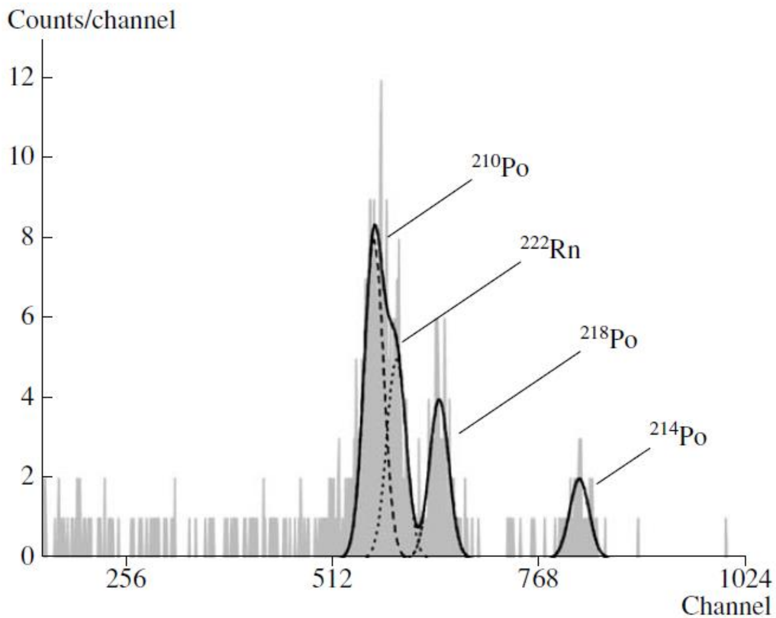

R&D of α-particle detector

The research and development of ultra-sensitive α-particle detector will include:

- Construction of a prototype of α-particle detector at Kavli IPMU (all technical documentation is ready)
- Development of improved signal processing techniques used for event's energy and track reconstruction
- Study of surface cleaning procedures and radiopurity of detector materials to reduce α-emitters background from inner surface of the detector
- Production of the 1000 cm^2 or larger ultra-sensitive α-particle detector

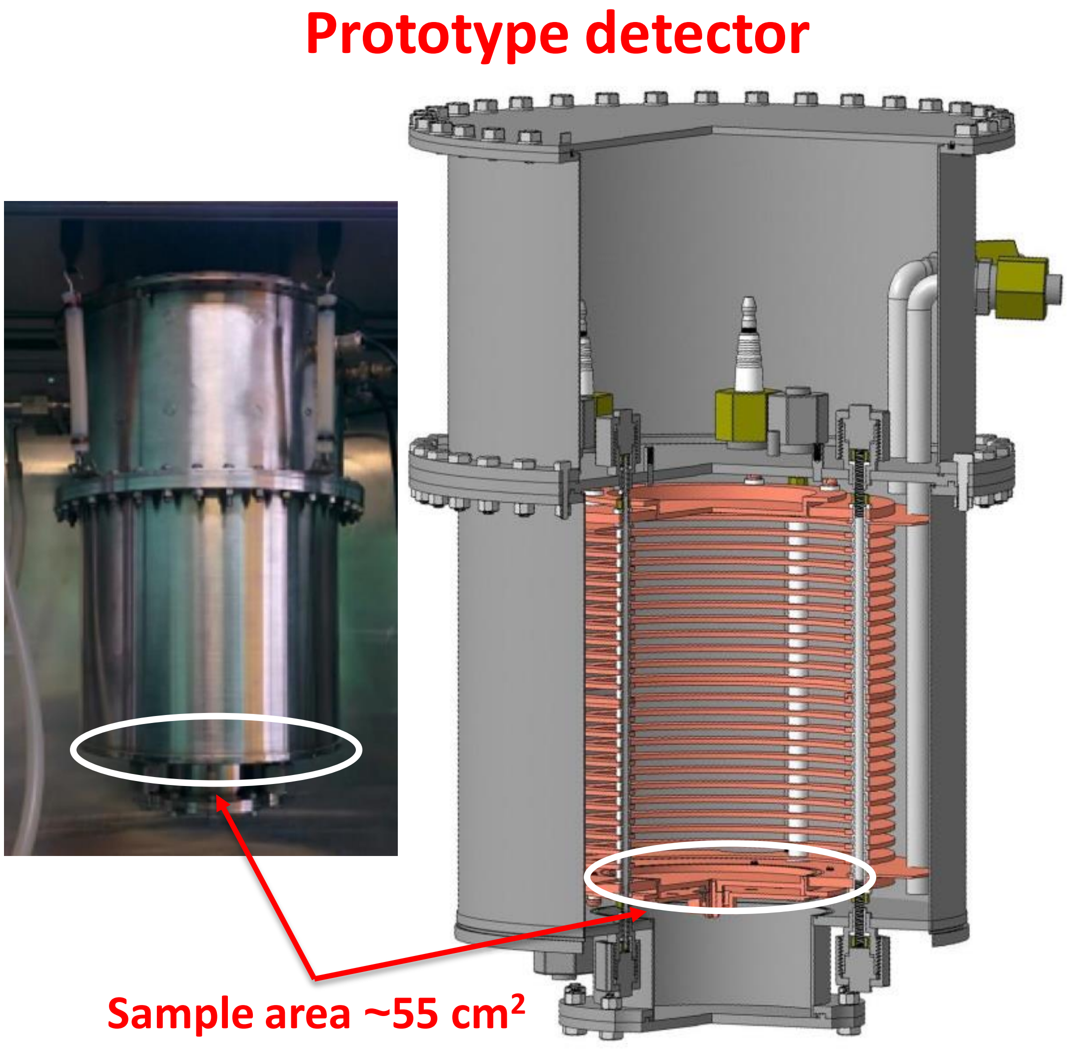

Postdoctoral position at Kavli IPMU

KAVLI IPMU INSTITUTE FOR THE PHYSICS AND MATHEMATICS OF THE UNIVERSE

THE UNIVERSITY OF TOKYO

Zero neutrino double beta decay search KamLAND-Zen

As a postdoc position at Kavli IPMU experiment I would like to actively participate in several research projects:

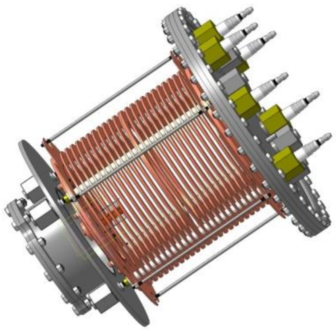

Development of ultra-sensitive gas detector of α-particles to control the surface contamination of the nylon film and other materials

Development and optimization of NaI(Tl) detector modules and large NaI(Tl) Dark Matter detector using GEANT4 simulations

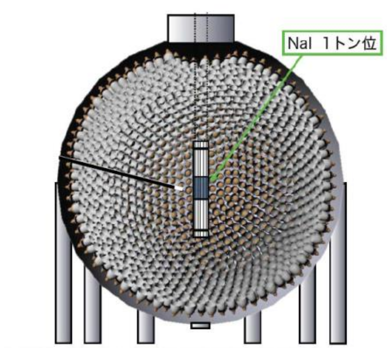

NaI(Tl) prototype tests, data analysis, and development of new experimental techniques used for background reduction in Dark Matter and double beta decay experiments


どうもありがとうございました！